VYSOKÉ UČENÍ TECHNICKÉ V BRNĚ

BRNO UNIVERSITY OF TECHNOLOGY

FAKULTA CHEMICKÁ
ÚSTAV FYZIKÁLNÍ A SPOTŘEBNÍ CHEMIE

FACULTY OF CHEMISTRY
INSTITUTE OF PHYSICAL AND APPLIED CHEMISTRY

BARRIER POLYMERIC LAYERS FOR INKJET PRINTS PROTECTION

BARIÉROVÉ POLYMERNÍ VRSTVY PRO OCHRANU INKJETOVÝCH TISKŮ

DIZERTAČNÍ PRÁCE
DOCTORAL THESIS

AUTOR PRÁCE — Ing. EVA ŠTĚPÁNKOVÁ
AUTHOR

VEDOUCÍ PRÁCE — doc. Ing. MICHAL VESELÝ, CSc.
SUPERVISOR

BRNO 2015

Brno University of Technology
Faculty of Chemistry
Purkyňova 464/118, 61200 Brno 12

Dissertation Thesis Assignment

Number of dissertation thesis **FCH-DIZ0109/2015** Academic year: **2015/16**

Institute:	Institute of Physical and Applied Chemistry
Student:	**Ing. Eva Štěpánková**
Study programme:	Physical Chemistry (P1404)
Study field:	Physical Chemistry (1404V001)
Head of thesis:	**doc. Ing. Michal Veselý, CSc.**

Title of dissertation thesis:

Barrier Polymeric Layers for Inkjet Prints Protection

Dissertation thesis assignment:

To prepare a protective varnish for inkjet prints with barrier qualities. This varnish should protect prints against ozone and UV light. To study protective characteristics using colour gamut volume calculation.

Deadline for dissertation thesis delivery: 30.9.2015

Dissertation thesis is necessary to deliver to a secretary of institute in the number of copies defined by the dean and in an electronic way to a head of dissertation thesis. This assignment is enclosure of dissertation thesis.

Ing. Eva Štěpánková Student	doc. Ing. Michal Veselý, CSc. Head of thesis	prof. Ing. Miloslav Pekař, CSc. Head of institute

In Brno, 1. 9. 2014

prof. Ing. Martin Weiter, Ph.D.
Dean

Printed by: Mgr. Alena Sýkorová
08.09.2015 13:58

ABSTRACT

This paper gives a brief overview on the published and accepted standards and methods for colour photography and print lightfastness measuring and evaluating. A comparison of selected valid standards and evaluation suggestions has been made.

The aim of this work was to protect inkjet prints by varnishing. Varnish compatible with photographic media was prepared. Composition was enriched by EVERSORB UV absorber addition in two concentrations. For comparison also three commercial varnishes were also used. Prints made with three types of dye-based ink sets proofed with varnish layer were exposed to accelerated lightfastness test in xenon test chamber as well as to accelerated gasfading test in ozone test chamber. Print gamut volume was calculated using measured reflectance spectra and VolGa software. The change in gamut volume during ozone and light induced ageing was monitored until the endpoint criterion was reached or test ended. Test endpoint was set to be 30% of gamut volume loss. A reciprocity law failure was observed, which indicates a lower credibility of long lifetime predictions. Gamut volume change was used to judge the effectiveness of UV and ozone protection provided by prepared composition.

Studied varnish layers were further tested on oxygen and water vapour transmission.

Key words:

Inkjet prints, varnishing, lightfastness, dye-fading, UV absorber, VolGa

ABSTRAKT

Práce podává přehled o dostupných a využívaných metodách, normách pro testování a hodnocení světlostálosti barevných fotografií a tisků. Bylo provedeno porovnání jednotlivých platných norem a návrhů na hodnocení.

Tato práce pojednává o ochraně inkjetových tisků pomocí lakování. Byl připraven lak kompatibilní s fotografickými médii. Připravená kompozice byla obohacena o UV absorbéry EVERSORB ve dvou koncentracích. Pro srovnání byly také testovány tři druhy komerčních ochranných fotografických laků. Výtisky se třemi barvivovými inkousty opatřené lakovou vrstvou, byly vystaveny jak urychlenému světelnému stárnutí v xenonové testovací komoře, tak urychlenému stárnutí v ozonové testovací komoře. Na základě měřených odrazových spekter byl vypočítaný objem barvového gamutu pomocí softwaru VolGa. Byl sledován úbytek gamutů v průběhu světelného stárnutí i při expozici ozonem. Stárnutí vzorků probíhalo do ukončení testu, nebo do dosažení kritéria 30% úbytku objemu barvového gamutu. Také bylo pozorováno selhání recipročního zákona, které ukazuje na jistou nepřesnost při předpovědi dlouhé životnosti vzorků. Pomocí změny barvového gamutu byla posuzována ochrana připraveného laku před UV zářením a ozonem.

Studované vrstvy laků byly dále charakterizovány na prostupnost kyslíku a vodní páry.

Klíčová slova:

Inkjetový tisk, lakování, světelná stálost, blednutí barviv, UV absorbér, VolGa

ŠTĚPÁNKOVÁ, E. *Bariérové polymerní vrstvy pro ochranu inkjetových tisků.* Brno: Vysoké učení technické v Brně, Fakulta chemická, 2016. 123s. Vedoucí dizertační práce doc. Ing. Michal Veselý, CSc.

PROHLÁŠENÍ

Prohlašuji, že tato disertační práce byla vypracována samostatně a že všechny použité literární zdroje byly správně a úplně citovány. Tato práce je z hlediska obsahu majetkem Fakulty chemické VUT v Brně a může být využita ke komerčním účelům jen se souhlasem vedoucího diplomové práce a děkana FCH VUT.

.....
podpis doktoranda

Poděkování:

Chtěla bych poděkovat svému školiteli doc. Ing. Michalu Veselému, CSc. a kolegům Ing. Petru Dzikovi, Ph.D. a Ing. Silvii Káčerové, Ing. Evě Bartoníčkové Ph.D. a Ing. Tomáši Opravilovi Ph.D. za jejich vstřícnost, čas a cenné rady. Dále bych chtěla poděkovat celému kolektivu laboratoře 3078. A v neposlední řadě bych chtěla poděkovat všem blízkým a hlavně rodičům, kteří mne v průběhu studia podporovali a bez nichž by tato práce nemohla vzniknout.

CONTENTS

1 INTRODUCTION

Throughout the history, humans always tried to depict images of their lives or emotions. Starting from first cave paintings (40,000 years ago[1]) to modern art, every generation tried to preserve the cultural heritage of the bygone era. Among this large group of imaging art surely belongs colour photography and print.

Photography was at the crossroad from the beginning of the 21st century. The technology for how the images are printed changed at a ferocious pace. In 1995, an inkjet print was largely an object of derision, suitable for amateurs and hobbyists, especially if they did not care (or know) that the print would likely discolour and fade in months. Today an inkjet print from one of Epson's pigment-based printers has an expected life span of between 100 and 200 years, longer than any previously available colour print media, including Cibachrome and Dye Transfer.[2]

According to the Image Permanence Institute, approximately 80 percent of cultural heritage institutions have inkjet prints in their collections and are concerned about the increasing influx of these materials. A survey showed that noticeable deterioration of these objects has already occurred, including fading, yellowing, colour bleed, surface cracking, and delamination. In total, 71 percent of institutions have identified deterioration of portions of their digital print collections.

The instability of inkjet prints have improved in recent years, however the need to protect and study these prints has stayed. One approach how to prevent print fade-out and protect them from harm of the environmental influences is varnishing.

2 CURRENT STATE OF RESEARCHED TOPIC

Colour photographs are still mainly produced electro-photographically. But the aim of this work is to focus on the colour "photograph" prints made with inkjet.

2.1 Inkjet print

Printing technology, inkjet, is a computer to print process, where ink is transferred directly onto the substrate via print head directed by electronic signal. Printing head shoots out droplets of ink on the medium, where the ink dries. Modern printing machines are able to change size (volume) of the ink droplet.

Generally the inkjet technology can be divided by the droplet forming method to continual stream (CS) and to drop on demand inkjet (DOD).[3,4,5]

2.1.1 Continuous inkjet

In the continuous inkjet technology, is generated a constant stream of small ink droplets, that are charged according to the imaging signal and are controlled electronically. The charged droplets are deflected by a subsequent electric field, while the uncharged ones flow onto the paper. This means that the imaging signal for charging the droplets corresponds to a negative print image. Continuous inkjet printing usually feeds only a small proportion of the stream of droplets to the substrate. The rest is fed back into the system.[3]

Continuous inkjet can be further subdivided into the CS process variations of binary deflection and multi-deflection.[3,6]

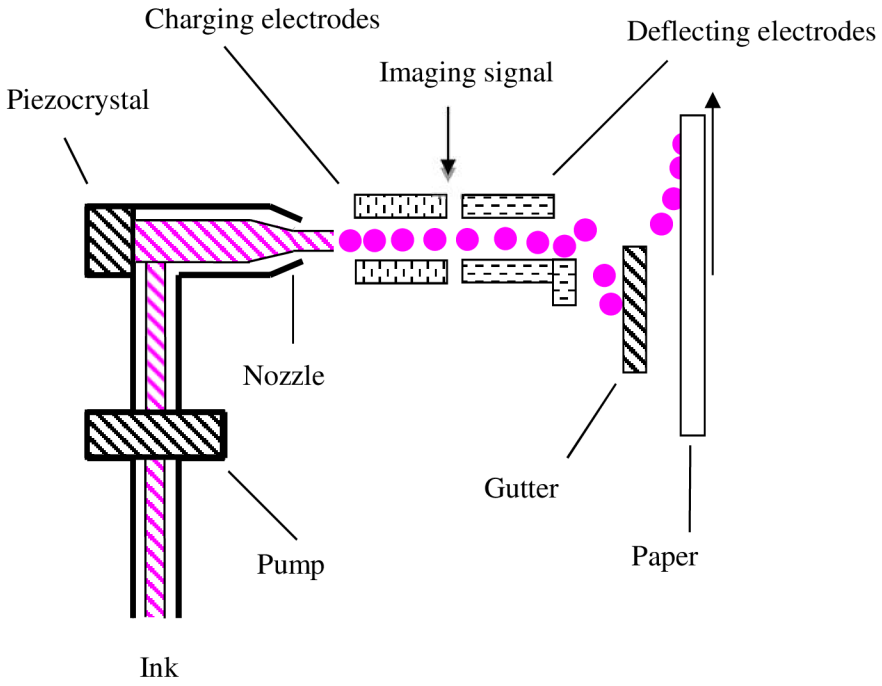

Figure 1 *Continual stream inkjet technology – binary deflection – the principle*[3]

2.1.2 Drop on demand inkjet

With the so-called "drop on demand inkjet" technology (DOD), on the other hand, a droplet is only produced if it is required. There are a number of variations of DOD technique, among the most important "drop on demand" methods are thermal inkjet (Figure 2) and piezo inkjet (Figure 3).[3]

2.1.2.1 Thermal inkjet

Thermal inkjet (also known as "bubble jet") generates the drops by the heating and localized vaporization of the liquid in a jet chamber. With passing of the electric current, the thermo-element heats up. Evaporation of ink continues and bubble is formed, which pushes out ink droplet though nozzle (Figure 3). Temperature of thermo-element drops suddenly and capillary forces refill the ink to the chamber.[3] Up-to date bubble-jet printers are capable of producing variable-size dots, instead of the uniform size dots, that are usually associated with this technology.[7]

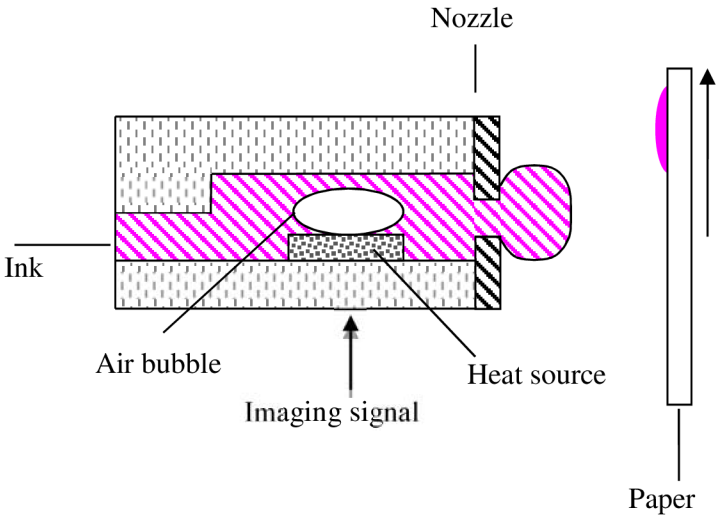

Figure 2 *Thermal inkjet – the principle*[3]

2.1.2.2 Piezo inkjet

Piezo inkjet technology is based on ink droplet formation and catapulting out of the nozzle by mechanical displacement in the ink channel (Figure 3), an action resulting from an electronic signal and the piezoelectric properties of the chamber wall.[6]

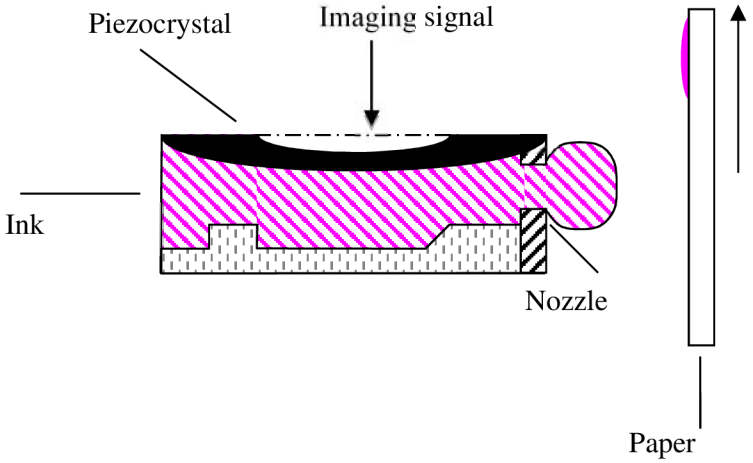

Figure 3 *Piezoinkjet – the principle*[3]

2.2 Print media materials

2.2.1 Inkjet papers

With the progress of digital photography the term photo paper no longer exclusively means light sensitive paper. It includes variety of other papers, designed to have image printed on them.

In late sixties, photo paper began to be manufactured with a polyethylene laminate on both sides of the sheet. The laminate keeps the print flat after wet processing and reduces the processing time. The top layer of laminate is often pigmented white, to enhance optical properties. These paper/plastic laminates have surface characteristics comparable to regular paper. Since then, these papers are sorted into inert media and called resin coated (RC papers).[8,9]

The base paper is coated with several layers consisting of pigments, vehicles (binders) and additives.[3]

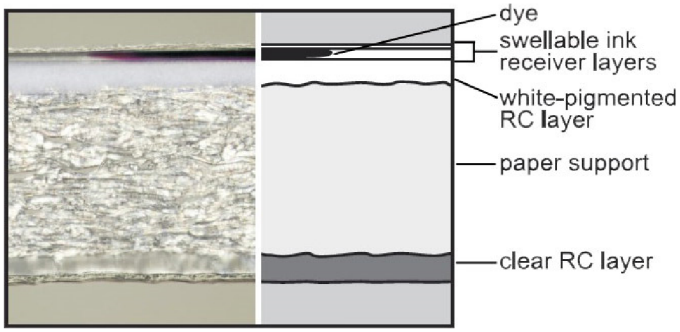

Figure 4 *Cross-section of swellable inkjet photo paper*[8]

2.2.1.1 Swellable Inkjet Coated Paper

The receiving layer of swellable inkjet paper is formed by a mixture of hydrophilic polymers, mainly polyvinylalcohol with modified starch and gelatine, with various degree of cross-linking.[4]

When ink droplets hit the surface, the swellable photo coating on inkjet papers swells and absorbs the liquid. Ink penetrates directly into the receiving layer, creating selectively coloured xerogel.[8.4] Freshly made prints become dry (or in moisture equilibrium with the surrounding atmosphere) within maximum of approx. eight hours after printing.[10] Handling the prints while they are wet can lead to smearing of the dye.[8]

Lately mainstream manufacturers stopped production of this type of papers.[11]

2.2.1.2 Porous Inkjet Coated Paper

The term porous inkjet paper really refers to three sub-types: macro-, micro- and nano-porous papers. Their similarity lies in presence of small pores that absorb the ink, their difference in the type of chemicals used to make the coatings and in the size of the pores.[8]

Porous inkjet paper is basically a thin layer of microceramic nano-particles held to the paper by a hydrophilic polymer binder.[12.8]

When ink droplet falls on this type of surface, liquid is quickly drawn inside further into a deeper layers of pores in seconds due to capillary mechanism, resulting in an “instant dry” prints, that are non-sticky shortly after emerging from the printer.[4] However, the absorbed liquid (water or solvents) will slowly diffuse from the microporous structure and evaporate until equilibrium with the surrounding air is reached.[13]

2.2.2 Inks

Ink is a colour carrier media, which is selectively applied on substrate. It is either low viscosity homogeneous, or heterogeneous liquid. Inks are consisting of solvent, colour carrier and other support components (surfactants, viscose controllers and preservatives).[14] Nowadays due to interest in

ecology, water based inks are preferred to oil or solvent based ones.[5] In large scale inkjet printing is nowadays mostly used eco solvent inks.[15]

According to the colour carrier medium we can divide inks into dye-based and pigment based.[3,4] Inks still go through constant development to obtain better qualities: better light fastness, less bleeding on the paper, wider hue range etc.[16]

2.2.2.1 Dye based inks

Dyes are molecules that are surrounded by solvents, which create a true analytical solution – a true homogeneous blend. This leads to higher colour intensity and more luminous colours. Solutions of dyes are very clear with high brilliancy, but every dye molecule can react with incident light. They have a larger hue range and are naturally transparent since the molecules are significantly smaller than the visible wavelength of 380 nm. The disadvantage with most dyes is their limited light-fastness (oxidation leads to bleaching).

Light stability of dye-based ink is limited, but recent changes in composition showed significant increase in lightfastness.[3,4]

2.2.2.2 Pigment based inks

Pigments consist of molecules that are cross-linked with one another as crystals. Normally pigments have a particle size of 0.1–2 µm and can consist of several million molecules. Only around 10 % of the molecules lie on the surface, and only these molecules and a few underneath that can absorb light. Pigments disperse light, have a wide absorption band and are therefore not as "pure" as dyes, which possess an extremely narrow absorption band.

Pigment based inks have foundation in insoluble pigments, which make heterogeneous blend. Dispersed pigment particles are stabilised against sedimentation and coagulation. The pigment content in ink, depending on the colour tone, is between 5 % and approximately 30 %. These inks have lower colour brightness, because only surface can react with incident light. Modern inks have very small particles and big surface area for the surface light reaction, which reaches the colour quality of the dye-based inks. This makes them perfect for the combination of wide gamut and good light stability.[3,4]

2.2.2.3 Pigmented inks

There is also another type of ink, which is the combination of both inks described above. The idea of combining both inks was to bring down the disadvantages and bring forward the advantages. Unfortunately, the downsides were not overcome, so pigmented inks were not manufactured.[3,4]

2.3 Factors influencing fading of the inkjet prints

Illumination intensity and spectral power distribution, method of framing or its absence (display without glass), temperature and relative humidity are the factors that can influence fading and its rate, degree, direction of colour balance changes, and yellowish stain formation that occurs over time from exposure to light, when prints are displayed or the dark phase when are the prints stored. In normal display, storing and use, prints are naturally "aged" for periods of months and years. Among factors that influence the print's stability belong temperature, humidity in which are prints present and also choice of receiving substrate type and its pH.[22,17] Influence of the main factors is described in further chapters.[13]

2.3.1 Light

The cause of degradation of colour prints is the fact that all print parts selectively absorb parts of ultraviolet and visible part of the electromagnetic spectra. Light induced degradation is caused by shot wavelength photons, from blue-violet to UV part of the spectra. These photons are high in energy. When the light/energy is absorbed, not only molecules of dyes and pigment particles are excited, other parts of print absorb light too. Excited molecules and particles usually dissipate redundant energy as heat, but excited molecules are unstable, and they can participate in reaction prior to their de-excitation, e.g. burnout of optical brightening agents (OBA's).[4]

Dyes present in inkjet prints are usually degrading by a photodegradation oxidation mechanism (see Figure 5). The principle of this is the fact that airborne pollutants generate free radicals that are degrading the inkjet ink. This degradation reaction produces more free radicals, which speed up the fading process.[18]

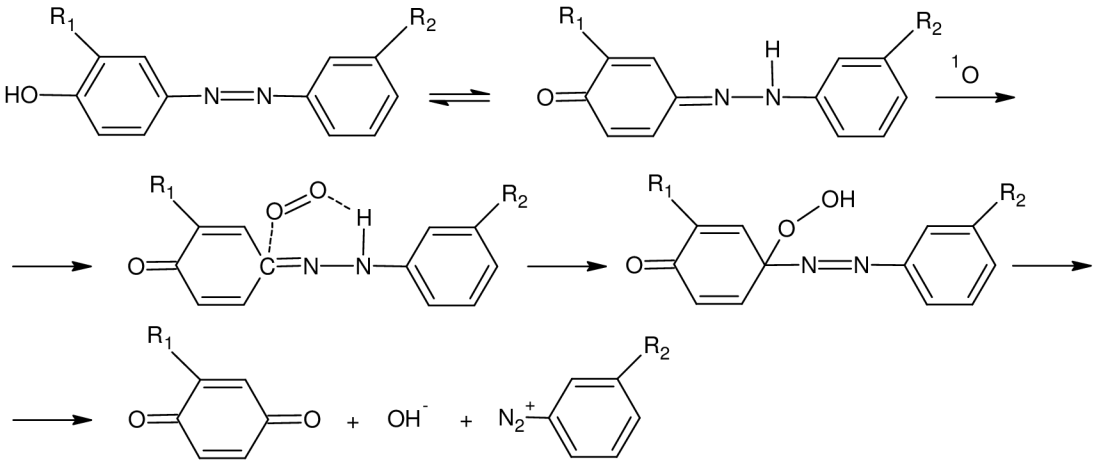

Figure 5 *Oxidation mechanism of light fading for ink colorant–azo dye.*[19]

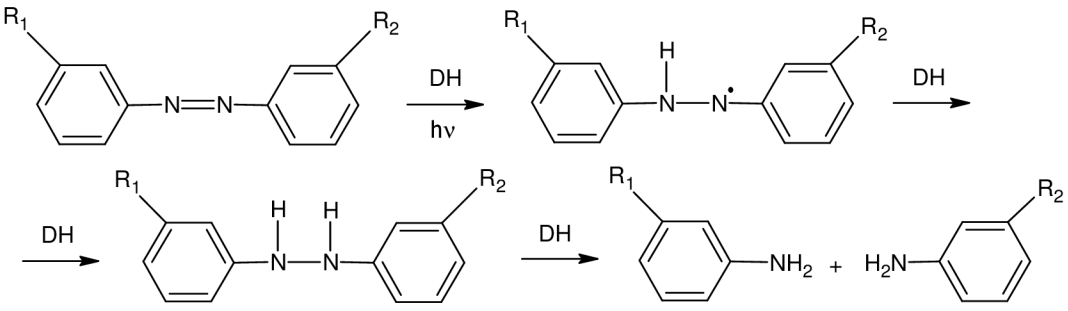

Figure 6 *Reduction mechanism of light fading for ink colorant–azo dye.*[19]

2.3.1.1 Additives enhancing the lightfastness of prints

Additives that enhance the photo-stability, usually water soluble, can be added to inks in low concentrations, to protect chromophores. When the dyes fade in oxidative manner the antioxidants are added or reductive manner then reductive reagents are added respectively. Additives can be added also to the receiving layers, but in that case much higher concentrations are used.[20,23]

2.3.2 Airborne pollutants

Image stability of unprotected prints is affected by pollutant gasses in the indoor and outdoor atmosphere.[21] Inkjet print degradation caused by these airborne pollutants is called "gas fading". And it occurs not only in light but also when the prints are stored in dark.[22]

Among airborne pollutants that are harmful for inkjet prints, in terms of stability, belong ozone $^3O_2$, sulphur oxides (mainly sulphur dioxide) and nitrogen oxides (nitric oxides, dinitrogen pentoxide, nitrogen peroxide and their mixture).[23,24,25] From all airborne pollutants the major influence on image stability has ozone and other gasses have just minor influence or cause different problems (e.g. yellowing of the substrate).[21] As well as environmental conditions influence ozone-induced degradation process; it is speeded up when humidity and temperature is elevated. Proved by studies, there is a correlation between changes in the residual optical density and the total ozone exposure.[26]

During the fading, oxygen, water and surface hydroxides may lead to a formulation of hydroperoxyl and hydroxyl radicals, who could attack the colorants present in the print.[27] An example of ozone induced degradation is shown in Figure 7 on phtalocyanine dye molecule, which is present in cyan inks.[26]

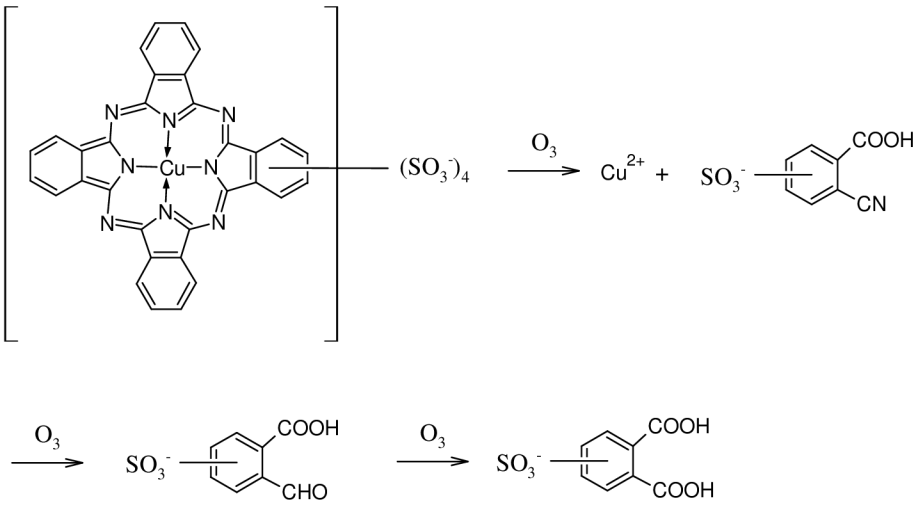

Figure 7 *Phtalocyanine ozone induced degradation.*[26]

From receiving layers the least resistant to airborne pollutants is the microporous type. The reason is their open structure, high porosity. Vast specific active area of synthetic sorbents allows even very small concentrations of ozone induce degradation.[23] The differences between microporous and conventional cast coated photopaper when interacting with light and airborne pollutants is clearly portrayed in Figure 8. When inkjet prints fade the higher the concentration of ozone, the bigger the degradation, so the reciprocity law is valid (for explanation see chapter 2.5.3).[28]

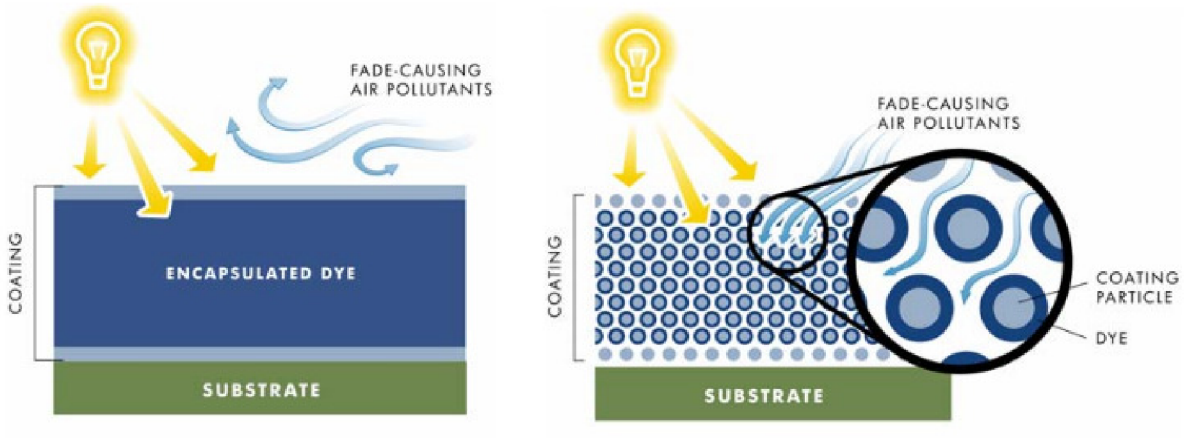

Figure 8 *The difference between microporous and cast coated receiving layers and their interaction with light and air pollutants.*[29]

2.3.3 Humidity

Regardless the imaging technique, the storing humidity level in which the print resides is very important. Humidity induced changes of line and edge quality in inkjet prints are due to lateral migration of the colorants within the image layer, whereas colour and tone scale changes can be caused by both lateral and vertical diffusion of the colorants. The migration effects vary with colorants mixtures and ink loadings.[30] Individual colours can change at different rates depending on the humidity level of the environment in which the print resides. In extreme cases, when the surrounding humidity exceeds approx. 70 %, it can lead to unacceptable decline in print quality due to lateral bleeding or line smearing due to sorption of water vapour, which augments the dye molecule migration.[31,30]

Especially swellable inkjet papers are threatened in environment with high humidity. Water adsorbed in hydrophilic polymers, present in the layer, works as a plasticizer thus lowering the glass transition temperature of these materials. Even in normal storage conditions there are significant changes in mechanical properties of the layer e.g. sticking, change in surface topology, bleeding etc.[4]

2.3.4 Catalytic fading

This phenomenon refers to the fact that a given dye may fade faster when it is in contact with another dye as a result of an image area containing more than just one ink. Components in the ink or their degradation reaction products or the printing substrate can also act as photocatalysts.[32]

2.3.5 Dark fading

The colour change occurs under light exposure as well as during dark storage period.[33] Degradation caused during this period is called “dark fading”. Degradation factors include temperature, humidity and atmospheric constituents. The atmospheric constituents, in order of their degradation strength during dark fading, are nitrogen oxides, sulphur oxides and ozone. Usually, this type of degradation manifests as yellow stain formation, which occurs with inkjet prints, as well as with traditional colour photographs. The degradation may damage imaging layer, paper or the other support material or all.[34,35,36]

When inkjet prints are subjected to the high-intensity illumination employed in accelerated light stability tests, the print may suffer from light induced yellowing that only shows itself during a dark period of storage after the prints are removed from light exposure.[13]

2.4 Colorimetry and colour perception

Colorimetry deals with the objective description of the physical correlates of colour perception. Initially, coloured samples were used to give an objective description of colour, and only in the

beginning of the twentieth century, when the objective measurement of coloured light became possible, did physicist develop methods for direct comparison of coloured lights with reference light.[37]

In 1931 the Commision Internationale de l'Éclairage, the CIE, defined the basics for system of colorimetry. It is founded on classic series of colour matching experiments that allowed the trichromatic properties of human vision to be studied and characterized.

Colour is a perception and as such, it is not accessible to engineering measurement. Metrology can access only the stimulus that will be produced as the consequence of the perception. Thus, CIE colorimetry is the metric of the psychophysical colour stimulus. The colour perception comprises of three irreplaceable elements (Figure 9); light source, observed object and observer.

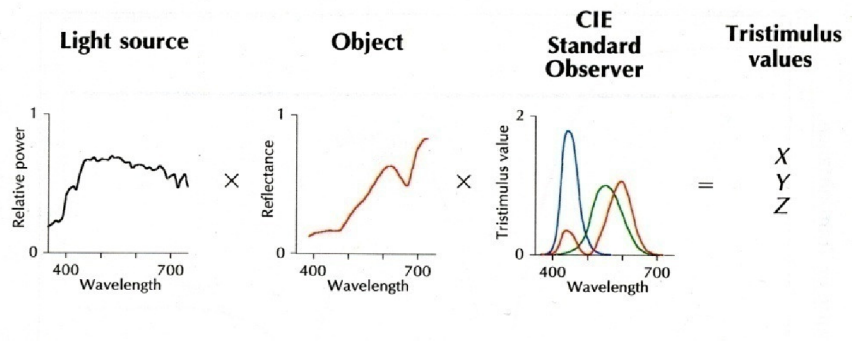

Figure 9 *Light source, object and observer (or any receiving detectors) make together colour perception defined by tristimulus values.*[48]

Light sensation is produced by visible radiation, electromagnetic radiation falling within the wavelength limit of 380 nm and 780 nm. Wavelength range of colour perception limits are not well defined, and the actual perception depends strongly on the adaptation state of the eye and on light stimuli surrounding the test object.[37]

There are two fundamental methods of producing colour stimuli: additive and subtractive colour mixing.[38] In additive colour mixing all colours are produced by the adding or blending together in different light proportions from the RGB primaries. By changing the intensity of lights, different mixed colours are produced. Subtractive colour principle, first described by du Hauron in 1862, is based on "removing" subtracting some part of the visible spectrum by colorants and is used in reproduction-printing.[37,45]

2.4.1 Light sources

As a source of light is considered an object that emits a large amount of photons whose wavelengths correspond with visible part of spectrum.[39] The most common source of light on Earth is the Sun. Electromagnetic radiation of the complete spectral power distribution is generated by thermonuclear reaction and is projected in all directions from the Sun into the space and approximately half of Sun's energy is absorbed by atmosphere or scattered. The spectral power distribution of daylight – a mixture of sunlight and skylight – can vary greatly depending on solar altitude and on weather and atmospheric conditions.[48,40] In Figure 10, note that the relative spectral radiant power distributions derived have a common value of 100 at the wavelength of 560 nm (CIE, 1964). The undulations in each of the spectral power distribution are the result of filtration effects due to the atmospheres of the sun and earth, particularly the amount of water vapour.[48,42]

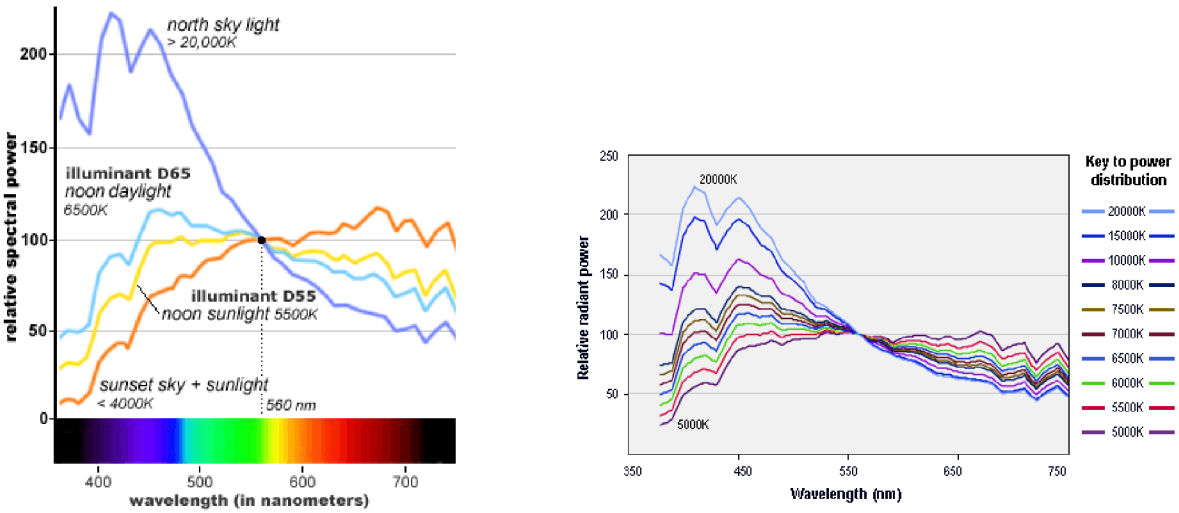

Figure 10 *Left: Spectral variations in natural light - standardized relative spectral power distributions for daylight phases across the visible spectrum.*[41] *Right: Relative radiant power distribution of 10 different phases of daylight.*[42]

The infinite variety and variance of natural daylight spectra makes it impossible to evaluate quantitatively an electric light source in terms of its ability to emulate natural daylight. Choosing a particular reference spectrum for daylight for comparison would not only be completely arbitrary, it would also undermine a basic marketing argument for manufacturers of full-spectrum light sources. Since daylight is a naturally varying light source, a light source that emulates one particular daylight spectrum is, by definition, unnatural. Nevertheless, all electric full-spectrum light sources have fixed spectral power distributions.[42] The CIE recommends either Standard Illuminant A (SA) or Standard Illuminant D65, which is a very good representation of average daylight but it is not available as a light source.[46] Standard practices and standards use various light sources as sunlight – e.g. xenon arc, tungsten lamp.

2.4.2 Standard observer

In 1931 the CIE defined a 2°standard observer for colorimetry, which incorporates both colorimetric and photometric behaviour.[43] The essential data are based on two experimental investigations, conducted by W. D. Wright and J. Guild.[37] Two equivalent statements of the colour matching behaviour of the CIE standard observer were embodied in the RGB and XYZ systems of units. There are two types of standard observers distinguished by the angle of incoming ray of light into the eye and retinal area, which perceives.[50]

The 2° observer has spectral characteristics concordant with typical human eye and it is used mostly for the colour specification in industry.[43,51,44]

The 2° measuring field was considered too small for many practical purposes, so a 10° field was adopted by the CIE convention in 1964. Although it has never been accepted as a standard for photometry, it is used for colorimetric calculations and measurements concerning large areas.[45] When compared together spectral characteristics of the two observers do differ from each other very slightly (Figure 11).[46]

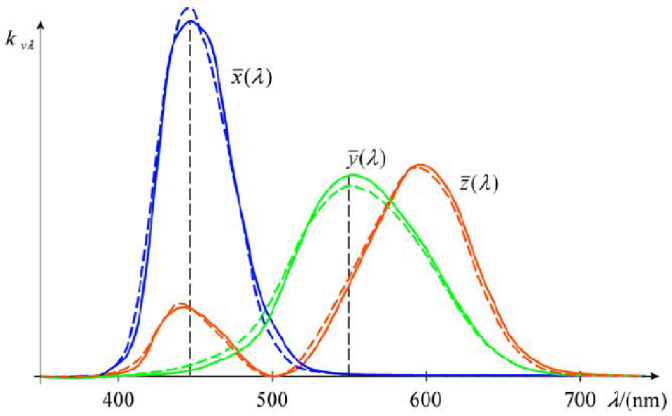

Figure 11 *Spectral characteristics: 2° (full line) and 10° (dashed line) standard observer.*[46]

2.4.3 Tristimulus values

CIE tristimulus values X, Y, and Z quantify the trichromatic characteristics of colour stimuli. The tristimulus values for a given object (characterised by its spectral reflectance $R(\lambda)$ or transmittance), that is illuminated by a light source (characterised by its spectral power distribution $\Phi_0(\lambda)$) can be calculated for the CIE Standard colorimetric observer (characterised by the CIE colour-matching functions $\bar{x}(\lambda)$ by summing the products of these distributions over the wavelength (λ) range of 380 to 780 nm.[50]

The calculation of the tristimulus values are shown in following equations (1–3) (ref.[50,3]):

$$X = K \sum_{\lambda=380}^{780} \phi^0(\lambda) \cdot R(\lambda) \cdot \bar{x}(\lambda) \quad (1)$$

$$Y = K \sum_{\lambda=380}^{780} \phi^0(\lambda) \cdot R(\lambda) \cdot \bar{y}(\lambda) \quad (2)$$

$$Z = K \sum_{\lambda=380}^{780} \phi^0(\lambda) \cdot R(\lambda) \cdot \bar{z}(\lambda) \quad (3)$$

K is a normalizing factor. By convention, K is usually determined according to the equation (4) such, that $Y = 100$ when the object is perfect white. A perfect white is an ideal, nonfluorescent, isotropic diffuse object with a reflectance (or transmittance) equal to unity throughout the visible spectrum. The brightness of a perfect white object is therefore independent of the direction of viewing (ref. [47,48]).

$$K = \frac{100}{\sum \phi^0(\lambda) \cdot \bar{y}(\lambda)} \quad (4)$$

2.4.4 CIE colour spaces

The CIE defined among others colour spaces. The definition of colour spaces is based on trichromatic values XYZ, which describe colours in terms of human colour vision; these spaces are considered as machine independent.[49]

*2.4.4.1 Colour space L*a*b**

Before CIELAB colour space was presented other model preceded, but eventually their use has stopped because of their technical difficulties when worked with. In 1976 CIE came with two alternative colour spaces CIELAB and CIELUV, which encompass all perceivable colours. With these they tried to compensate the problem of non-uniformity of the previous colour spaces, to allow more precise evaluation of colour differences (e.g. ΔE) and tolerances.[46,50,51] However, the desired perceptual uniformity of CIELAB colour space has not been realized. Studies have shown that as the chroma of a colour increases CIELAB increasingly overstates the magnitudes of perceived chroma

and hue differences. CIELAB colour space is also non-uniform regarding hue angle, although the specific nature of the non-uniformity is not yet definitively determined.[52]

The CIELAB colour space is square three-axis systems, with achromatic colours (white, black and shades of grey) placed on vertical axis, represented by lightness L^*. Chromatic axes a^* and b^*, lie in direction red-green (a^*) and yellow-blue (b^*). The scheme of colour space depicts Figure 12.

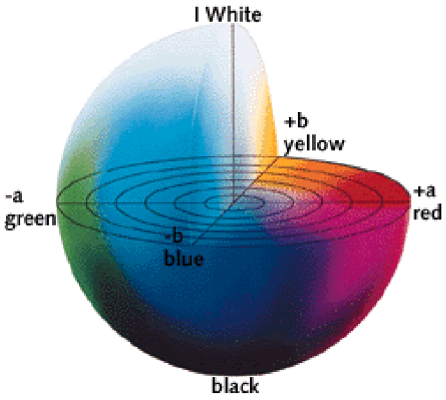

Figure 12 *Colour space CIE 1976 L*a*b**

Colour's position data in these systems are calculated from trichromatic values. For colour space $L^*a^*b^*$; equations 5–7 are valid only if values of illumination D65 and 10° standard viewer are $X_n = 94.811$; $Y_n = 100.00$; $Z_n = 107.305$ (ref. [50])

$$L^* = 116 \cdot \left(\frac{Y}{Y_n}\right)^{\frac{1}{3}} - 16 \tag{5}$$

$$a^* = 500 \cdot \left[\left(\frac{X}{X_n}\right)^{\frac{1}{3}} - \left(\frac{Y}{Y_n}\right)^{\frac{1}{3}}\right] \tag{6}$$

$$b^* = 200 \cdot \left[\left(\frac{Y}{Y_n}\right)^{\frac{1}{3}} - \left(\frac{Z}{Z_n}\right)^{\frac{1}{3}}\right] \tag{7}$$

Basic way to determine in $L^*a^*b^*$ space colour difference between two colours is the Euclidean distance between 2 points in CIELAB space.[53] Colour difference ΔE can be calculated according to equation 8.[54,55]

$$\Delta E^*_{ab} = \sqrt{(L^*_2 - L^*_1)^2 + (a^*_2 - a^*_1)^2 + (b^*_2 - b^*_1)^2} \tag{8}$$

It is advised to exercise appropriate caution when interpreting results and quantitative evaluation of colour accuracy.[56] ΔE was intended to judge a small incremental differences between two colour patches presented side by side.[67,56]

Table 1 *ΔE value and perceived colour difference*

Value ΔE^*_{ab}	Colour difference
0.5–2	perceived as colour accord
2–4	perceived as colour accord until direct comparison
4–8	colour difference perceived even without direct comparison
>8	perceived as distinctive colour difference

2.5 General principle of fastness evaluation

Inkjet prints exposed to surrounding environment (light, airborne pollutants, humidity etc.) loose in time their image information. The loss speed depends on many factors, e.g. processing, material combination, influence of the environment, and their combined effect. The most accurate is exposure of samples to actual source of harm e.g. daylight in real–time, but this form of test is time demanding (test can go on for years) and not very practical (tested product manufacture may be discontinued during test duration). Then there are accelerated tests which give reproducible results and take much shorter time. When prints are tested for light-fastness (in accelerated way), they are exposed to specified light source at given conditions. Usually the tests are carried out with special targets in test chambers with controlled conditions. In certain intervals test targets are measured spectrometricaly. And after a given endpoint criterion is reached, the test is ended. From the collected data, it is possible to calculate estimated lifetime of the image.[68]

There are, as mentioned above, two possible ways of testing light stability – time consuming long-term tests and accelerated ageing, where reciprocity law needs to be taken into account. The variety of different specific conditions for both tests is almost endless, taken into account variety of indirect daylight, their intensity, humidity, ozone and other airborne pollutants.[57] Conditions for reporting print permanence test data and image-quality loss metrics can be tested for following (ref.[58,59,30]):

- Indoor light stability during long term display
- Resistance to gas-fading
- Humidity-fastness
- Thermal degradation and yellow staining – dark storage
- Water fastness
- Stability of optical brighteners (OBA's)

2.5.1 Accelerated–lightfastness tests

For testing the accelerated lightfastness of inkjet print there are no ISO standards, which administer the test parameters. There is ISO standard that is for all types of tests for classical chromogenic materials but, with its translation to inkjet materials many issues arise. First and foremost is densitometry, the measuring method. Due to the composition differences this method, prescribed by the ISO standard, is not suitable for inkjet prints. The wide range of colorants used is not compatible with RGB filters in densitometer and in most cases absorption maxima of the dyes will miss the absorption maximum of the filter.[60]

Still used standard is the ISO standard dealing with all types of artificial ageing tests of classical chromogenic photographic materials. It is based on optical density loss of neutral and CMY pure patches with starting optical density of 1.0 ± 0.05 above the minimal optical density of the substrate. The endpoint criteria are complex but the most basic one is, that the photograph is considered faded when the loss of optical density on the neural patch or CMY is equal or greater than 30%.[61] This approach does not correlate with the psycho-physical based research on the human perceptiveness of the optical density loss and colour shift. According to the Shibahara et. al. the endpoint criterion can be augmented by 10% to 40% of density loss for CMY patches, but 23% for neutral patch, for the image to be rated as unacceptably faded. But this psycho-physical approach to the rating of prints and determining of endpoint criteria is not applicable in general, even though when done with professionals with trained eyes.[62,63] In some cases total impression of images is still at an acceptable level even if any one of the criteria has reached the threshold.

2.5.1.1 Test target

General term target covers an image with certain number of patches, which changes according to the test. The size of the patches differs from used machine and its recognition ability. For example, the ISO 18909 defines the minimum patch as a square 5 by 5 mm.

The number of patches is a moot point. On one hand, single patch does not provide enough information and on the other hand great patch number prolongs the measurement time and augments the requirements for the measuring machine and evaluation expenses.[68] A comparison of three targets is shown in Figure 13, very short and small one recommended by photographic ISO standard, reasonably sized test target used by Wilhelm Imaging group and big X-Rite standard profiling target TC9.18 RGB. [68,64,65]

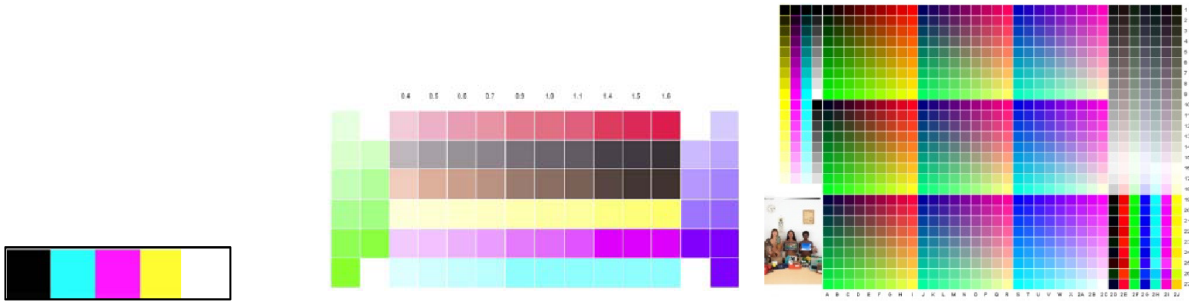

Figure 13 *The basic test target according to ISO 18909 (left)[68], test target used by Wilhelm et. al. (middle)[64] and standard printer profiling target TC9.18 RGB (right).*

2.5.1.2 Densitometry-based measuring methods

Densitometry is the recommended method for change monitoring by ISO 18909, the photographic standard.[68]Although it has no colour matching function or standard illuminants involved, it does provide its own brand of colour quantification in the form of a spectral density response, a density spectrum, or three integrated densities through three different colour-separation filters (RGB).[66]

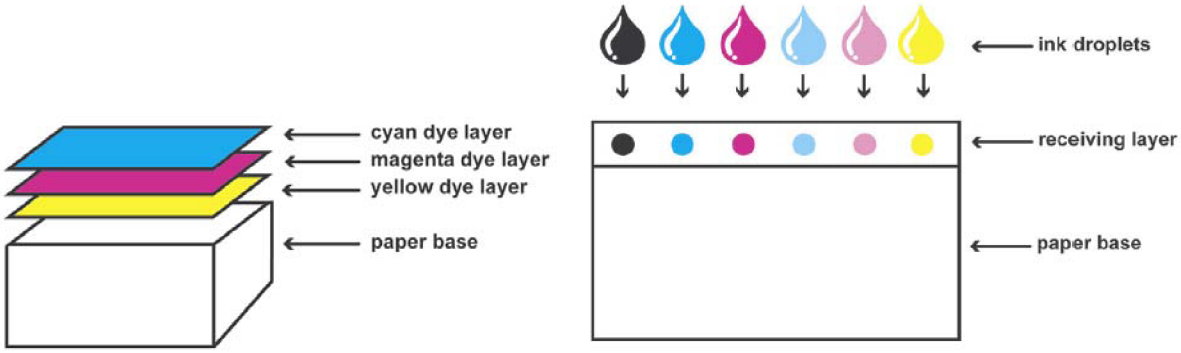

Figure 14 *Structure of traditional chromogenic dye-based photo material (left) and inkjet printing material (right).[81]*

Traditional dye-based chromogenic systems lose density uniformly across the full tonal scale (due to their structure, where colorants are sealed in separate layers (Figure 14), resulting in more or less parallel shift (light fade) or linear slope change (thermal ageing).

On the other hand modern digital printing systems employ a wide variety of pigment and dyes based colorants with markedly different spectral properties and use more than four CMYK colorants, present in one layer, to achieve enhanced colour gamut and improved continuous tone properties.[13] Catalytic fading, non-uniform printed dot dispersion, multi-colour sets (up to 12) with different bleeding levels, and varied black component placement by GCR techniques mean that the full tonal scale cannot be reliably concluded from measurements of just one or two initial density points. For

these reasons, it is essential to evaluate the full image tonal scale behaviour using colorimetric method.[67,81]

ISO 18909:2006 – Photography – Processed photographic colour films and paper prints – Methods for measuring image stability

Photographic standard ISO 18909 specifies test conditions for wide range of stability tests (dark and light). For purposes of this work only part containing indirect sunlight lightfastness tests, is presented.

The photographic material is to be exposed and processed according to manufacturer's recommendation to obtain patches of uniform density at least 5×5 mm. This International Standard requires measuring the changes in colour densities in minimum density area (d_{min}) and at a density 1.0 ± 0.05 above $d_{min.}$ These changes are to be monitored in neutral RGB areas, where initial red, green and blue densities are approximately equal as well as in areas selectively exposed to produce the purest possible cyan (C), magenta (M) and yellow (Y) dye scales (see recommended test target Figure 13-left). The following densities of the specimens, prepared as described, shall be measured before and after the treatment interval.[68]

This ISO describes five different light stability tests, which tend to simulate common use situations. For the purposes of this work both outdoor and indoor test have been described. Density values that are measured and life-time parameters are shared by all tests in this standard.

Simulated outdoor sunlight (xenon arc) 100 klx – CIE spectral distribution

Test unit shall be xenon high pressure arc lamp, or its equivalent, containing outer borosilicate glass filters of 1.5 and 2.5 mm thickness giving an illuminance of 100 klx (for relative spectral power distribution for outdoor daylight CIE illuminant D65 see Figure 15). Chamber temperature shall be 40 °C ± 5 °C, chamber relative humidity 40 % RH ± 5 % RH and black panel temperature 65 °C ± 5 °C.

Prints shall be backed with non-reactive and non-yellowing white material such as 100% cotton cellulose mount board or metal. In this test routine, there are two cycle steps: light (hot less-humid day) and dark step (cool humid night). It is strongly recommended to keep the change light/dark cycles accordingly, because excessive heat can potentially desiccate specimens

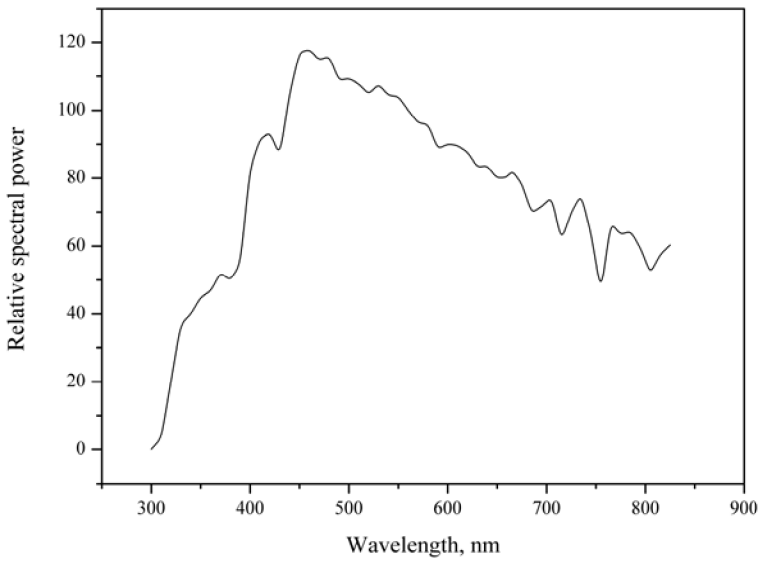

Figure 15 *Relative spectral power distribution for outdoor daylight CIE illuminant D65*[68]

High intensity filtered xenon arc D65illuminant for simulated indoor indirect daylight through window glass

For simulated indoor indirect daylight through window glass, a high-intensity filtered xenon arc ID65 illuminant is used. In this test routine, there are two cycle steps: light (hot less-humid day) and dark step (cool humid night). It is strongly recommended to keep the change light/dark cycles accordingly, because excessive heat can potentially desiccate specimens. Irradiation is to be maintained in range of 70–100 klx. The specimens shall be surrounded by air at 30 ± 5 °C maintained by an adequate airflow across the specimens. The ambient relative humidity shall be 50 RH ± 5 % RH.

Density values to be measured and parameters

The following densities of the specimens, prepared as prescribed, shall be measured before and after the treatment interval (ref. [68]):

- change in optical density of neutral patches that initially had densities 1.0 above d_{min}
- change in the red, green and blue minimum densities of specimen d_{min} (reflexion materials in dark and light stability tests have ½ d_{min} correction - for starting densities of 0.7 to 1.0
- change in the red, green and blue densities of cyan, magenta and yellow colour patches that initially had densities of 1.0 above d_{min}

Optical density of reflexive materials in time t is calculated according to equation. Correction of d_{min} is lowered by half, because of multiple internal reflexions. (Ref. [68])

$$D_{\mathrm{M}}(G) = d_{\mathrm{M}}(G)_{\mathrm{t}} - d(G)_0 \tag{9}$$

$$D_{\mathrm{N}}(B) = d_{\mathrm{N}}(B)_{\mathrm{t}} - d_{\mathrm{min}}(B)_{\mathrm{t}} + {}^{1}/_{2}\,[d_{\mathrm{min}}(B)_{\mathrm{t}} - d_{\mathrm{min}}(B)_0] \tag{10}$$

Colour balance in neutral density patch is calculated as the percent of the average density (ref. [68]):

$$d_{\mathrm{N}}(R-G)_{\mathrm{t}} = \frac{d_{\mathrm{N}}(R)_{\mathrm{t}} - d_{\mathrm{N}}(G)_{\mathrm{t}}}{0.5[d_{\mathrm{N}}(R)_{\mathrm{t}} - d_{\mathrm{N}}(G)_{\mathrm{t}}]} \times 100\% \tag{11}$$

From the measured density values, five image-life parameters can be computed. These image life parameters and illustrative end-points are listed in Table 2. The image life parameters listed are the critical characteristics that have practical significance for the visual degradation of colour images; however, the numerical end-points given are merely illustrative.[68]

Table 2 *Image life parameters for which times shall be reported*[68]

Parameters	Illustrative endpoint criteria for colour transmissive and reflection materials
Change in neutral patches of D_{N}(R), D_{N}(G) and D_{N}(B) (d_{min} corrected)	30%
Change in colour patches of D_{C}(R), D_{M}(G), and D_{Y}(M)(d_{min} corrected)	30%
Change in colour balance of neutral patch:%D_{N}(R – G), %D_{N}(R – B), %D_{N}(G – B)(not d_{min} corrected)	15%
Change in d_{min}(R), d_{min}(G) and d_{min}(B) in the d_{min} patch	0.10%
Shift in colour balance: d_{min}(R – G), d_{min}(R – B), d_{min}(G – B) in the d_{min} patch	0.06%

JEITA standard

Standard made by Standard of Japan Electronics and Information Technology Industries Association CP-3901 specifies conditions for Digital Colour Photo Print Stability Evaluation.

Specimens must have CMYK patches with starting optical densities (OD) 0.5; 1.0 and 1.5. Size of the sample is 89×127 mm and it is produced with printer.

Changes in these data are to be monitored:

- change in optical density of neutral patches d_N that initially had densities0.5 ± 10 %, 1.0 ± 10 %, 1.5 ± 10 % above d_{min}
- change in the red, green and blue minimum densities of specimen d_{min}
- change in the red, green and blue densities of cyan, magenta and yellow colour patches d_C, d_Y, d_M
- Changes in optical densities are monitored densitometricaly. Calculations of d_{min}, percentual change in OD and colour balance are made according to equations (13)–(15). Measurement goes by ISO 18909.[69]

$$\Delta d_{\min}(R)_t = d_{\min}(R)_t - d_{\min}(R)_0 \tag{12}$$

$$\Delta d_M(G)_t = \left[\frac{d_M(G)_t - d_M(G)_0}{d_M(G)_0}\right] \times 100 \tag{13}$$

$$\Delta d_N(R-G)_t = |\Delta d_N(R)_t - \Delta d_N(G)_t| \tag{14}$$

The conditions for lightfastness tests are specified thus: As a light source xenon arc is used with continual irradiance in range 300–1000 nm with window filter defined by ISO 18909 and intensity 30–100 klx. Other specifics of the testing in chamber: temperature and humidity are to be kept in ranges 20 ± 5 °C and 50 ± 5 % RH. Temperature of the black panel should not exceed 40 ± 2 °C.[69]

Table 3 *Colour image endpoints by JEITA standard*[69]

Permissible limit of reflection density change	Image change parameter
30%	Decline in red density in a neutral patch
30%	Decline in green density in a neutral patch
30%	Decline in blue density in a neutral patch
30%	Decline in red density in a single-colour patch
30%	Decline in green density in a single-colour patch
30%	Decline in blue density in a single-colour patch
15%	Colour imbalance in the differential between red density and green density in a neutral patch
15%	Colour imbalance in the differential between green density and red density in a neutral patch
15%	Colour imbalance in the differential between red density and blue density in a neutral patch
15%	Colour imbalance in the differential between blue density and red density in a neutral patch
15%	Colour imbalance in the differential between green density and blue density in a neutral patch
15%	Colour imbalance in the differential between blue density and green density in a neutral patch

Table 4 *Colour image endpoints by JEITA standard*[69]

Permissible limit of the reflection density in white patches	Image change parameter
0.06	Increase in red density or green density
0.1	Increase in blue density
0.05	Imbalance between red density and green density
0.1	Imbalance between red density and blue density
0.1	Imbalance between green density and blue density

Wilhelm Imaging Research

With the absence of ISO and industrial standards for inkjet media, the advised testing procedure set by Wilhelm imaging research (WIR) became used by the industry. During time WIR published two sets of test specifics and endpoint criteria – 3.0 and 4.0. For both sets the measuring and the test properties are similar to the ISO standard 18909 – they are densitometry based.

In the set 3.0 the initial patch densities are 0.6 and 1.0. Endpoint criteria are based on psychometrical scaling.

Set 4.0 differs from the previous just by augmenting the patch number. The CMYKRGB patch base is widened with violet and skin tone. For each of the previously mentioned colours, there are three initial densities 0.5, 1.0 and 1.5.[13]

2.5.1.3 Colorimetry-based measuring methods

Colorimetry solves the technical issue of identifying visually neutral colorant mixtures across the diverse range of modern materials.[67]

ASTM F 2366 – International Standard Practice for Determining Relative Lightfastness of Ink Jet Prints Exposed to Windows Filtered Daylight Using a Xenon Arc Light Apparatus

This standard practice covers specific procedures that are applicable for xenon arc exposure of inkjet media prints. The accelerated laboratory procedure is intended to determine the relative lightfastness of inkjet prints in office environment, where window filtered daylight is used for illumination. Printed inkjet media are exposed to radiant energy from a xenon arc source equipped with a window-glass filter. The duration of the exposure may vary widely depending on the light fastness of the ink/media.

It is recommended to maintain the irradiance level of 0.35 $W \cdot m^{-2} \cdot nm^{-1}$ at 340 nm. Immediately before and after exposure the specimens shall be measured on a spectrophotometer, spectrocolorimeter or colorimeter using CIE1964 supplementary standard observer and standard illuminant D65. The change in exposed specimens is evaluated instrumentally using CIE 1976 $L^*a^*b^*$ and ΔE^*_{ab} is calculated. Also percent of retained optical density is calculated.[70]

WIR I* Retained Image Appearance metric 1.0

WIR retained image appearance is a tool for calculation of colour change. I^* consists of two parts I^*_{colour} and I^*_{BW}. I^*_{colour} metric incorporates chroma changes, hue changes and changes in grey sector picture elements.

Factor w presents the ratio between colour and B&W information. I^*_{colour} approaches zero as chroma, C^*, is lost.[67]

The hue is in $L^*a^*b^*$ defined by ratio of a^* and b^*. The $L^*a^*b^*$ space is divided into six equal pieces – yellow, red, magenta, blue, cyan, green – and grey. I^*_{colour} covers change in the hue, saturation and shifts in grey area.[67]

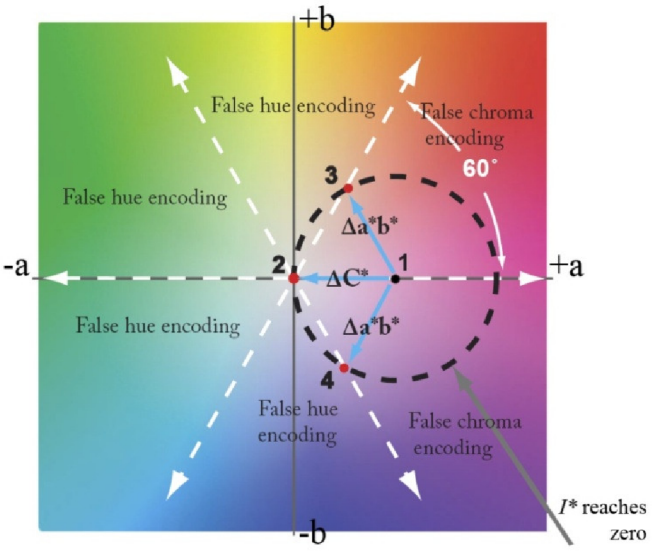

Figure 16 *I* presentation in L*a*b colour space cut.*[67]

$$I^* = \frac{I^*_{colour} + (I^*_{B\&W} + w)}{1 + w} \quad (15)$$

Function $I^*_{B\&W}$ is directly dependent on contrast. In context, this method can be considered complex, but the endpoint criteria determining the tolerable change have not been published.[67]

ICC profiles and gamut volumes

Utilizing ICC profiles and the associated colour gamuts give a measure of the entire colour space in the permanence evaluation. Results presented by Chovancova et. al. provide general framework for accessing image permanence.[71,67] The gamut is usually specified in a colorimetric or visually based space such as CIE *XYZ* or *L*a*b**.

VolGa

Using colorimetry includes also Colour management system (CMS) and gamut volume. Gamut volume is a subset of colours that certain device is capable of reproducing. During ageing, gamut changes, its volume usually decreases.

Relative gamut volume changes plotted as a function of exposure dose can be conveniently used to determine the fading rate and corresponding lifetime. However, with use of commercial software, it is not clear how the gamut volume is calculated.

Calculating the gamut volume is a challenge on its own, as gamuts might not be necessarily convex bodies. This problem can be overcome by a non-linear "convexing transformation "of the measured data points. A set of isolated points in three-dimensional space does not define a unique body in any obvious way. The convex hull of the set is a well-defined notion (resembling the gamut), however, it may over-estimate the gamut substantially (see Figure 17). The use of the convex hull might be satisfactory for device comparison, but is certainly not sufficient for print fading monitoring. Dzik et. al. developed a method for estimating the volume of the gamut by identifying its "vertices", approximating it by a generally non-convex polyhedron and calculating the volume of the polyhedron.[72]

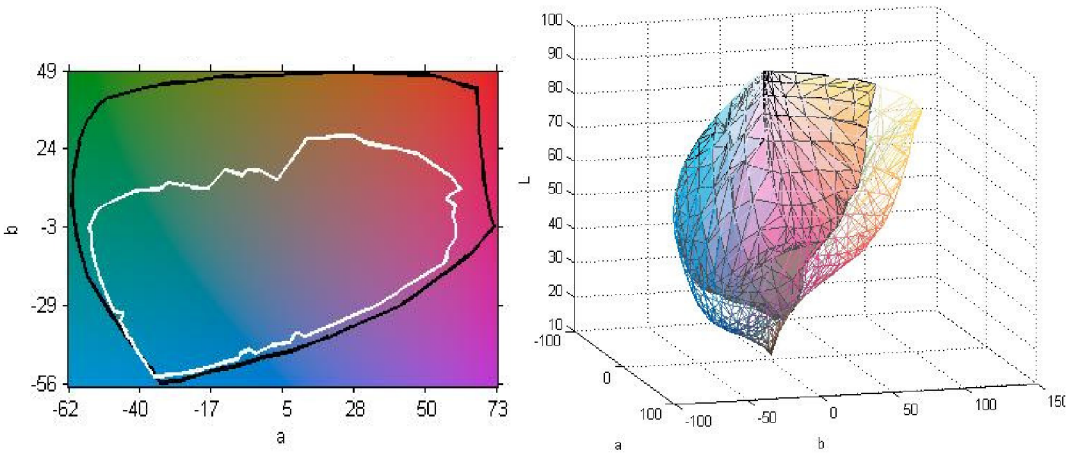

Figure 17 *Most gamuts of real printers are not convex. The departure from convexity may further be enhanced during print fading. Screenshots from Volga software illustrate this behaviour on sample made on Foma paper with MIS Dye ink set. Left – gamut volume 2D cross section at L=50, where black line is gamut volume before ageing and white line is gamut volume after 2-year indoor display; Right-same gamut volumes but in 3D visualization. Wired surface belongs to original volume and the full one to gamut after ageing.*[72]

I* retained image appearance

Wilhelm et. al. did provide a concept of *I** lightfastness evaluation colorimetry-based full tonal scale "retained image appearance" metric. However no further specification or theory testing has been provided.[64]

2.5.2 Airborne pollutants – Gasfading tests

Barrier properties of protective films are very important. There are a number of international standards, which are dealing with this matter. Standards used in this work are mentioned below.

2.5.2.1 ISO 18941 – prints sensitivity to ozone

The standard method for testing prints sensitivity to ozone ISO 18941, describes the equipment, methods and procedures for generating a known ozone exposure and the subsequent measurement and quantification of the amount of change produced within both digitally printed hardcopy images and traditional analogue photographic colour print images due to that exposure.[73]

A minimum of two duplicate specimens before testing shall be placed in dark in controlled conditions (23 ± 2 °C, 50 ± 10 % RH) in ozone free environment (≤ 2 nl/l over 24 hours).

The colorimetry values of the specimens *L**, *a**, *b**, and Status A densities shall be measured before and after treatment interval. Colour balance by colorimetry in the d_{min} patches is calculated according to the equation (9).

Ozone can be generated e.g. by UV lamp or corona discharge unit. Air used for ozone generation shall be firstly purified, pollutants are likely to influence the generation of ozone. It is known, that corona discharge units can generate pollutants, such as nitrogen oxides.

Tests shall be carried out at ozone concentration equal to 1.0 µl/l with an operational uniformity of ± 0.1 µl/l. if other concentrations of ozone than 1.0 µl/l are used, the operational uniformity shall be ± 10 %. If the ozone concentration is higher, the reciprocity tests are recommended. The preferred air temperature and relative humidity is 23 ± 2° C and 50 %, but other are accepted as well if they reflect the product use conditions.

This test method does not contain endpoint criteria and therefore the measurement results shall not be used independently to predict any aspect of print image life. The results are reported as cumulative, i.e. ozone concentrations is given in microliters per litre and the exposure time in hours – [(µl/l) h].[73]

2.5.2.2 JEITA CP-3901

This standard described method for testing the indoor ozone stability of digital colour photo prints produced by household printers that re not under glass frame.[69]

Test conditions

Test chamber is a sealed apparatus that is from a material that isn't easily corroded by ozone. Air used for ozone generation is first passed through an activated carbon filter for purification and ozone is generated by silent electric discharge or ultraviolet lamp, provided the amount and purity of ozone are met.

The ozone concentration is measured within test chamber should be measured either electrochemically or by ultraviolet absorption spectrometry (ISO 13964). Also the gas flow should be controlled so, that the concentration of ozone inside the chamber has no non-uniformities.

Specimens shall be placed parallel to the gas flow. And temperature shall be 23 ± 2°C and the relative humidity 50 ±5% RH. Ozone concentration inside chamber shall be 1–5 ppm ± 10%.[69]

Density values to be measured and predicted print life

In chapter 2.5.1.2 are in subsection JEITA standard specified density measurements ad endpoint criteria. Predicted print life for ozone stability is calculated in years according to eq. (16). Integral ozone concentration is product of the set ozone concentration and time.[69]

$$\text{indoor ozone stability(years)} = \frac{\text{integral concentration (ppm·h)}}{40\text{(ppm·h/year)}} \tag{16}$$

2.5.2.3 ISO 18946:2011 – Imaging materials – Reflection colour photographic prints –Method for testing humidity fastness

ISO 18946:2011 describes test methods for evaluating reflection colour photographic prints with regard to changes in image appearance resulting from exposure to both low and high relative humidity.

The observed changes relate to colour, tone and loss of sharpness caused by horizontal and vertical diffusion of colorants from exposure to elevated humidity levels. Other humidity-related factors are outside the scope of this test method.

The method and procedures described in ISO 18946:2012 are particularly appropriate to systems where the colorants are applied by a mechanism involving the diffusion of colorant into image-receiving layers and to certain types of inkjet media that are susceptible to D_{min} yellowing.[74]

2.5.2.4 ČSN 77 0332 – Determination of transmission of water vapour trough thin areal films

This method is designated for testing thin areal materials like paper, carton, plastic foils, metal foils and their combinations. The maximum thickness of the material for this standard to be applicable is 3 mm.

The number of samples for one experiment is 5 to 10 and their dimension correspond to the size of the measuring cup, but should have area between 25–50 cm^2 with 0.5 % accuracy. Thickness of samples is measured with precision on 0.01 mm three times.

The test is performed in air conditioned chamber between 20–40 °C at 65–90 % RH with air flow 0.5–2.5 metres per second. The test device should be from solid, vapour impermeable and light material e.g. aerospace aluminium (Figure 18).

Figure 18 *Water vapour permeable cup*[75]

Siccative should be either silica gel with grain size1.5–5 mm or anhydrous calcium chloride with grain size 1.6–4 mm. The siccative amount is 25 g, its layer height is 1–2 cm and the minimal siccative distance from sample is 3–4 mm. The amount of absorbed water vapour is determined gravimetrically by subtracting the weight before the test from the weight after the test. The difference is the amount of absorbed water vapour in siccative. There are four test regimes A, B, C and D. Their specification is described in Table 5 and Table 6.[76]

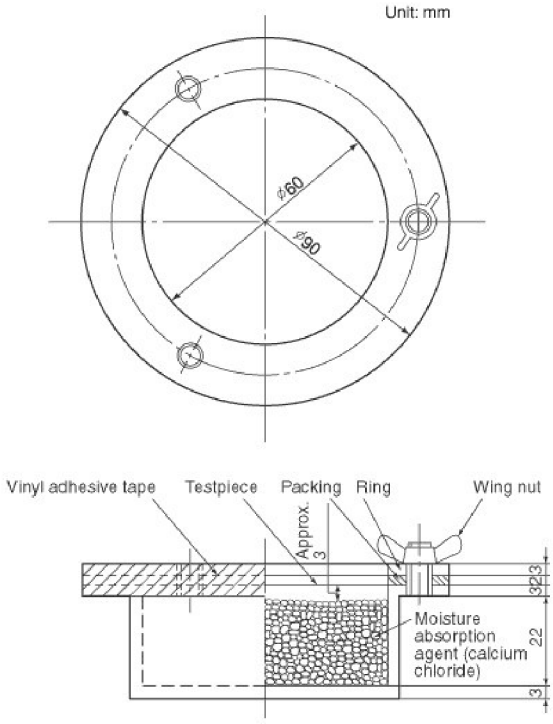

Figure 19 *Water vapour permeable cup–scheme*[76]

Table 5 *Specification of test regimes*[76]

Regime type	Regime parameter	
	Air temperature, °C	Relative humidity, %
A	25 ± 0.5	90 ± 2
B	38 ± 0.5	90 ± 2
C	25 ± 0.5	75 ± 2
D	20 ± 0.5	65 ± 2

Table 6 *Saline solution recommended for use in test regimes*[76]

Regime type	Saturated saline solution
A	$Na_2C_4H_4O_6 \cdot 2H_2O$
B	KNO_3 or $Na_2C_4H_4O_6 \cdot 2H_2O$
C	NaCl
D	KCl

2.5.2.5 DIN 53380-3–Determining the gas transmission rate of plastic film, sheeting and mouldings by the carrier gas method

This industrial standard is focused on determining the oxygen transfer trough plastic films. The diffusion cell has two inlets and two outlets and the middle 5 mm rim is sealed with vacuum grease, to prevent any leakage (Figure 20). Total internal volume of the halves is 25 and 50 cm^3. Each diffusion chamber half is equipped with separate thermometer. If the test is carried out in temperature range 20–50 °C, there is need of liquid or blanket thermostat. Otherwise, test chamber is placed in temperature-controlled cabinet/room.

Each of the cells half is filled with different gas, but both gasses are CO_2 free:
- N_2–dry nitrogen containing maximum 0.5–3 % H_2 and less than 0.01 % O_2
- O_2–oxygen must be at least 99.5 % pure

Oxygen sensitive coulometric sensor is with Ni, Cd and graphite electrodes saturated with NaOH solution. During long exposures, there is a risk of sensor dry out. As a humectant, serves saturated salt solution, which produces 12, 33, 53, 75, 85 and 93 % relative humidity.

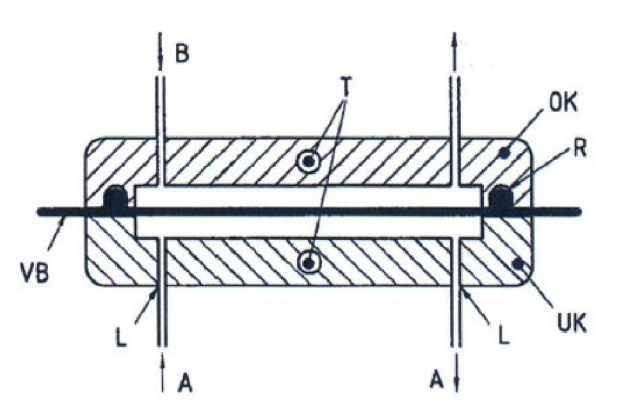

Figure 20 *Test chamber scheme for oxygen transmission; B-oxygen or carrier gas inlet; t-thermometer wells; OK-upper half of diffusion cell; R-O-rim; VB-specimen; L-metal tubes; UK-lower half of diffusion cell; A-inlet/outlet of carrier gas*

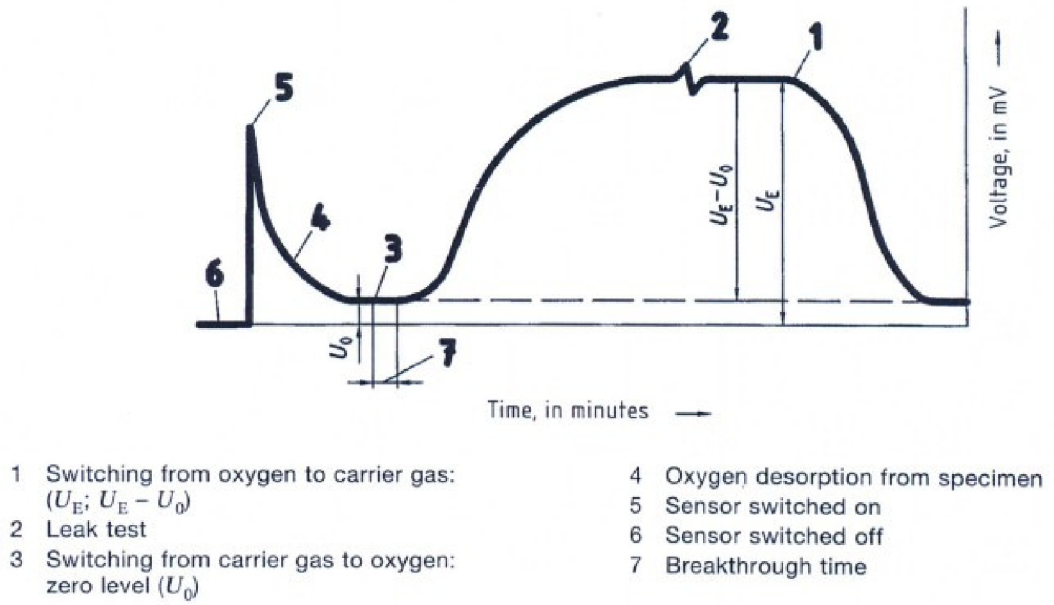

Figure 21 *Progress of the measurement*[77]

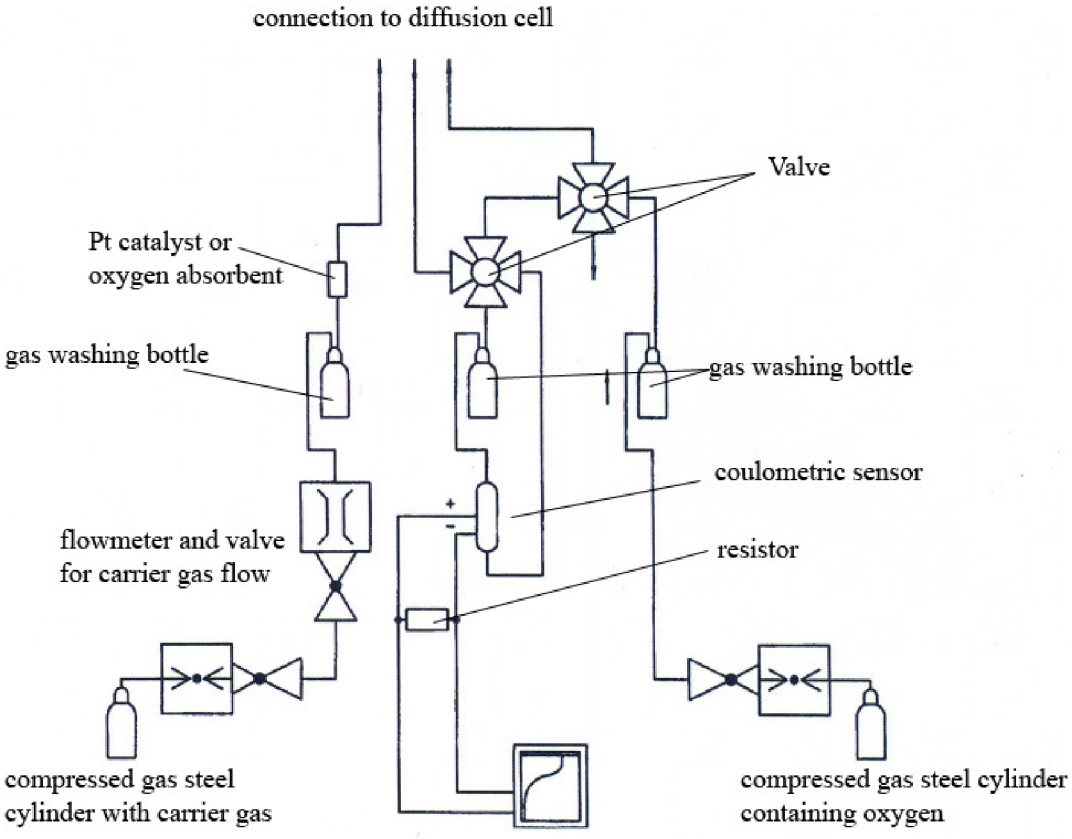

Figure 22 *Reactor scheme*[77]

Residual oxygen from the diffusion cell inner surface and sample is removed by Pt/Pd catalyst on aluminium tube. Amount of transmissed oxygen is expressed in $cm^3/(m^2 day\ bar)$ and calculated from Equation (16).

$$q_A = \frac{(U_E - U_0)\cdot Q_A \cdot 100}{A \cdot R \cdot \rho_{O_2} \cdot P_{amb}} \quad (17)$$

Where U_E is steady state voltage (mV), U_0 is zero level voltage (mV), A is test area of the specimen (cm^2), Q_A is the calibration constant ((cm^3 cm^2 Ω)/(m^2 day mV)), R is resistance of the resistor (Ω), P_{amb} is the atmospheric pressure (bar), ϱ_{O_2} is the volume percentage of oxygen in the test gas.[77]

2.5.3 Bunsen-Roscoe Reciprocity law, lifetime estimation

Methods, which count the rate at which the photons arrive, obey photochemistry law, namely Bunsen-Roscoe Reciprocity Law, in which the response is proportional to the quantity of photoproduct, irrespective of whether that quantity is produced by brief pulses of high photon irradiance, or longer periods of low photon irradiance.[78] The definition of the law is: One quantum of light is absorbed per molecule of absorbing and reacting substance that disappears.[79]

However, exception to this rule is high intensity accelerated lightfastness tests. At very high intensities the reciprocity failure occurs, because the incident number of energy quanta overcomes absorption maximum of the material and remaining energy dissipates as thermic energy.[4]

Wilhelm et. al. conducted a lightfastness test with two different illumination levels–35 klx for 9.5 days and 0.6 klx for 550 days. At lower irradiation intensity the endpoint criteria are met 1.4 times sooner that predicated by the high-intensity test.[80]

Almost all manufactures do their lightfastness calculations with "standard" day illumination – 450 lux/12 h/day or 500 lux/10 h/day. According to Wilhelm et. al. the only exception is Eastman Kodak comp., which considers a 120 lux/12 h as a "standard" day illumination. This presumption enhances the lifetime of their product by 3.75 times more compared to the other manufacturers.[81] Epson in their paper extends the use of "Kodak" conditions (120 lux/12 h/day) to one more user – Agfa Photo.[82]

The issue of reciprocity behaviour if inkjet prints in ozone atmosphere has been studied and the results of real-time test and accelerated test with higher O_3 concentration have been compared. And there are opinions approving that reciprocity law is not contravened when it comes to ozone induced fading of inkjet prints.[83,84] But there are cases, where with certain combinations of inks and receiving layers reciprocity law is contravened, exist.[85,86]

2.6 Optical surface characterisation

Spectroscopy is a domain focused on measurement and evaluation of electromagnetic radiation emitted by matter or matter interaction or characteristics of products made by this interaction. Majority of spectral methods (except for luminescence methods) are based on radiation absorption. In case of radiation transition through a layer of homogeneous absorbing system, the absorption is quantified usually by absorbance or transmittance.[87]

2.6.1 Infrared spectroscopy

Infrared spectrometry deals with measuring and evaluation of absorption spectra of matter in wavelength range 800 nm to 1000 µm, i.e. wavenumbers 12 500 $cm^{-1}$to 10 cm^{-1}. Nowadays, most important analytical technique can be used to identify molecules, confirm new compounds, investigation in chemical balance, chemical reaction kinetics and many others.

In normal conditions in every molecule, atoms vibrate. Molecule parts vibrate and create the vibrational state of the molecule, which can change after radiation is absorbed. Differences between individual vibrational and rotational states are very small and for absorption to occur, nothing more than simply a radiation with small energy and long wavelength is needed.

When infrared radiation reacts with matter, some part with certain frequencies is absorbed and the rest of the frequencies are transmitted. The absorbed IR radiation causes the change in vibrational-rotational states.[87]

IR radiation can be divided into IR-A (near IR) 780–1400 nm, IR-B (short wavelength IR) 1400–3000 nm and IR-C 3000 nm^{-1} mm.[88] These stated limits are conventional and are connected to construction possibilities of measuring devices.

Low energy radiation in far IR causes change in rotational molecule states. IR-A and IR-B affect vibrational-rotational transitions and also vibrational and rotational state of the molecule changes. When evaluating IR spectra it is important to observe the shape, location and number of absorption bands as well as their intensity.[87]

2.6.1.1 Attenuated total reflectance method

Attenuated total reflectance (ATR) principle of this method is shown on Figure 23. ATR spectroscopy is using the effect of total inner reflection. If the incident coherent ray of light falls on the interface, firstly coming through the phase with higher refraction index and if the incident angle is bigger than the critical angle, the total reflection occurs.

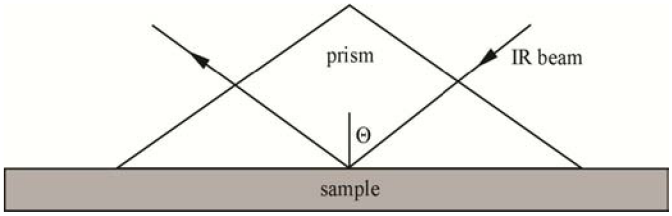

Figure 23 *Total reflection*

Sample is placed on the base surface. Part of the infrared radiation goes in the sample into depth of several μm, where are absorbed wavenumbers that correspond to the frequencies of the molecule vibration. The depth of the penetration d_p depends on the index of prism refraction, incidence angle and wavelength of radiation (See Eq. 18).

$$d_p = \frac{\left(\frac{\lambda}{n_1}\right)}{2\pi\left[sin\Theta - \left(^{n_1}/_{n_2}\right)^2\right]} \tag{18}$$

Preceding equation describes the depth of the beam penetration n_1 is sample refraction index and n_2 is ATR prism refraction index. After attenuated reflected radiation is analysed, absorption spectra, similar to the classic IR spectra, is obtained. The difference is in the obtained band intensities, because the penetration of infrared radiation into the sample is dependent on radiation wavelength.[87]

2.6.1.2 IR spectra interpretation

In basic terms, infrared spectrum is formed as a consequence of the absorption of electromagnetic radiation at frequencies that correlate to the vibration of specific set of chemical bonds from within a molecule.[89]

IR spectra contain an amount of absorption bands, which correspond to certain bonds and atom groups and are useful for compound characterisation and identification. As stated, vibrational frequency and wavenumber absorbed by the molecule is given by the atom type, bond type and molecule geometry. By analysing the IR spectra it is possible to specify the presence of functional groups in molecule, as well as identify unknown compounds. Unknown compound can be identified by comparing the spectra to series of other reference spectra of known compounds. If a perfect match is found, with any of the reference spectra, it is possible to attribute this reference structure to a structure of unknown compound.

For IR spectroscopy were created many correlation charts and diagrams. When interpreting spectra, one needs to be aware of that not all bands in spectra can be easily assigned to vibration of certain

band or part of molecule. Among factors that complicate the identification are overtones, combination bands, hydrogen bonds and Fermi resonance.[87]

The infrared spectrum can be fundamentally divided into two parts.[87]

1. Characteristic group vibration region – 4000–1500 cm^{-1}; on these is based the structural compound diagnostics.
2. "Fingerprint" region – 1500–600 cm^{-1}; this region is usually used for whole molecule structure.

2.6.1.3 Alkanes

Alkanes contain C–H and C–C bonds. Bands for valence saturated hydrocarbons vibrations C–H are found in region under 3000 cm^{-1}, opposed to the aromatics that absorb over 3000 cm^{-1}. Symmetrical and asymmetrical stretching of CH_3, CH_2 and CH groups is found in range 2880 and 2960 cm^{-1} region. Absorption bands of these groups in fingerprint region for valence vibrations are very weak and have very small diagnostic value. Planar deformation vibrations of C–H can be found in region 1340 and 1470 cm^{-1}.[87]

2.6.1.4 Alcohols

The most important bands of alcohols and phenols result from valence vibrations of –OH groups. Except these bands thee are also bands of valence vibrations of groups C–O and deformation vibration bands C–O–H. Band wavenumbers ν(OH) of alcohols are influenced by substituent character, spherical effect and mainly hydrogen bonds. Wavenumbers of bands ν(OH) connected in hydrogen bond are always lower than bands wavenumbers of free –OH groups. In spectrum they are observed in quite broad range 2500 to 3700 cm^{-1} in dependence on hydrogen bond type.[87]

2.6.1.5 Carbonyl compounds

Wavenumbers of bands ν(C=O) in various carbonyl compounds, e.g. ketones, aldehydes, carboxyl acids, esters, lactones etc. are located in the 1620 to 1870 cm^{-1} region. Presence of C=O band in organic molecule is easy to recognize, because bands ν(C=O) are very intense and their wavenumber is quite stable. But when are the wavenumbers shifted the identification is made more difficult, e.g. by electron donor substituents bonded to carbonyl groups to region in which other groups absorb (C=C and C=N). The wavenumber and band intensity ν(C=O) is influenced by form, electron effects of substituents bonded directly to carbonyl group, conjugation, ring tension and hydrogen bonds.[87]

2.6.1.6 Esters

On ester spectra are observed two characteristic absorption bands ν(C=O), saturated esters in region 1735 to 1750 cm^{-1} and unsaturated esters 1715 to1730 cm^{-1} and bands of valence vibration of groups C–O. Wavenumbers of bands ν(C–O) in esters are in region 1100 to 1300 cm^{-1}.[87]

2.6.2 Raman spectroscopy

The way in which radiation is employed in infrared and Raman spectroscopy is different. In infrared spectroscopy, infrared energy covering a range of frequencies is directed onto the sample. Absorption occurs where the frequency of the incident radiation matches that of a vibrations of that the molecule is promoted to a vibrational excited state. The loss of this frequency of radiation from the beam after it passes through the sample is then detected. In contrast, Raman spectroscopy uses a single frequency of radiation to irradiate the sample and it is the radiation scattered from the molecule, one vibrational unit of energy different from the incident beam, which is detected. Raman scattering doesn't require matching of the incident radiation to the energy difference between the ground and excited states.

In Raman scattering, the light interacts with the molecule and distorts (polarizes) the cloud of electrons around the nuclei to form a short-lived state called a 'virtual state'. This state is not stable and the photon is quickly re-radiated.

If only electron cloud distortion is involved in scattering, the photons will be scattered with very small frequency changes. This scattering process is elastic and is the dominant process. For molecules it is called Rayleigh scattering. However, if nuclear motion is induced during the scattering process, energy will be transferred either from the incident photon to the molecule or from the molecule to the scattered photon. In these cases the process is inelastic and the energy of the scattered photon is different from that of the incident photon by one vibrational unit. This is Raman scattering. It is fundamentally a weak process in that only one in every 106–108 photons which scatter is Raman scattered.

At room temperature, most molecules are present in the lowest energy vibrational level. Since the virtual states are not real states of the molecule but are created when the laser interacts with the electrons and causes polarization, the energy of these states is determined by the frequency of the light source used. The Rayleigh process will be the most intense process since most photons scatter this way. It does not involve any energy change and consequently the light return s to the same energy state. The Raman scattering process from the ground vibrational state leads to absorption of energy by the molecule and its promotion to a higher energy excited vibrational state (n). This is called Stokes scattering.

Compared to Stokes scattering, anti-Stokes scattering will be weak and will become weaker as the frequency of the vibration increases, due to decreased population of the excited vibrational states. Usually, Raman scattering is recorded only on the low-energy side to give Stokes scattering but occasionally anti-Stokes scattering is preferred.

Strictly speaking, Raman scattering should be expressed as a shift in energy from that of the exciting radiation and should be referred to as Δcm^{1} but it is often expressed simply as cm^{1}.

The intensities of the bands in the Raman spectrum are dependent on the nature of the vibration being studied and on instrumentation and sampling factors. Sampling has a large effect on the absolute intensities; bandwidths observed and band positions.[90]

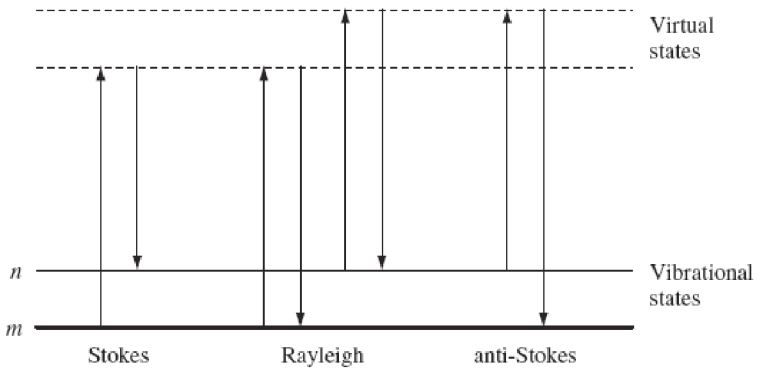

Figure 24 *Stokes anti-Stokes and Rayleigh scattering*[90]

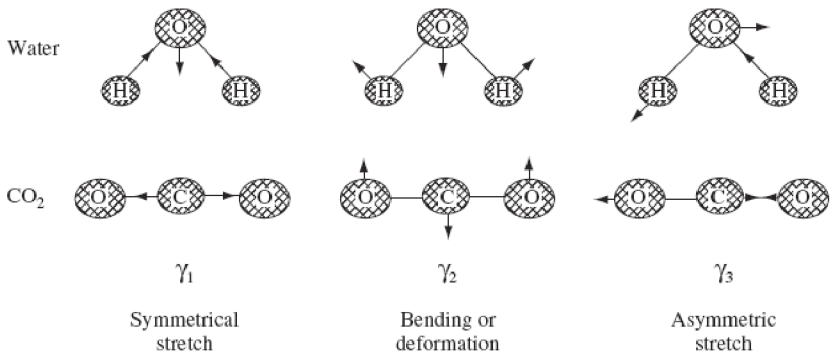

Figure 25 *Three modes of vibration for non-planar molecule H_2O and planar molecule CO_2.*[90]

2.6.2.1 An Approach to Interpretation of Raman spectra

It is possible to give energy ranges in which the characteristic frequencies of the most common groups which are strong in either infrared or Raman scattering can occur. The relative intensities of specific peaks help to confirm that the correct vibration has been picked out.[90]

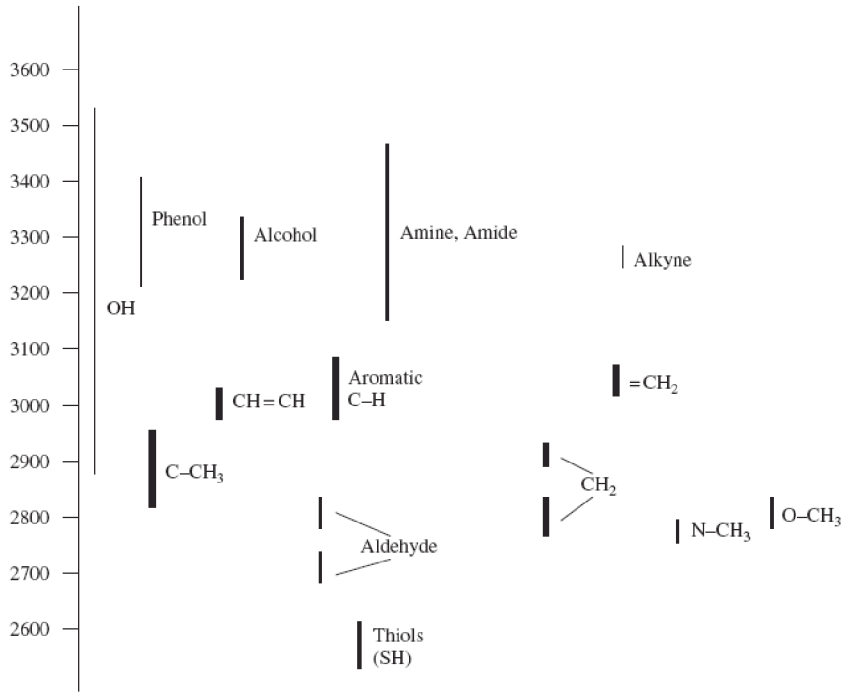

Figure 26 *Single and group vibration frequencies and possible peak intensities commonly identified in Raman scattering.*[90]

2.6.3 Spectroscopy in ultraviolet and visible

Currently is UV-VIS absorption spectral analysis one of the most used methods for its quick experimental unpretentiousness, precision and sensitivity.[87]

Molecular UV-VIS absorption spectrometry deals with measurement and interpretation of electron molecular matter spectra, which absorb electromagnetic radiation in range 200 to 800 nm. Substances that absorb only radiation with wavelength smaller than 380 nm (UV part of the spectra) seem colourless. Substances that absorb radiation from "white" sunlight in range 380 to 770 nm seem as chromatic, coloured.[87]

UV-VIS spectrometry is used for study of compound colour, which is given by the wavelength of VIS light, which is not absorbed. Review of absorptions and colour of matter is in Table 7.

Table 7 *Regions of certain radiation energies, characterised by wavelength and corresponding compound colour*[87]

Absorption region	*Colour of absorbed radiation*	*Compound colour (complementary colour)*
400–435	violet	greenish-yellow
435–480	blue	yellow
480–490	green-blue	orange
490–500	blue-green	red-orange
500–560	green	magenta
560–580	greenish-yellow	violet
580–595	yellow	blue
595–610	red-orange	blue-green
610–760	red	cyan

Visible light can go through matter, it can be completely reflected (white) and can be absorbed by the matter completely (black). If only some wavelengths are absorbed or particular wavelengths are absorbed unevenly, the matter seems as coloured. So, human eye or detector can detect the complementary wavelengths that have not been absorbed.

By absorbing radiation photons from UV or visible part of spectra an electron configuration is changed, resp. electron spin and molecule are transitioning to excited state. Persistence in this state is very short (in order of 10^{-15} s) and it goes through various radiant and non-radiant transitions back to the ground state. This keeps absorption system in balance. Absorption transitions can be in progress from various vibrational and rotational ground states of molecule to various vibrational and rotational excited states. Because energetic transitions between energetic states in molecule (ΔE_e~150 to 600 kJ·mol^{-1}) are much more demanding than vibration state transitions (ΔE_v~2 to 60 kJ·mol^{-1}) and rotational ones (ΔE_r~3 kJ·mol^{-1}), the total radiation absorption with enough energy for electrons transitions can mean at once excitation in vibrational and rotation levels of molecule. The final spectrum is in bands, because particular transitions merge together.[87]

2.7 Surface Characterisation

2.7.1 Profilometry

Profilometry is a measuring technique where topography of the surface is scanned to determine roughness. There are optical and contact measuring methods. Only contact profilometry is described, because it was used.

2.7.1.1 Contact profilometry

Tactile profilometers are pointwise contact measuring instruments used to sequentially acquire a 2D and 3D topography of a small surface (1–50 mm). During the measurement a stylus (with submicrometer accuracy) is brought vertically in contact with a sample using a specified contact force. It is then moved laterally across the sample for a specified distance. Small surface variations are detected as vertical stylus displacements (10 nm to 1 mm) during the scanning process. The coordinates of the sample points are referenced against an intrinsic coordinate system, which is supplied by the machine after a calibration process. The aim is to measure the shape as well as the roughness.[91,92,93]

2.7.2 Gloss measurement

Gloss provides printed products with better overall look. It is basically, a visual impression resulting from light reflected from a surface.[3,94]Sensing of the gloss depends heavily on the response of the human eye and the gloss sensation on surface roughness, texture and spectroscopic properties of the object.[95]

The intensity is dependent on the material and the angle of illumination. In case of non-metals (coatings) the amount of reflected light increases with the increase of the illumination angle. The remaining illuminated light penetrates the material and is absorbed or diffusely scattered dependent on the colour.[94]

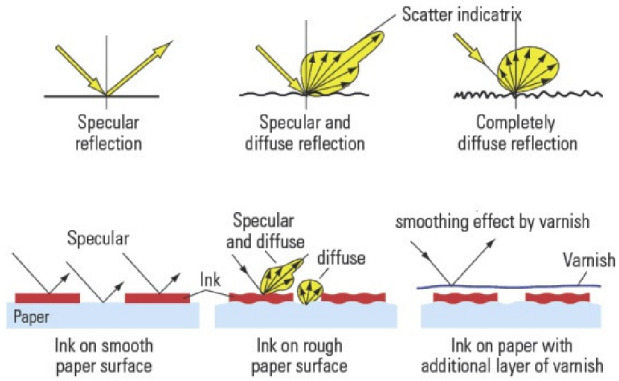

Figure 27 *Reflection properties of different surfaces in printing. Front row: scatter indicatrix on various rough surfaces; second row: scatter behaviour of printed papers: smooth and rough papers and varnished image.*[3]

Glossmeters

A glossmeter measures the specular reflection (the angle of incidence equals the angle of reflection). Specularly reflected light is collected by another lens to a photo detector.[94]

The measurement of gloss is standardized in ASTM and ISO standards. In the standard is described a standard reference surface as a highly polished black coloured glass that has refractive index of 1.567, and it should give 100 specular gloss units (GU) at all angles of incidence. Glossmeters typically make use of the 20, 45, 60, 75 or 85°angle of light incidence. The measurement results of a glossmeter are related to the amount of reflected light from a black glass standard with a defined refractive index, and not to the amount of incident light. Materials can have a GU count higher than 100 (e.g. films). Low angle of incidence is used for shiny and high for dull surfaces, respectively.[95] When gloss is measured on porous media bulk scattering has to be taken into account.[94]

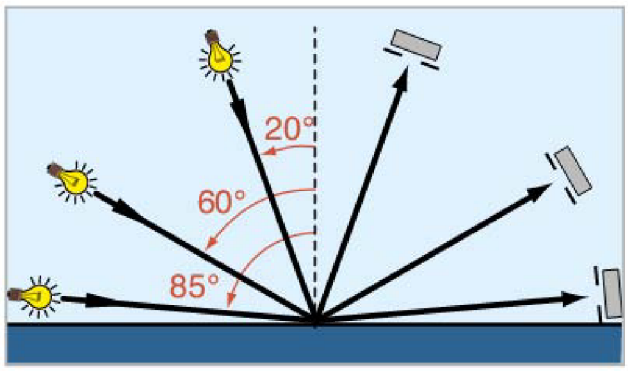

Figure 28 *Typical measurement geometry of conventional glossmeter.*[94]

2.8 Varnishes

During time, there have been different opinions on varnishes and their influence on colour photographs (mainly they varied with varnish composition). Producers proclaimed that their marketed UV varnishes would prolong the lifetime of colour prints from six to eight times, but the results were naught.[96] Varnishes should not be applied on colour photographs without full knowledge of how they behave over time.[97]

If varnishes are applied on print, they have two important properties. The first is protective function. Layer of varnish shields the prints from mechanic staining, e.g. humidity, grease, impurities, etc. The second is augmenting the optical qualities of the print. If the surface of the print is smoothened by colourless transparent layer of varnish, reflective surface properties change, usually

they are enhanced. Visually the observer perceives this change in properties as augmentation of saturation, sharpness and hue range.

2.8.1 Methods for varnish application

There are two methods for applying varnish on the paper sheet:

- Off-line varnishing – paper sheets are printed on and then stacked. Pile is delivered into the varnishing machine, where are the prints coated. By this method, the producer is able to create thicker layer of the varnish. The disadvantages of this method are possible damage of the images and low productivity.[98,49]
- In-line varnishing – in one go-trough the printing machine the paper is printed and varnished at one time. With this technology, it is hard to produce thicker varnish layers, because of stickiness of the printed ink.[98,49]

Varnish and ink interaction is in these two cases different.

2.8.2 Basic principles for varnishing

If on the surface of the print should be created a smooth optically perfect even varnish layer, few physical premises have to be met (ref.[49]):

- Surface tension of the varnish has to be lower than the surface tension of the printed surface, so the varnish spreads well and wets the surface well. The best difference of the values is by 10 $mN \cdot m^{-1}$.
- To obtain a smooth surface, if the surface is uneven, the varnish layer must be that thick to cover the defects.
- Adhesion of the liquid and cured varnish to the printed substrate must be higher than varnish cohesion to prevent the varnish from exfoliating.
- Flexibility of the varnish layer must be adapted to the substrate to prevent cracking.
- When the varnish is dried and cured it lowers its volume. The volume difference is dependent on the amount of dry mass and the drying process.

2.8.3 Varnish types

Mostly the only difference between an ink and a varnish is the presence of a suspended pigment in the former, the composition of the liquid phase is the same in both instances, for a given printing and drying process.

According to the material composition, the varnishes can be divided to:

- solvent based
- oily
- dispersive
- reactive (binary)
- UV varnishes

Only solvent based varnishes are described into further detail, since they are used in this work. ***Solvent based*** varnishes consist of film-forming material dissolved in volatile solvent. According to the solvent or film-forming substance, they are divided to alcoholic and nitrocellulose. They are applied in special machines and dried by solvent evaporation.[49,50]

As film-forming resins, which are insoluble in water but soluble in organic solvents are: natural resins or synthetic film forming polymers such as cellulose ester, polyvinyl acetate, polyvinyl chloride, polystyrene, cellulose ether, formaldehyde condensation resins and other resins.

Nitrocellulose lacquers and various natural resins have the disadvantage that they show yellowing to a greater or lesser degree under the action of heat and light, and this is particularly undesirable in connection with photographic colour pictures. Polystyrene, polyvinyl acetate, cellulose acetate and similar raw materials have an unsatisfactory adhesion with the layers containing gelatine, so that after

the coating has dried completely, it is easily detached when the layers are touched or under mechanical stress. This detachment can be prevented by an intermediate layer, but it is an additional working step. Ternary copolymers, which compose of vinyl chloride, vinyl acetate and unsaturated aliphatic dicarboxylic acid or anhydride (e.g. maleic acid) or vinyl alcohol units, are excellent binding agents for protective layers.

Additives such as UV absorption agents and matting agents can be introduced in sufficient quantity (up to 50 %) into lacquers without deleteriously modifying the bonding or the layer elasticity.[49,99]

2.9 Light Stabilizers

Photodegradation is degradation of a photodegradable molecule caused by the absorption of photons, particularly those wavelengths found in sunlight, such as infrared radiation, visible light, and ultraviolet light. However, other forms of electromagnetic radiation can cause photo-degradation. Photodegradation includes photodissociation, the breakup of molecules into smaller pieces by photons. It also includes the change of a molecule's shape to make it irreversibly altered, and the addition of other atoms or molecules. A common photo degradation reaction is oxidation.[100]

To ensure that certain objects made from natural or synthetic polymers keep their properties, there are additives needed (ref.[101]):

– UV screens, UV absorbers: deactivate excited states of molecules and inhibits creation of free radicals
– free radicals elimination and hydroxyperoxides decomposition by which is inhibited propagation of chain oxidization – hindered amines – HALS

Coatings, like all organic substances, are submitted to photoageing during their life time. To enhance the durability, stabilizer additives such as UVAs and/or HALS or combinations of them are added to the coatings formulation. The light stabilizers must be effective over a long period of time and must therefore not degrade, volatilize from the matrix, be leached out by solvents or be removed in any other way from the material. Furthermore, the additive must be evenly distributed, which requires that it is compatible with the composition.[102,103]

By the industry is often adopted the optimum combination of competitive UV absorption by UV absorbers in the wavelength range 290–350 nm and trapping of the radicals formed during polymer degradation by radical scavengers.[104]

2.9.1 UV absorbers

When used, many coatings are gradually degraded and destroyed the simultaneous influence of light, oxygen, moisture and often air pollution. To prevent changes in the coating, they are protected by light stabilizers from the consequences of the action of harmful UV light.[105]

UV absorbers have are compounds that are added as coatings to polymeric products. The UV absorbers (or light stabilizers) filter off the radiation via an internal conversion mechanism and return to the ground electronic state on a sub–picosecond time scale. UV absorbers, prevent photo-degradation by competitive UV light absorption.

Three types of UV absorbers, benzophenone, benzotriazole or triazine, are mainly used today as UV absorbers (ref. [106,105]):

– 2-hydroxybenzophenones

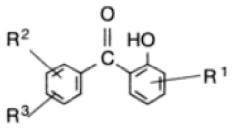

– 2-hydroxyphenylbenzotriazoles

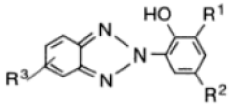

– 2-hydroxyphenyltriazines

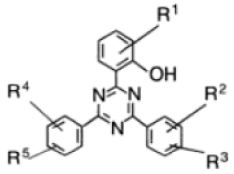

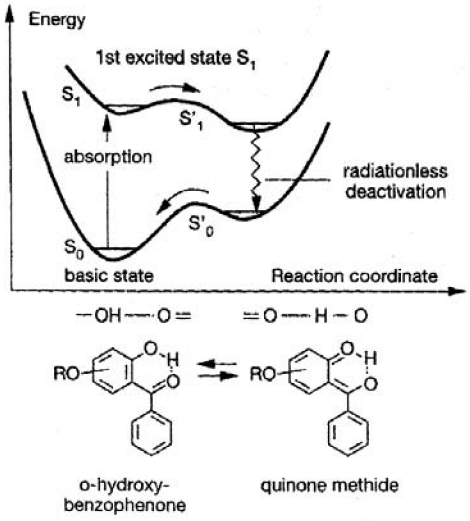

Figure 29 *Mechanism of energy conversion by phenolic UV absorbers, o-hydroxybenzophenone as an example*[105]

Figure 30 shows transmission spectra for specified absorbers.

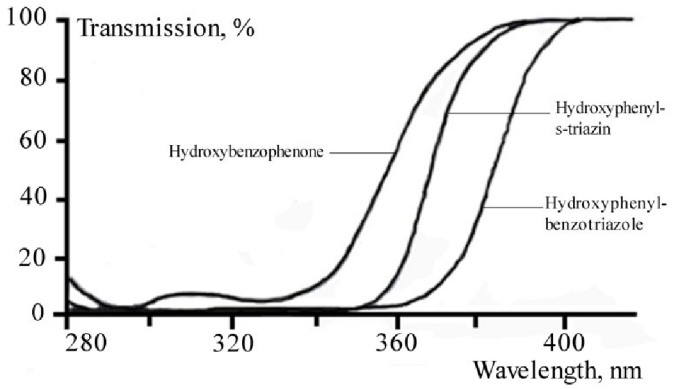

Figure 30 *Transmission spectra for various classes of UV absorbers ($c=1.4\times10^{-4}$mol/l in CH_3Cl)*[105]

Hydroxybenzophenones have two isomers which behave differently, o-hydroxybenzophenones are good photostabilizers and p-hydroxybenzophenones are photodegradation sensitizers.

Benzotriazole stabilizer (o-hydroxyphenylbenzotriazoles) may form H–bonds and their photostabilization mechanism is thought to be rapid tautomerism of the excited states. Benzotriazole quenchers are very efficient quenchers of photochemical excitation reactions, particularly the Norrish type I reaction.[107]

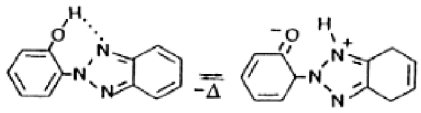

Figure 31 *Transformation of hydroxybenzotriazole.*[107]

Usually UV absorbers are used together in composition with HALS. The two component approach to absorber system is needed because as the UV light is absorbed by the chromophores, further damage is done to the film by free radicals. The combination of HALS with UV absorber has been widely applied to improve the photostability of a variety of polymers. However, the combination of HALS with UV absorber does not always have a positive effect on the photostabilization.[107]

2.9.2 HALS

Hindered amines light stabilizers, HALS, are without exception amine and amino ether derivatives of 2,2,6,6-tetramethyl piperidine.

The high efficiency HALS, the amine and amino ether derivatives of 2,2,6,6-tetramethylpiperidine, as inhibitors of polymer photo-oxidation is considered to be determined primarily by a complex set of reactions involving the scavenging of active alkyl and peroxy-radicals formed during oxidation. During polymer exposure, both amine and amino ether derivatives of HALS produce nitroxides which can intercept alkyl radicals to yield aminoethers which, in turn, can react with peroxy radicals to destroy the latter and to regenerate nitroxides which are then returned to the alkyl radical scavenging pool. Therefore, HALS of different structures are able to interconvert in cyclic pathways, destroying species which could lead to polymer degradation and creating species which protect the polymer against degradation.[108]

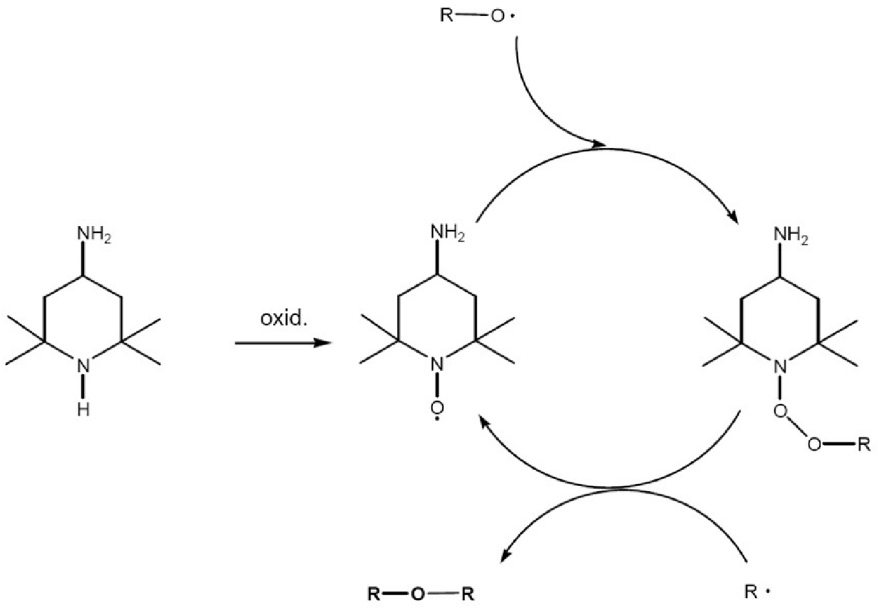

Figure 32 *Schematic view of the stabilisation mechanism of a HALS compound, taking amino-tetramethylpiperidine system as an example.*[105]

3 EXPERIMENTAL

3.1 Used laboratory equipment, chemicals and consumer goods

3.1.1 Laboratory equipment

- Spectral colorimeter X-Rite i-1 Pro
- Q-Sun Xenon test chamber Model Xe-1-B
- Spectrometer Ocean Optics Red Tide USB650UV
- Calibration light source Ocean Optics LS-1-CAL
- UV-VIS Spectrophotometer Spectronic Heλios α
- Nicolet™ iS™50 FT-IR Spectrometer with mid- and far-IR capable diamond ATR
- Raman microscope Solar T II Nanofinder S
- Glossmeter BYK Gardner micro-TRI-gloss µ
- Profilometer BrukerDetak XT
- Anton Paar Density Meter 4100M
- Rheometer TA Instruments AR GR
- Material printer FujiFilm Dimatix
- X1$_1$Optometer with probe XD-950
- Ozone generator
- Inkjet printer Epson Stylus Photo P50
- Inkjet printer Hewlett–Packard Design Jet 500PS
- Deuterium lamp Ocean optics DT-MINI-2GS
- Analytical balance SCALTEC SPB32
- Metrohm Flat-membrane electrode serial .nr. 6.0227.100
- Elcometer Baker Bar, film width 25 mm

3.1.2 Chemicals

- Ethanol for UV-VIS spectroscopy
- Cellulose acetate propionate (CAP-482-0.5)
- Triacetin (M_r=280.20)
- Ethanol, 99%
- Ethyl acetate, 99%
- EVERSORB UV absorbers AQ1, AQ2, AQ3, AQ4
- NaI
- KCl
- Deionized water, conductivity≤5 µS

3.1.3 Ink sets

3.1.3.1 MIS Dyebase - Dye based ink set, MIS Associates, Inc.

- Black ESC-R200-4-K
- Cyan ESC-R200-4-C
- Magenta ESC-R200-4-M
- Yellow ESC-R200-4-Y

3.1.3.2 Dye based ink set, Epson Claria Photographic Ink

- Black T0801
- Cyan T0802
- Magenta T0803
- Yellow T0804

3.1.3.3 Dye based ink set, HP invent

– HP ink Black 82
– HP ink Cyan 82
– HP ink Magenta 82
– HP ink Yellow 82

3.1.4 Inkjet paper

– Ilford Gallerie Smooth Pearl, 290 g m^{-2}– (ISP)
– Ilford Gallerie Smooth Gloss, 290 g m^{-2}– (ISG)

3.1.5 Commercial protective photo-varnishes

– Herma Anti-fade varnish for inkjet prints
– Hahnemühle protective spray for fineart inkjet prints
– Tetenal gloss light protective spray

3.1.6 Used software

– Microsoft® Office Word 2010
– Microsoft® Office Excel 2010
– OriginLab® 7.5
– Adobe® Photoshop® CS2 9.0
– Ocean Optics Ocean View
– VolGa software
– GretagMacbeth™ KeyWizard 2.5
– GretagMacbeth™ Eye-One Match 3
– GretagMacbeth™ Measure Tool 5.0.5
– Software for profilometer Vision 64
– Software for UV-VIS spectrophotometer Vision 3.6
– Software for Rheometer Rheology Advantage

3.2 Test target, inkjet prints preparation

3.2.1 Test target and sample printing

For the purposes of fading tests, both ozone and light, has been used test target i-1 1.5 (Figure 33), which is used for printer profiling and has 288 patches. Targets were printed from Adobe Photoshop software with no colour management. Test targets were printed on two printers Epson Claria and Hewlett Packard (HP) with three types of dye-based inks Epson Claria, HP and MIS Dye Associates. Printing substrate was microporous inkjet paper Ilford Smooth Pearl. Targets sizing and dimensions were modified for varnishing purposes (Figure 33) in accordance with Elcocometer Baker Bar (see Figure 34), which has 25 mm film width.

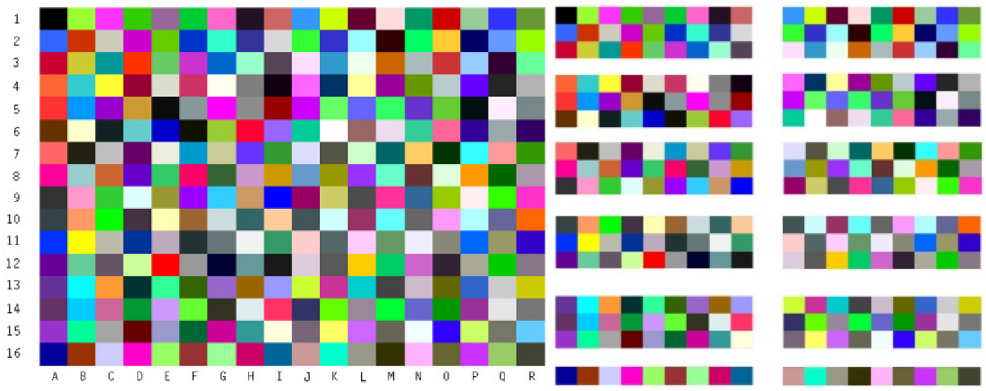

Figure 33 *Un-divided and divided test target i-1 1.5*

3.2.2 Dimatix – material printing

To obtain absorbance spectra of pure inks, from ink cartridges from HP, Epson Claria and MIS Associates Inc. were extracted inks and put into cartridges of material printer Dimatix and printed on Gallerie Smooth Gloss paper. The resolution of the printed image was modified in Dimatix Drop Manager. Optimal print drop span setting was 40 µm and 635 dpi.

Test patches of clear inks CMYK were printed with material printer Dimatix. After the patches dried, reflectance spectra of the patches were measured with X-Rite i-1 spectrophotometer.

3.3 Varnishes and varnishing

3.3.1 Varnishing, sample preparation, handling and storage

As previously stated, varnish was applied on test target strips with Elcometer Baker bar. Several tests with the bar were made in order to determine the best option for thickness of wet film for used varnish composition.

Figure 34 *Elcometer Baker Bar*[109]

All samples were treated the same after varnishing. The varnishes were let dry for 24 hours; test targets were reassembled and attached to a white carton backing. After this period of time they were stored in dark in EMBA archival paper envelopes and EMBA cardboard boxes with alkaline reserve. All paper samples were handled in white cotton gloves to protect them from dirt and skin residues.

3.3.2 Commercial varnishes

A total of 3 inkjet light protective commercial varnishes entered in the test; Tetenal gloss, Hahnemühle and Herma protective varnishes.

3.3.3 Prepared varnish composition

Cellulose acetate propionate (CAP) based overprint varnish has been prepared according to the further composition:

- Cellulose acetate propionate (CAP-482-0.5)[110] 21.7 w%
- Triacetin (M_r=280,20)[111] 1.8 w%
- 99% Ethanol 53.5 w%
- Ethyl acetate 99% 23.0 w%

All liquid components were mixed together and then CAP was added in two or three batches. Varnish was stirred on magnetic stirrer in tightly closed glass reagent bottle, until the CAP flakes were not visible.

EVERSORB UV absorbers were mixed in basic varnish composition in two concentrations, 5 and 10 w% to total weight of the varnish.

3.3.3.1 CAP – Cellulose acetate propionate

Cellulose acetate propionate (CAP) is a cellulose ester, where hydroxyl groups of cellulose are substituted with acetyl and propionyl.[112] Cellulose acetate is soluble in widely used organic solvents such as acetone, xylene or ethanol.

CAP Cellulose acetate propionate is a low-odour, free-flowing powder. It is especially adaptable for use in printing inks and clear overprint varnishes because of its wide solubility in ink solvents, compatibility with other resins used in printing inks, and high melting point. Films formed from CAP

have fast solvent release, very good anti-blocking properties, and grease resistance superior to that of other film-formers.[113]

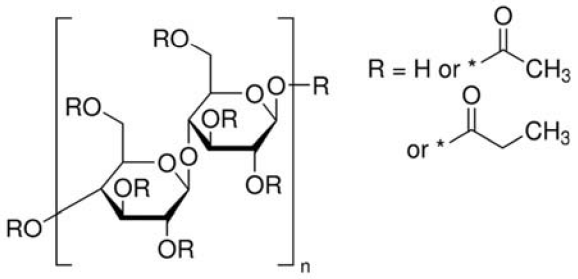

Figure 35 *Structure of cellulose acetate propionate*[113]

3.3.3.2 Triacetin

Triacetin (glyceryl triacetate) $C_9H_{14}O_6$ is used as a plasticizer for cellulosic resins and is compatible in all proportions with cellulose acetate, nitrocellulose, and ethyl cellulose. Triacetin is useful for imparting plasticity and flow to laminating resins, particularly at low temperatures, and is also used as a plasticizer for vinylidene polymers and copolymers. It also serves as an ingredient in inks.[111]

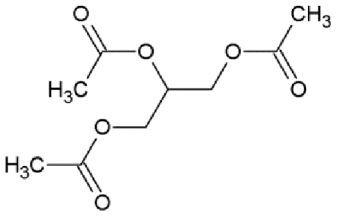

Figure 36 *Structure of triacetin*[114]

3.3.4 UV absorbers - EVERSORB series

Eversorb series is a series of UV absorbers made by Everlight chemicals; they produce mainly light stabilizers as well as UV absorbers. Everlight light stabilizers, coded EVERSORB, are additives that extend the endurance of organic substances to resist degradation caused by the UV rays naturally incorporated in sunlight or artificial lights.[115] Since they are protected by trade secret, information about the product is scarce and the description restricted.

3.3.4.1 EVERSORB AQ1

It's an amber liquid and a mixture of UV absorbers and HALS, which is soluble in water. Eversorb AQ1 is a liquid type and high performance UV stabilizer blending for waterborne coatings. It is versatile light stabilizer, which can be used in wide varieties of clear and pigmented coating systems. It enhances the gloss retention of clear coatings.[116]

3.3.4.2 EVERSORB AQ2

It is a mixture of UV absorbers, more precisely hydroxyphenyl-benzotriazole derivative and 1,2,2,6,6-pentaethyl-4-piperidyl sebacate derivative and cationic dispersive agent. It prevents discoloration and enhances gloss retention of clear coatings.[117]

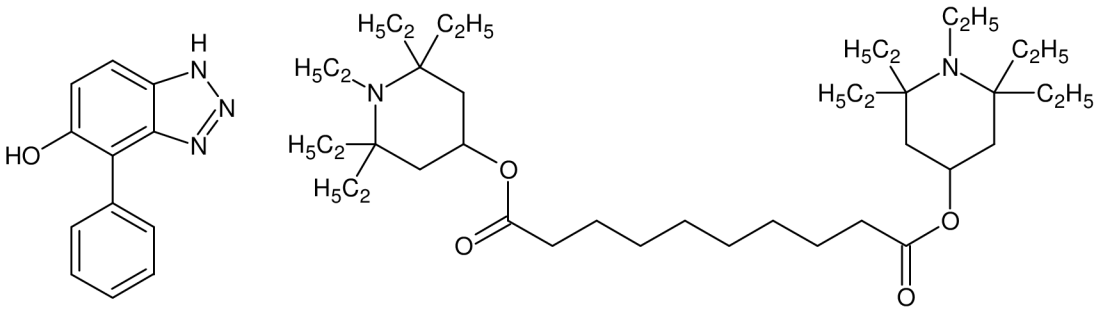

Figure 37 *Hydroxyphenyl-benzotriazole (left); Bis(1,2,2,6,6-pentaethylpiperidin-4-yl) sebacate (right)*

3.3.4.3 EVERSORB AQ3

EVERSORB AQ3 is a liquid type and high performance UV absorber for waterborne coatings. It is suitable for coatings under high baking temperature and extreme conditions. The product can be used with water borne systems directly. Is a hydroxyphenyl-benzotriazole derivate amber-yellowish liquid.

3.3.4.4 EVERSORB AQ4

EVERSORB AQ4 is a liquid type hindered amine light stabilizer (HALS) for waterborne coatings. It prolongs lifetime of coatings under outdoor exposure. It's a light yellow odourless liquid and it's a mixture of HALS and surfactant.

3.4 Optical surface characterisation

3.4.1 FTIR spectrometry

IR spectra of pure UV absorbers, clear varnish as well as varnishes with the 10 w% addition of UV absorbers were measured on Nicolet™ iS™50 FT-IR Spectrometer, with built-in diamond ATR. Total of 128 spectra were collected and averaged into one final spectrum for each sample.

3.4.2 Raman spectrometry

Raman spectra of clear varnish and pure UV absorbers were measured with Raman microscope Solar T II Nanofinder S at 633 nm with 20× magnification and 20 s measurement time.

3.4.3 UV-VIS spectrometry

3.4.3.1 Absorbance spectra of commercial varnishes

4 commercial varnishes (Ch. 3.3.2) were applied on 3×3 cm Pyrex glass substrates. After 24 hour drying period, samples were weighted to gravimetrically determine the applied amount of varnish. To obtain optical property of the varnishes, absorbance spectra were measured with spectrometer Heλios α in range of 250–400 nm.

3.4.3.2 Absorbance spectra of UV absorbers in ethanol

Absorbance spectra of the solutions were measured in spectrophotometer Heλios α in quartz cuvettes with optical length 10 mm. UV absorbers EVERSORB AQ 1, 2, 3 and 4 were diluted in 10 ml of ethanol for UV-VIS spectroscopy. Concentration of the solution 0.04 w% (3.15×10^{-3}g in 10 ml EtOH), reached absorbance values around 1.0 to be in accordance with Lambert-Beers law.

3.5 Surface characterisation

3.5.1 pH of the inkjet paper

pH of both paper substrates was measured (3.1.4) with Metrohm flat membrane electrode. 5 drops of deionized water were placed on paper receiving layer and pH on the surface was measured with the

electrode. Measurement was performed 5 times, the pH value averaged and standard deviation calculated.

3.5.2 Profilometry

Varnishes were applied (3.3.1) on to the Pyrex glass substrate and were let to dry at laboratory conditions. Thickness of dry varnish was measured after 24 hours with profilometer BrukerDetak XT. The measurement parameters are in the Table 8.

Table 8 *Profilometer scan setting*

Parameters	
Stylus radius	12.5 µm
Scan length	29 mm
Scan duration	200 s
Resolution	484 mm

3.5.3 Rheological properties

Viscosity of prepared varnish was measured on Anton Paar Density Meter 4100M. First the sample was deaerated with use od ultrasonic cleaning bath. Then 2 ml of clear varnish was entered into measuring capilary cell. The temperature was set to 25 °C and the tilt angle to 70°.

And the varnish viscosity was also measured at TA Instruments AR GR rheometer. After the measuring head was lowered the edges were covered with oil to prevent varnish to dry out.

3.5.4 Gloss measurement

The measurement of gloss was done with portable gloss meter BYK micro-TRI-gloss µ (Figure 38). Glossmeter was calibrated with black glass calibration standard. To determine the right measuring geometry, first measurement was done with three measuring angles 20°, 60° and 85°. And since the values of gloss were in range 10–70 GU (gloss units), further measurement were done with 60° geometry.

Table 9 *Definition of gloss range and use of measuring geometries*[118]

Gloss range	***Measured value at 60°geometry***	***To be measured with***
high gloss	>70 GU	20° geometry
semi-gloss	10–70 GU	60° geometry
low gloss	<10 GU	85° geometry

Unprinted samples were coated with clear varnish and varnishes prepared according to the composition described in chapter 3.3.3. And then 25×10 mm samples were cut and put to accelerated lightfastness test with same conditions as described in chapter 3.6.1.Gloss was measured after each exposure step, up to 60 hours.

On printed samples is the gloss measurement influenced by the colour of the printed substrate, so samples were measured on the same three places on the test target, where the glossmeter was placed (see Figure 39).

Table 10 *Glossmeter measurement area dimensions at various measurement geometries*[118]

Measurement geometry	***Measurement area dimensions [mm]***
20°	10×10
60°	9×15
85°	5×38

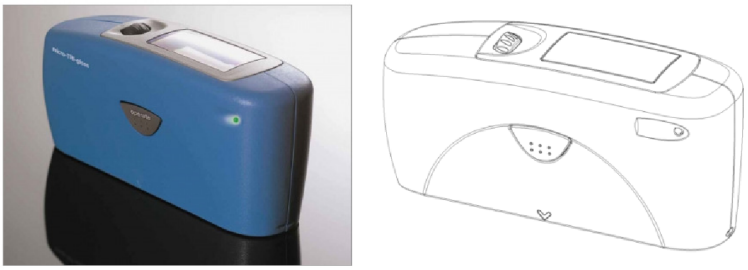

Figure 38 *Micro-TRI-gloss μ - BYK Gardner. Right – scheme of device. Small arrow points out mark for measure aperture.*[118]

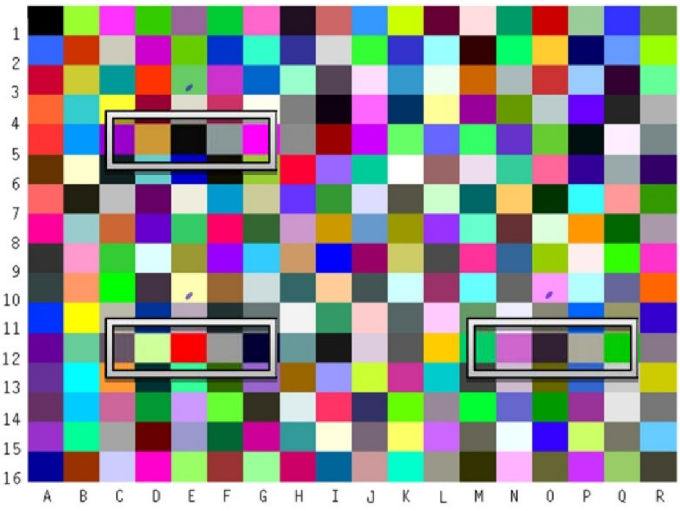

Figure 39 *Position of the glossmeter measuring area on the target. The violet dots represent the positioning of the mark for the measurement aperture and the grey rectangles represent the three measurement areas.*

3.6 Fastness tests

3.6.1 Accelerated lightfastness tests

Accelerated tests were done in Xenon test chamber Q-Sun Xe-1-B with xenon lamp and daylight "outdoor" filter. The test chamber setting is summarized in Table 11. The exposure step was 16 hours, but to ascertain the first change on inkjet prints the first two exposure steps were 4 hours (at HP samples) and the third was 8 hours. The end point criterion fort the test was 30% gamut volume loss.

Table 11 *Test parameters*

Parameter	***Value***
Intensity	0.35 $W \cdot m^{-2} \cdot nm^{-1}$ at 340 nm
Black panel temperature	63 °C
Exposure step	16 h

3.6.1.1 *Spectrum of xenon test chamber lamp*

Emission spectrum of xenon lamp filtered with daylight "outdoor" filter was measured with spectrometer Ocean Optics Red Tide USB650UV and software Ocean Optics Ocean View. For measured spectrum see Figure 40.

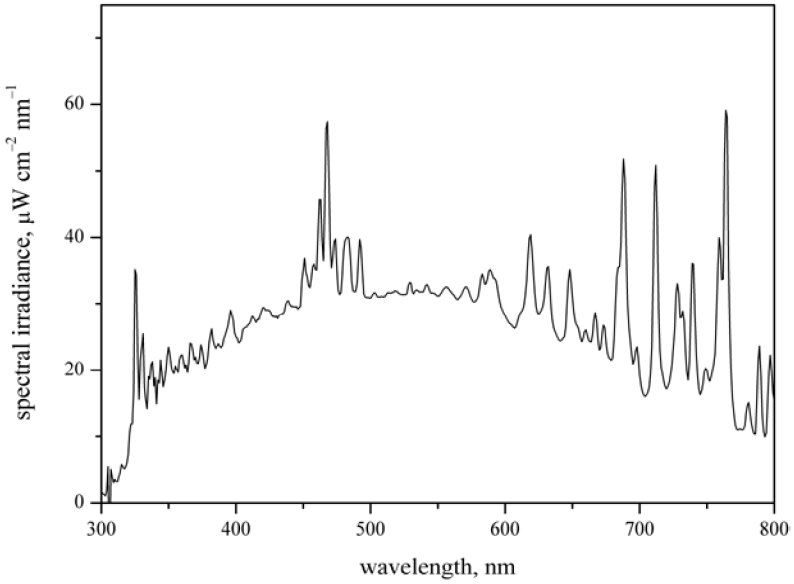

Figure 40 *Emission spectrum of used xenon lamp with daylight "outdoor" filter*

3.6.1.2 *Integral illumination dose*

To determine the total integration dose in xenon test chamber, data from relative intensity spectrum E_r stated in previous sub-chapter were used (Figure 40). These measured values of relative intensity were normalized E_n (divided by the highest intensity value E_{max}) and multiplied by a constant number so, the value at 340 nm is equal to 0.35 W·m^{-2}.

$$E_{n,i} = \frac{E_{r,i}}{E_{max}} \tag{19}$$

$$E_i = E_{n,i} \cdot \text{const.} \tag{20}$$

$$E = \sum_{300\,nm}^{800\,nm} E_i \tag{21}$$

A sum of E_i, integral irradiance dose, in range 300–800 nm from used chamber setting is 295.1 W/m^2.

3.6.1.3 *Estimated lifetime*

For evaluating the estimated lifetime, light conditions set on Q-Sun xenon test chamber have been measured with optometer X1$_1$with probe XD-9502-4. See Table 18 for overview of xenon lamp with daylight filter and set irradiance intensities at 340 nm.

Figure 41 *Optometer X1$_1$ with probe XD-9502-4*

Equivalent prints lifetimes have been calculated according to the equation 21, as an incident illumination recalculated on standard day. A standard illumination day is apprehended dose of 450 lx during 12 hours.[80]

$$S = \frac{H}{450 \cdot 12} \tag{22}$$

3.6.1.4 Commercial varnishes

Prepared samples were adjusted with strong magnets on metal plate in Xenon test chamber Q-Sun Xe-1-B with xenon lamp and daylight "outdoor" filter. Samples were irradiated with light intensity set to 0.35 $W \cdot m^{-2} \cdot nm^{-1}$ at 340 nm (for full chamber setting see Table 11). Exposure steps were 4, 8, 16, 32, 48, 64, 80, 96, 112 hours and so on until the endpoint threshold is achieved. This threshold is set to 30% loss of gamut volume.

3.6.1.5 Prepared varnishes

Prepared varnished prints were adjusted with strong magnets on metal plate in Xenon test chamber Q-Sun Xe-1-B with xenon lamp and daylight "outdoor" filter (for full chamber settings see Table 11). After 304 hours or 30% of gamut volume loss accelerated test was stopped.

3.6.2 Gas fastness

3.6.2.1 Ozone-fastness

The important quality of the prints gas-fastness was tested in an ozone apparatus is shown in Figure 42. Compressed technical air was lead trough gas flow regulator to ozonizator. Ozonized air passed through light absorption cell, where absorption spectra of deuterium light source were measured at 254 nm to continuously determine ozone concentration. The ozonized air flow was adjusted to measured absorbance value of 0.1. Samples were exposed to the ozonized air in reaction cell with 1600 cm^3 volume. Even air distribution was assured by inserted magnetic stirrer with attached scapulae. And this even reaction gas distribution was tested on cyan test target. To prevent ozone emission to ambient environment, two consecutive wash bottles with 0.2M NaI solution were placed to the outflow from the reaction chamber. After the exposure, assembled apparatus was rinsed with technical air for 10 minutes.

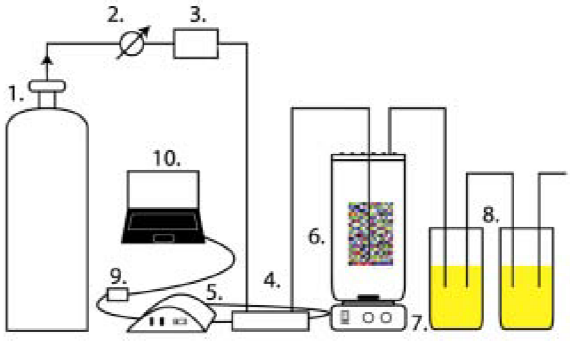

Figure 42 *Scheme of ozone apparatus; 1-compressed air tank, 2-air flow regulator, 3-ozone generator, 4-light absorption cell, 5-deuterium light source, 6-reaction chamber with magnetic stirring bar, 7-magnetic stirrer, 8-two wash bottles with NaI solution, 9-spectrophotometer, 10-computer*

Sample patches reflectance spectra were measured before the test and after each exposure step with X-Rite i-1 spectrophotometer. Exposure steps were 1.5, 3, 4.5, 6, 7.5, 9, 12, 15, 18 etc. Ozone doses corresponding to hours of exposure were calculated (Table 21). Endpoint criterion was 30% of gamut volume loss. Test was stopped either if the test endpoint criterion was achieved or after 72 hours of exposure. Evaluation was performed in the same manner as in case of lightfastness test (Ch.3.7).

Even ozone distribution test–cyan test target

Test chart (288 cyan patches) to confirm the even distribution of the reaction gas was printed on Hewlett–Packard Design Jet 500PS printer and Ilford Smooth Pearl paper and let dry for 24 hours at laboratory conditions. After this time it was placed into test chamber and exposed to ozone. Reflectance spectra were measured before and after exposure, CIE *L*a*b** values were calculated using Gretag MacBeth Measure Tool 5.0.5. and colour difference was calculated according to the Equation 8. A heat map of colour differences was created in order to determine whether the distribution of the reaction gas is uniform.

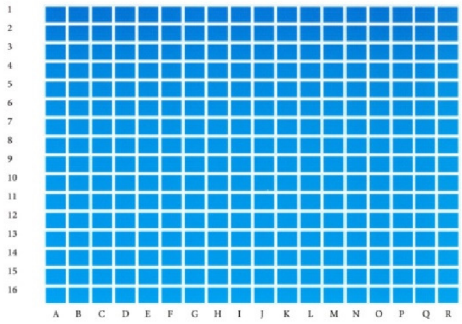

Figure 43 *Used cyan test target*

3.6.2.2 Water vapour permeability test

Water vapour permeability test was done according to ČSN 77 0332. Circles of 4 cm diameter were cut out from calendered paper coated from one side with PE. Prepared samples were sprayed with commercial varnishes. The applied varnish amount was determined gravimetrically after 24 hours (samples were weighted before and after varnish application). For the prepared composition, the samples were first varnished using Mayer rod and then cut out.

According to the standard (Ch. 2.5.2.4)[76] a measuring regime was chosen – type D. After drying period, samples were adjusted into water vapour permeable cups with silica gel, weighted and placed into desiccator, where they were let for 24 hours with saturated solution of KCl.

To determine the amount of absorbed (into paper substrate) and transmissed water (absorbed by silicagel), directly after the end of the test, test cups and samples were weighted.

3.6.2.3 O_2 permeability test

As a substrate for O_2 permeability test was chosen a calendered paper coated from one side with polyethylene. Permeability of clear substrate was tested, to determine its characteristics. For the varnish application was due to the size of the OTR measuring device used Mayer rod, with wet film thickness 50 µm (2 mills). Sheets of paper of size 12×12 cm were coated with prepared varnish as well as commercial varnishes, which were sprayed on. The amount of applied commercial varnish was determined gravimetrically. For every varnish type, 5 samples were prepared.

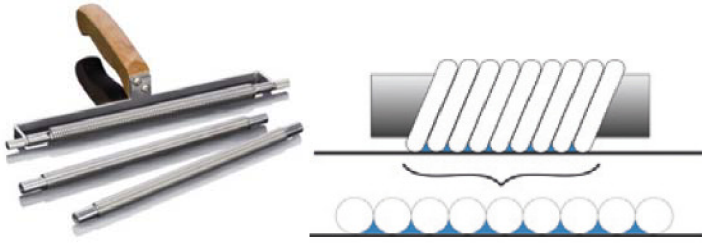

Figure 44 *Mayer rods with handle holder (left); principle of coating with Mayer rod (right).*[119]

Sample was placed in the cell (Figure 45). Test chamber was rinsed with nitrogen gas, until a threshold of 5 ppm O_2 concentration was achieved. After the cell was rinsed, the concentration of permeated oxygen trough substrate with applied varnish layer was measured ten times for each sample. From each peak in the measurement (Figure 46) oxygen transmission rate was calculated (Equation (16)), averaged for every sample and the standard deviation has been calculated.

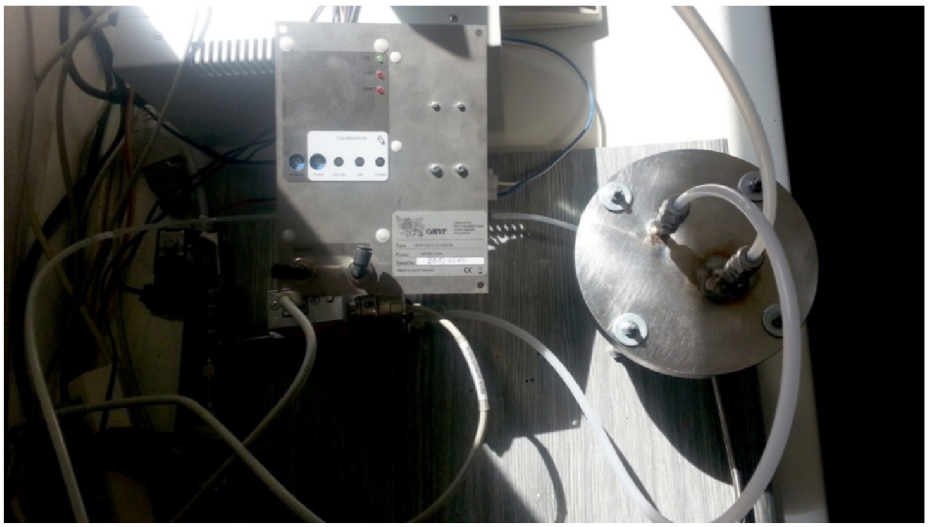

Figure 45 *OTR measuring device; round measuring cell is on the right. (apparatus scheme Figure 20)*

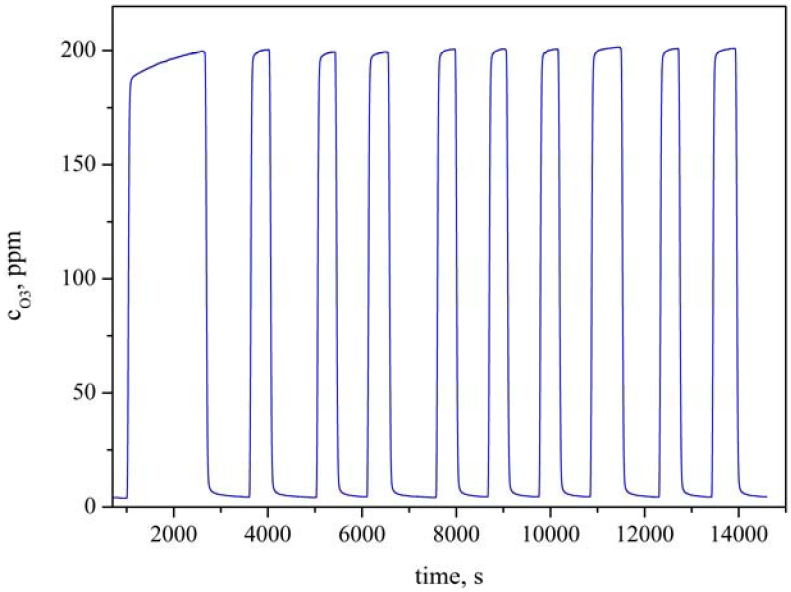

Figure 46 *Normal OTR measurement progress.*

3.7 Colorimetry

All spectrophotometric measurements were done by X-Rite i-1 Pro (Figure 47) with Gretag Macbeth Eye-One Match 3 software.

Figure 47 *Spectrophotometer X-Rite i-1 Pro*

3.7.1 Gamut volume calculation–Volga

CIE *L*a*b** values were calculated from measured reflectance spectra of test target i-1 1.5, in Gretag MacBeth Measure Tool 5.0.5. Then CIE *L*a*b** values corresponding to each measurement (exposure step) were entered into VolGa software, to calculate gamut volume and its change during ageing.[120]

From VolGa software the data were exported as visualizations of the change in gamut volume (Figure 48-left). The initial gamut volume has always grid-like see-trough surface and the end of the test has full one. Change in relative gamut volume has been plotted to illuminance (lightfastness test) or ozone exposure dose (gasfastness test) – Figure 48-right. The results are in both fastness tests arranged in the same manner for HP, MIS Dye and Claria (in this exact order), first are results of commercial varnishes, then unvarnished print, clear varnish and 5 and 10 w% addition of each UV absorber.

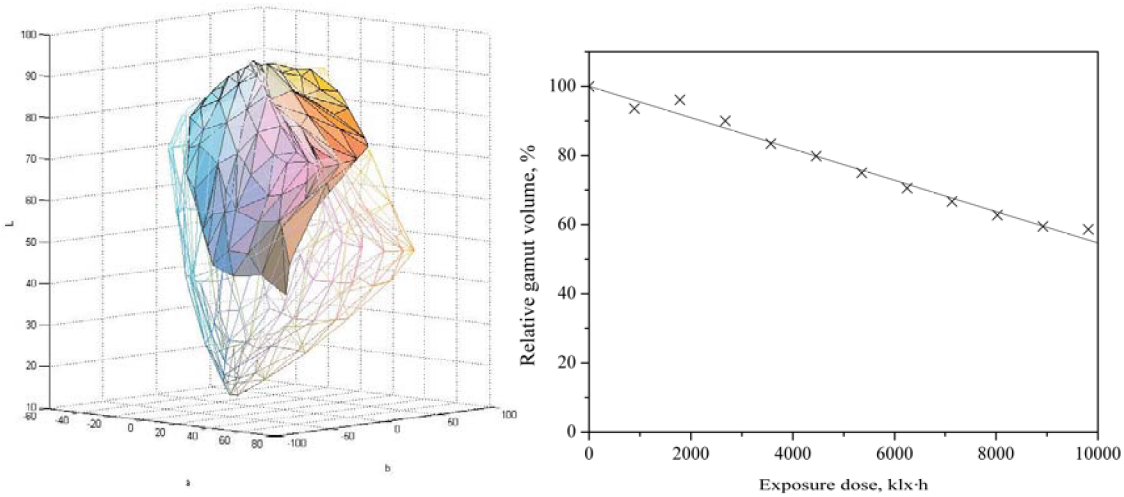

Figure 48 *Example of data evaluation; Left – gamut loss visualization in 3D CIE L*a*b* space. The grid belongs to the gamut before exposure and the full surface to the gamut volume after certain exposure dose. Right – Plot of change of gamut volume and exposure dose with linear regression.*

3.7.2 Change in colour after varnishing

3.7.2.1 Unprinted paper

Unprinted paper pieces were varnished (for more detail see chapter 3.2) and the CIELAB values as well as reflectance spectra were measured with X-Rite i-1.

3.7.2.2 Colour change after varnish application

Eight patches representing important colours (Figure 49) on the target were measured in order to determine the colour change caused by the varnish application. The patches were measured with Spectral colorimeter X-Rite i-1 Pro and the L*a*b* values and reflectance spectra were recorded.

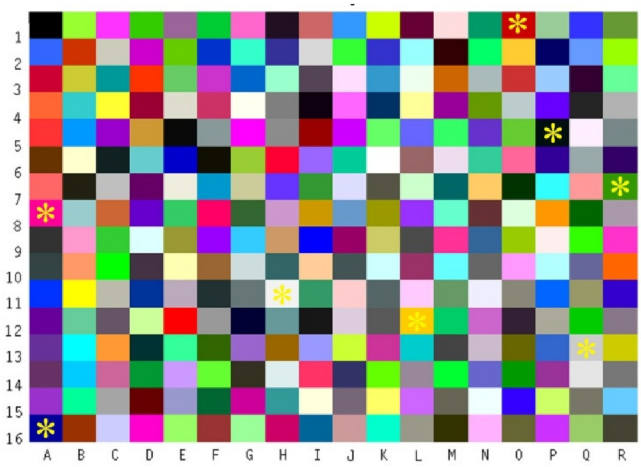

Figure 49 *Measured patches for colour change on I11.5 test target after varnish application are marked with yellow star.*

4 RESULTS AND DISCUSSION

4.1 Varnishing

Several tests with the bar were made in order to determine the best option for thickness of wet film. Most homogeneous films with tested varnish composition proved to be with 60 µm wet film thickness. Other thicknesses 30, 90 and 120 µm showed some problems like bubble formation, leaving lines, inhomogeneity etc.

4.2 Optical characterisation

4.2.1 FT-IR and Raman spectrometry

Broad peak in spectrum of clear varnish (Figure 50) range 3625 to 3100 cm^{-1} signalizes presence of –OH groups (strong intermolecular H bond). Broad diffuse band from 3600 to 3100 cm^{-1} can be attributed to either strong intermolecular H–bond in –OH groups or polymers. Peak at 2973, 2927 and 2880 cm^{-1} can be attributed to asymmetrical stretching of $–CH_3$ groups, asymmetrical stretching of CH_2 bond and weak stretching of –CH bonds. Pronounced peak at 1741 cm^{-1} is stretching of C=O bond of saturated ester groups. Region from 1260 to 1350 cm^{-1} signalizes deformation vibrations of C–OH in primary alcohols. Peak of 1374 cm^{-1}can be attributed to stretching of C=O ester groups present in Triacetin.

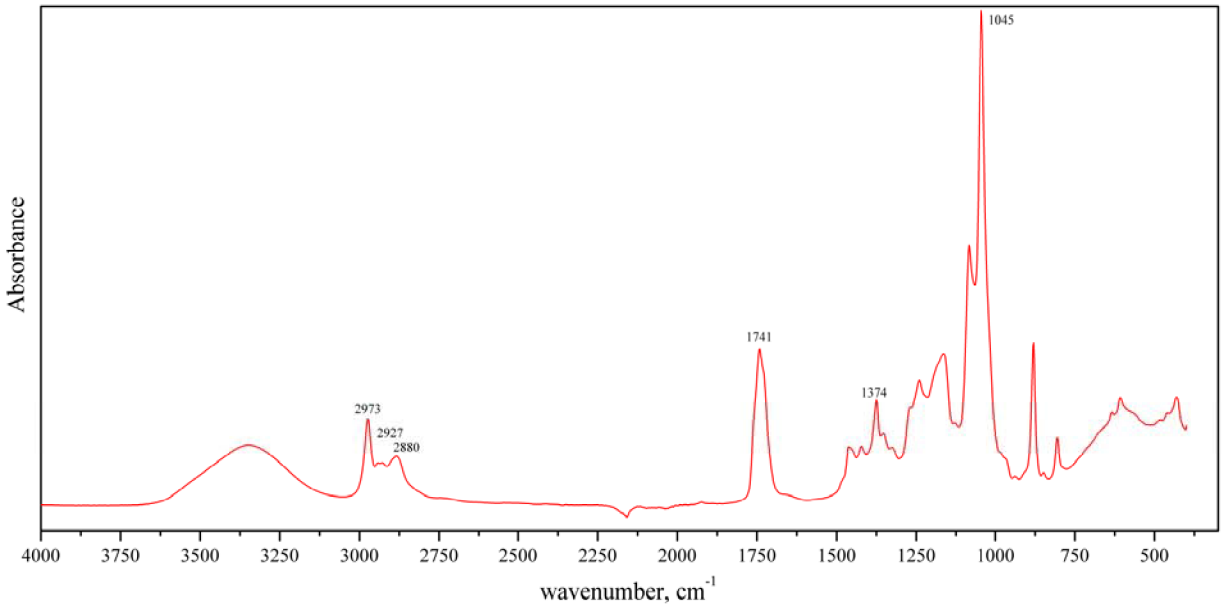

Figure 50 *IR spectrum of clear varnish*

All three UV absorbers have almost identical spectra (Figure 51). Broad diffuse band in region from 3625 to 3000 cm^{-1} signalises the presence of bonded –OH groups, since the band is broad and diffuse it could mean polymers; valence vibration of aromatic C–H and bonded –NH groups. Band in region 3000 to 2750 cm^{-1} can be attributed to $–CH_2$, $–CH_3$ groups. Distinctive peak at 1731 cm^{-1} ascertains the presence of an ester (sebacate) and peaks at 1440 cm^{-1} can be attributed to vibrations of C–H in $–CH_2$ group. Peaks at 1270–1230 cm^{-1} can be attributed to ether vibrations and broad peak at 1105 cm^{-1} belongs to C–O vibrations (C bonded in aryl).

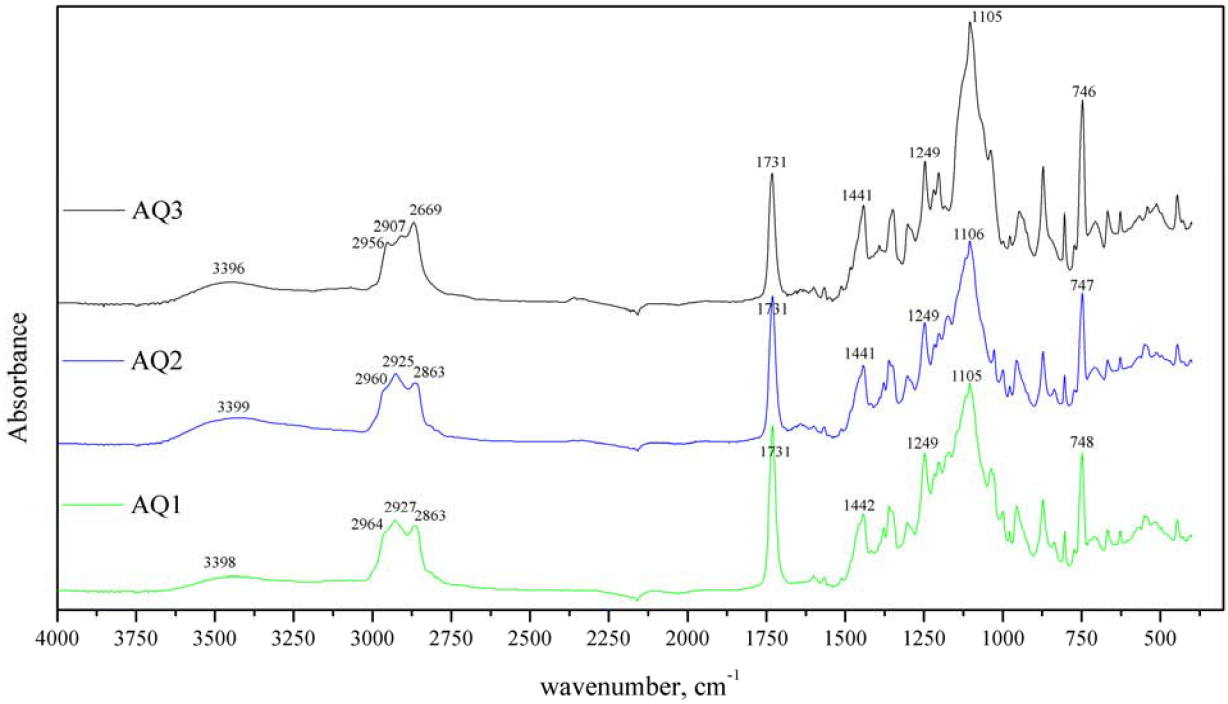

Figure 51 *Infrared spectra of Eversorb UV absorbers*

All spectra of clear varnish and varnishes with addition of 10 w% of UV absorbers have similar peak positions (Figure 52). In fact they are almost identical, and the differences are just in the intensity of certain peaks.

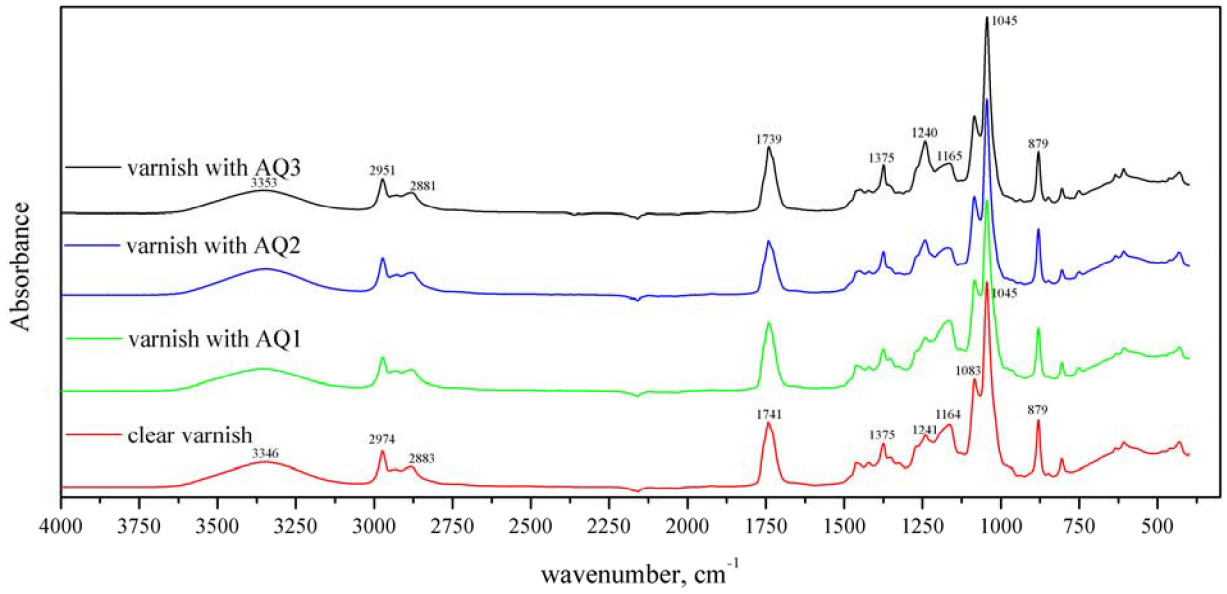

Figure 52 *Infrared spectra of clear varnish and varnishes mixed with 10 w% UV absorbers*

In Figure 53 to Figure 55, there are four spectra in each figure, spectra of varnishes with UV absorbers, those of printing substrate, clear varnish and UV absorber. So peaks belonging to the printing substrate can be recognized in varnish spectrum (varnish+UV absorber).

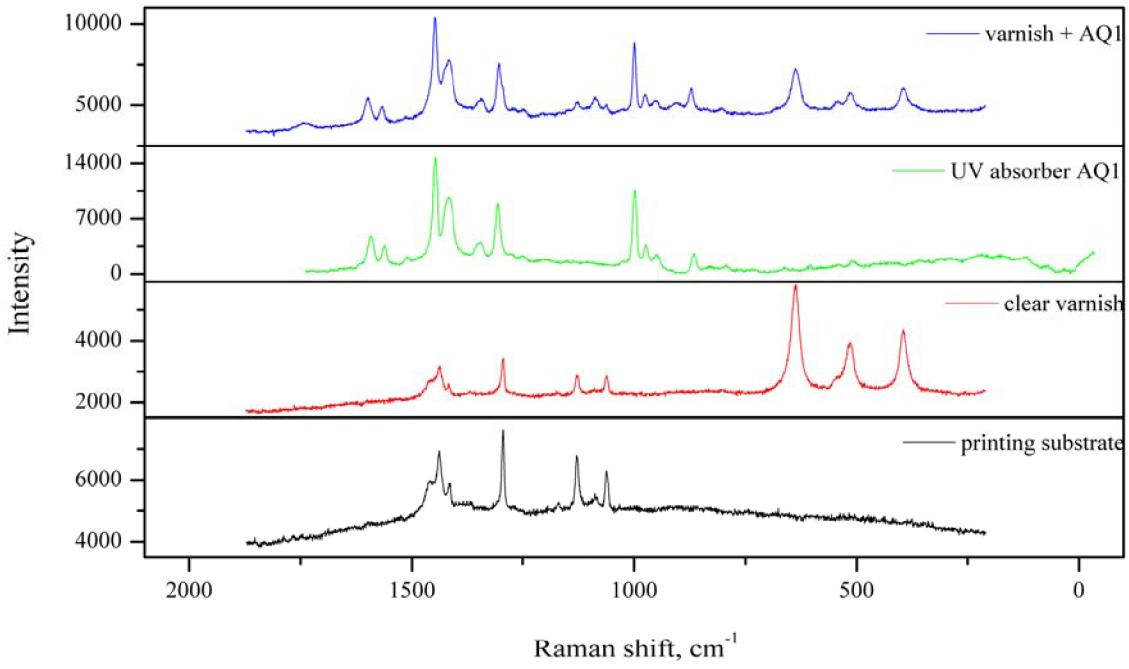

Figure 53 *Raman spectra of printing substrate, clear varnish applied on the paper, absorber AQ1 and varnish with the addition of UV absorber AQ1 applied on the printing medium.*

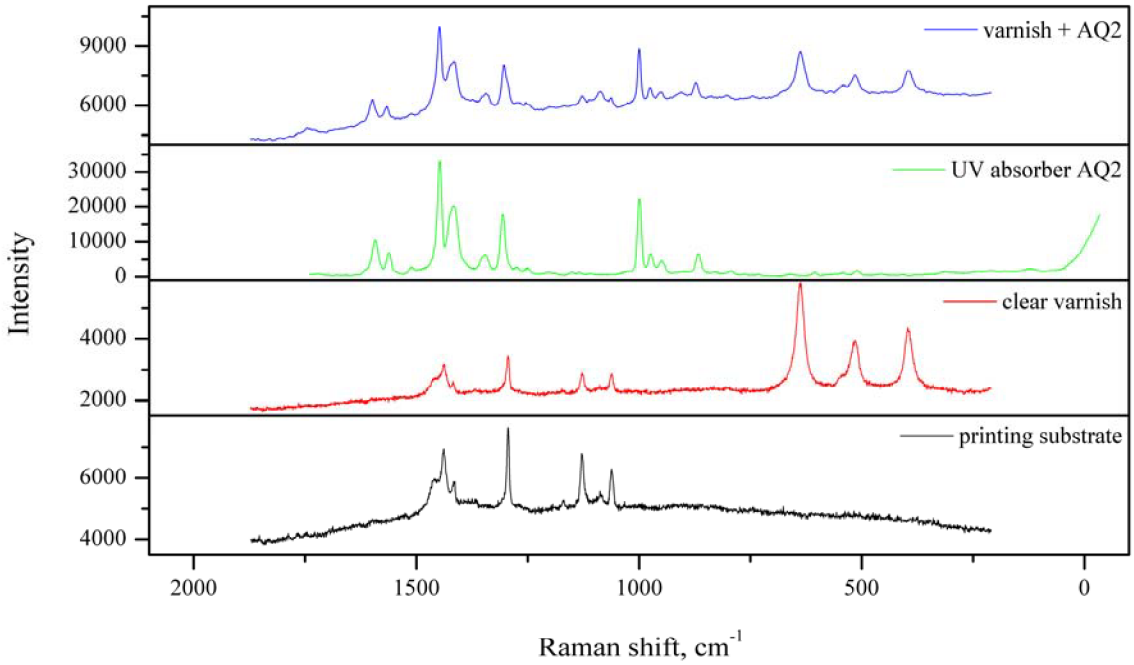

Figure 54 *Raman spectra of printing substrate, clear varnish applied on the paper, absorber AQ2 and varnish with the addition of UV absorber AQ2 applied on the printing medium.*

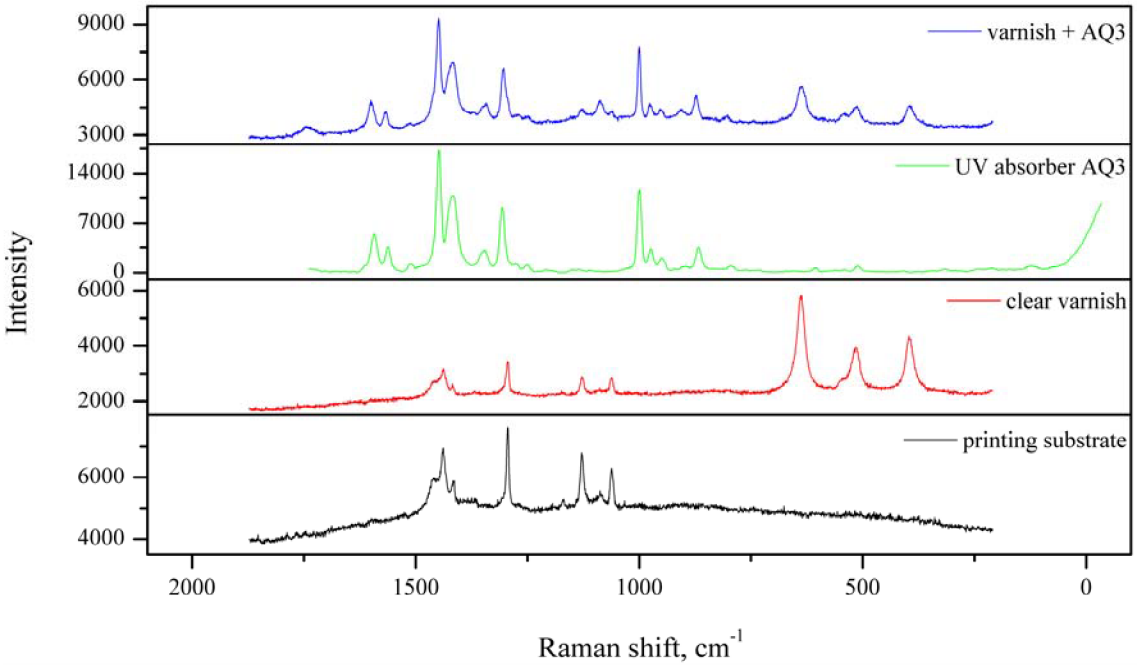

Figure 55 *Raman spectra of printing substrate, clear varnish applied on the paper, absorber AQ3 and varnish with the addition of UV absorber AQ3 applied on the printing medium.*

Previously interpreted UV absorber IR spectra (Figure 51) were put together with Raman spectra (Figure 56, Figure 57 and Figure 58). All three UV absorbers have same position of the main peaks, but slightly differ in intensity. Peak at 1614 cm^{-1} can be attributed to stretching of (>C=C<) group, two pronounced peaks in region 1400–1475 cm^{-1} to asymmetric stretching of CH_3 groups scissoring and bending of $–CH_2$. At 1341 cm^{-1} peak belongs to bending of CCH groups. Peak in 1048 cm^{-1} can be attributed to symmetrical stretching of >C–O–C< bonds.

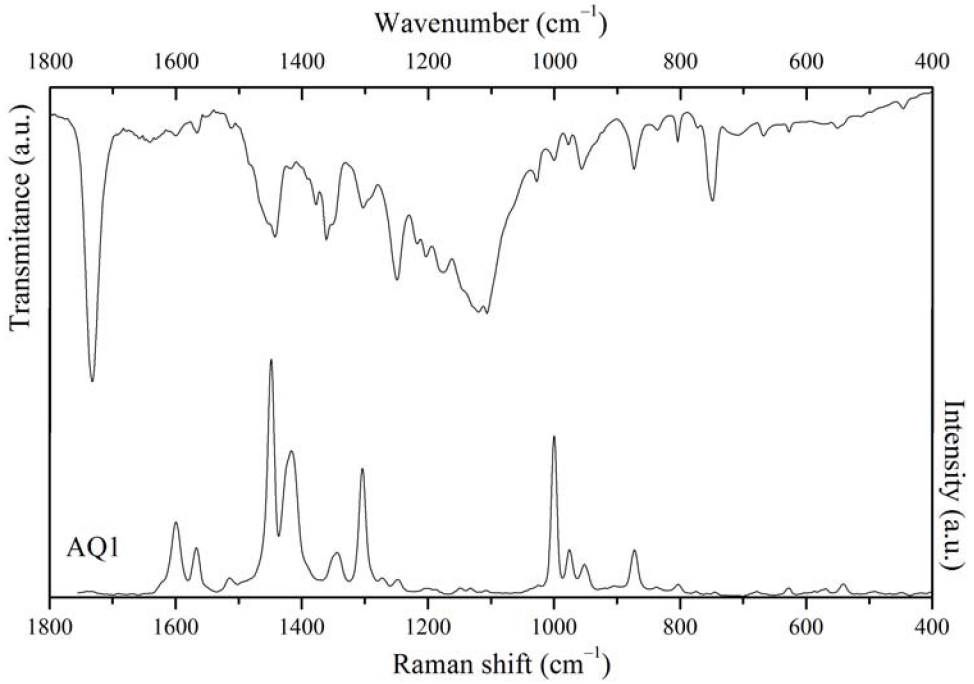

Figure 56 *IR and Raman spectra of UV absorber AQ1*

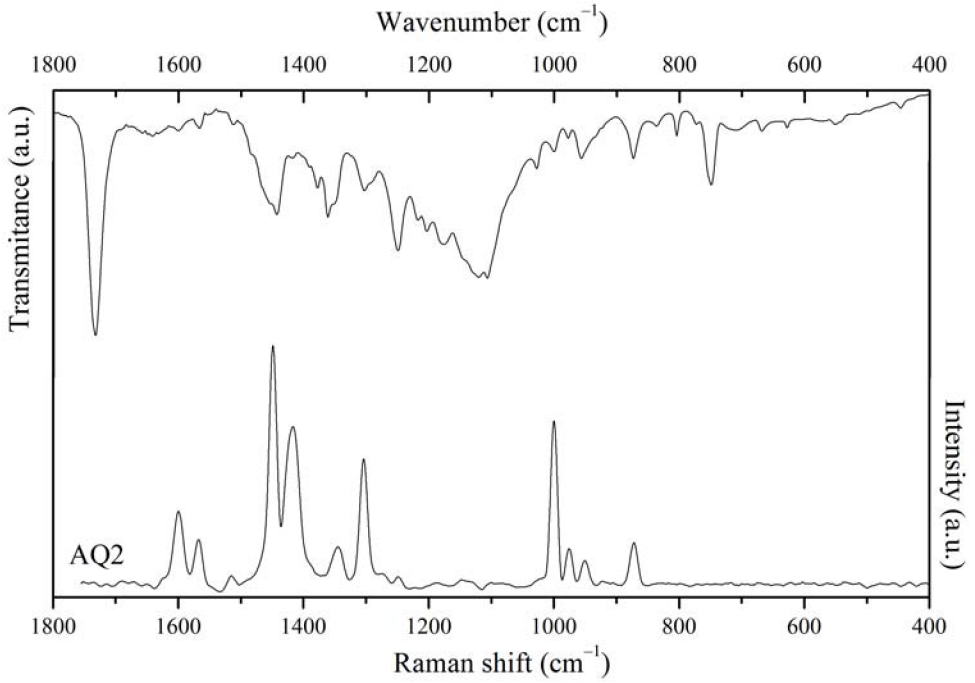

Figure 57 *IR and Raman spectra of UV absorber AQ2*

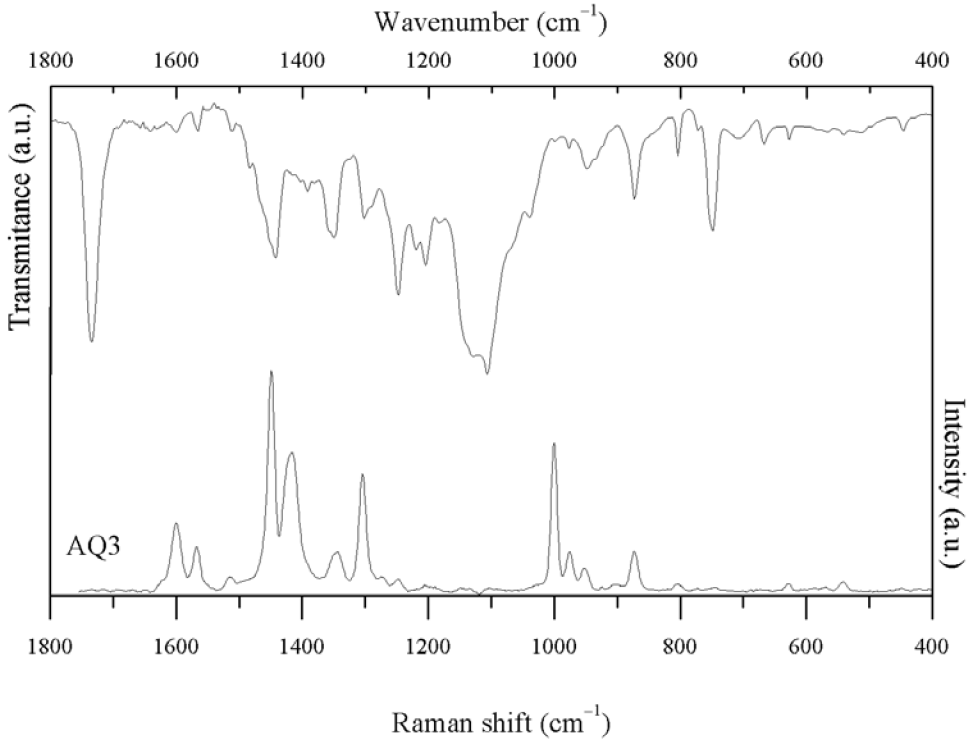

Figure 58 *IR and Raman spectra of UV absorber AQ3*

In next four figures (Figure 59, Figure 60, Figure 61 and Figure 62) there is comparison of Raman spectra acquired before the exposure in xenon test chamber and after 144 hours of exposure (which is approximately half of the total exposure time). Spectra are composed from the spectrum of the receiving layer and varnish (with or without UV absorber addition). From the spectra it can be assumed that in 144 hours of exposure the varnish didn't undergo degradation.

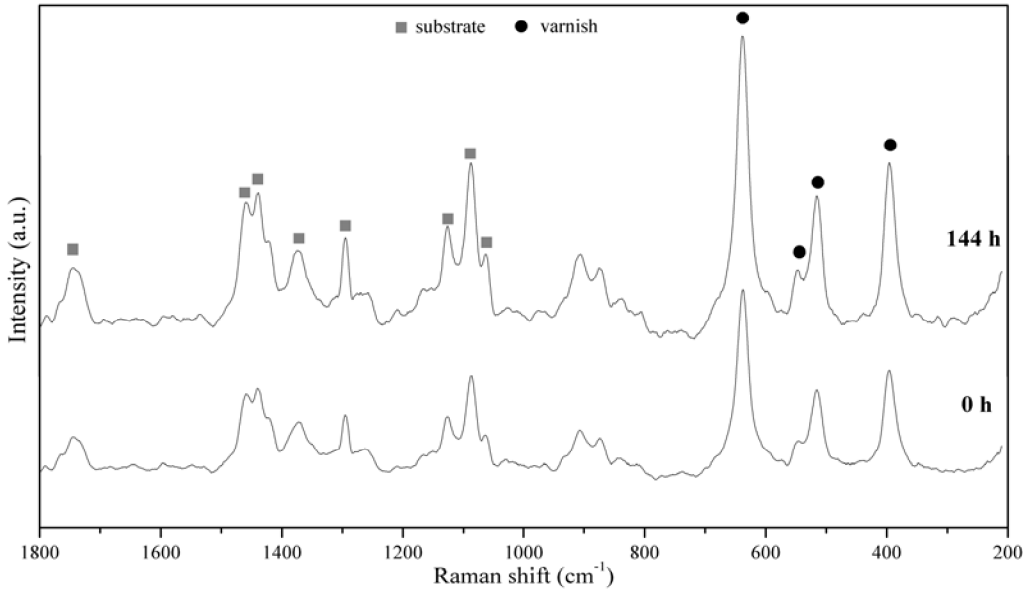

Figure 59 *Raman spectra measured on unprinted spectra after application of varnish; 0h spectrum was measured before the exposition in the Q-Sun test chamber and 144 h exposure in the test chamber.*

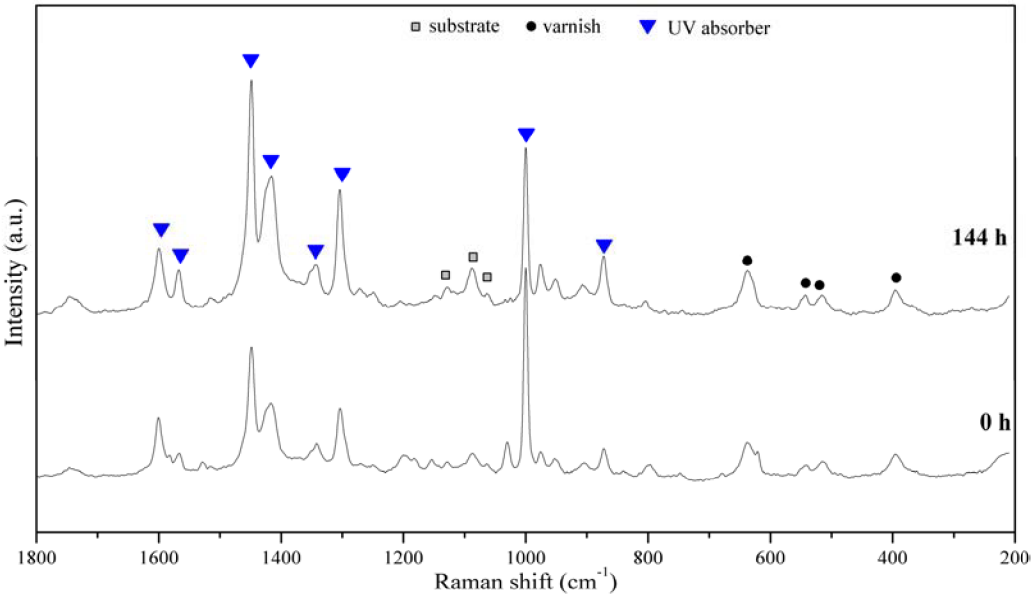

Figure 60 *Raman spectra measured on unprinted spectra after application of varnish mixed with 10w% AQ1 addition; 0 h spectrum was measured before the exposition in the Q-Sun test chamber and 144 h exposure in the test chamber.*

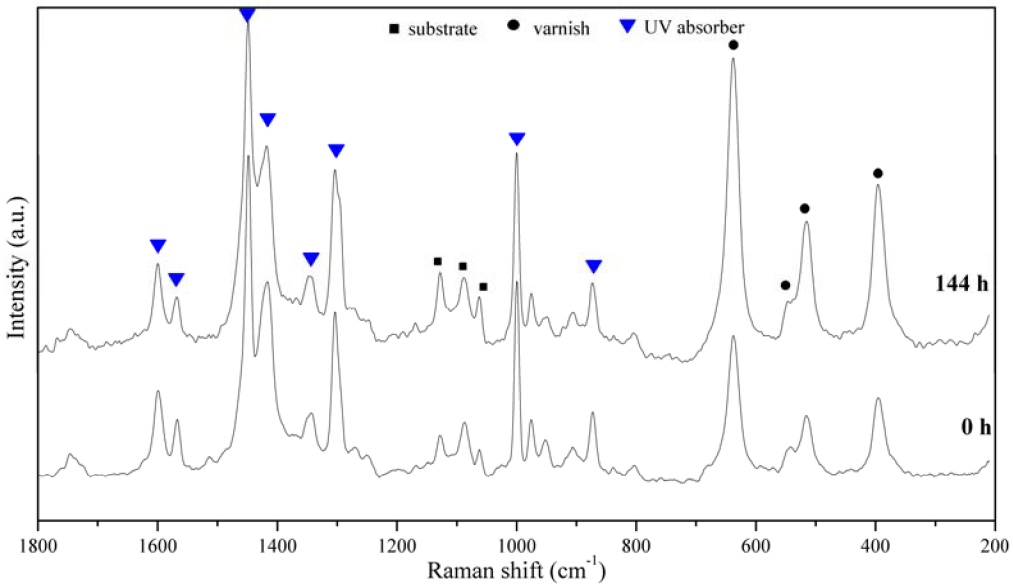

Figure 61 *Raman spectra measured on unprinted spectra after application of varnish mixed with 10w% addition of AQ2; 0 h spectrum was measured before the exposition in the Q-Sun test chamber and 144 h exposure in the test chamber.*

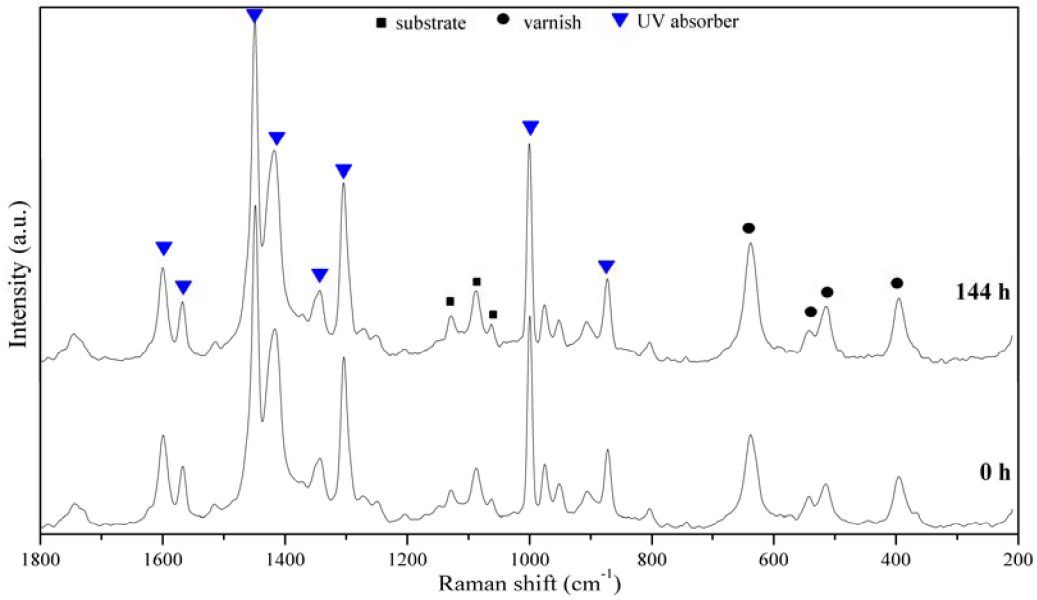

Figure 62 *Raman spectra measured on unprinted spectra after application of varnish mixed with 10w% AQ3 addition; 0 h spectrum was measured before the exposition in the Q-Sun test chamber and 144 h exposure in the test chamber.*

Figure 63 shows the places from where the spectra were acquired, from each one spectrum was chosen.

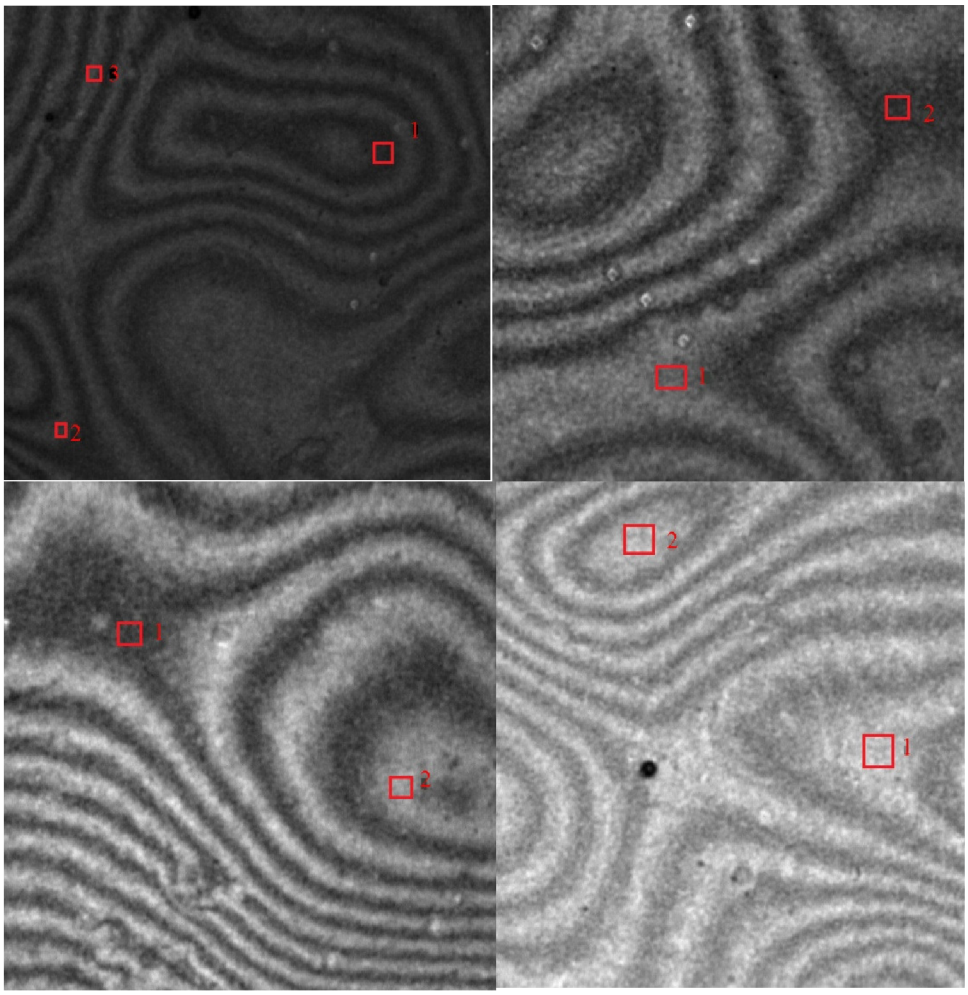

Figure 63 *Measurement spots for Raman spectra acquisition; on the top-left clear varnish, top-right varnish with AQ1, bottom-left varnish with AQ2, bottom-right varnish with AQ3*

4.2.2 UV-VIS spectrometry

4.2.2.1 Reflectance spectra of pure ink components

Following three graphs with reflectance spectra measured on CMYK patches printed with material printer show the differences between the particular ink sets, mainly cyan and black inks differ (more on of pure CMYK patches prep in Ch. Figure 33)

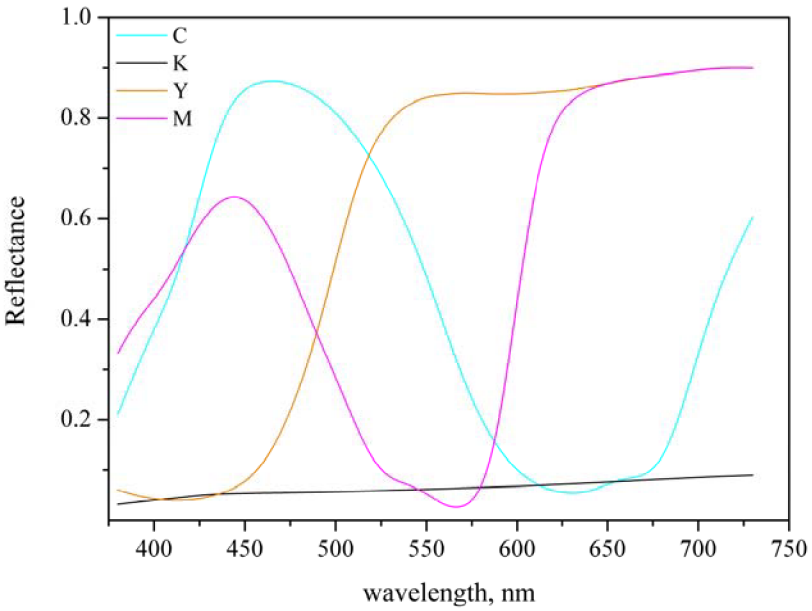

Figure 64 *Reflectance spectra of pure CMYK inks from HP ink set.*

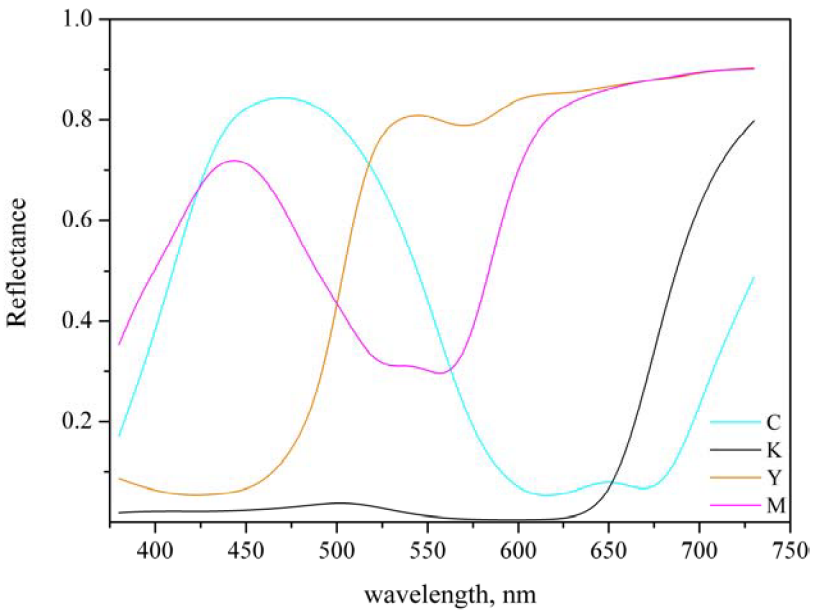

Figure 65 *Reflectance spectra of pure CMYK inks from MIS Associates Inc. ink set.*

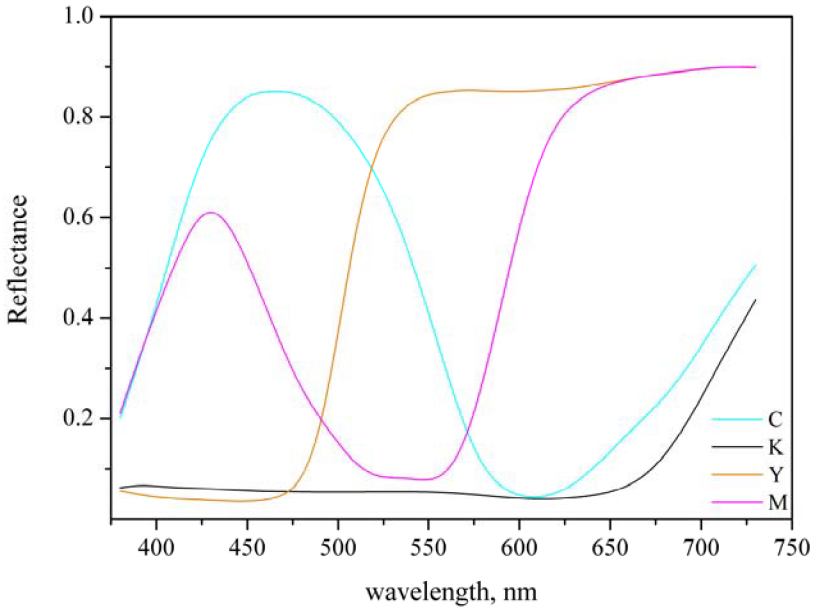

Figure 66 *Reflectance spectra of pure CMYK inks from Epson Claria ink set.*

4.2.2.2 Absorbance spectra of commercial varnishes

Amount of applied dry varnish was with all samples in range $34\pm5\cdot10^{-4}$ g on Pyrex glass ($9.61 cm^2$). As visible from Figure 67, Hahnemühle varnish has strong broad absorption band in 250–350 nm region, which could indicate to the presence of UV absorbers.

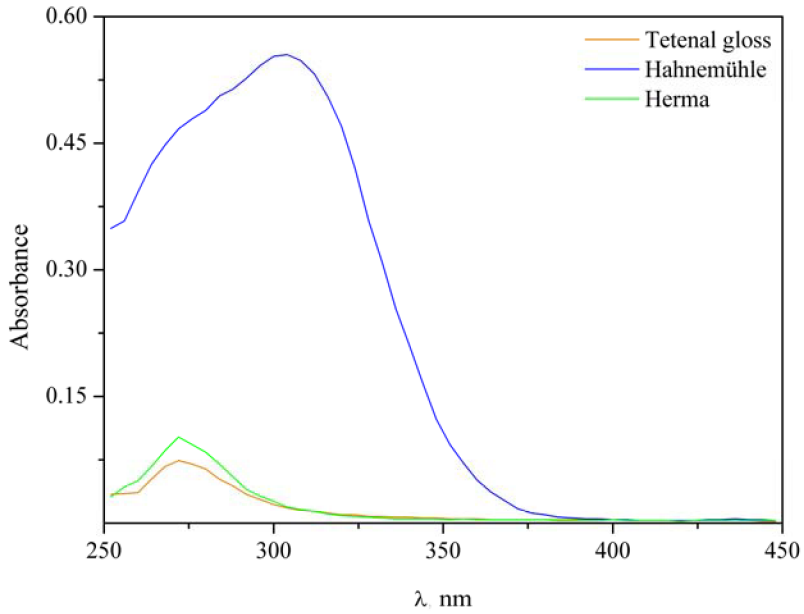

Figure 67 *Absorbance spectra of the commercial varnishes measured on spectrometer Helios α.*

4.2.2.3 Absorbance spectra of UV absorbers in ethanol

Concentration of the UV absorbers in ethanol was 0.04%, to achieve absorbance value around 1.0. UV absorbers AQ1, AQ2 and AQ3, diluted in pure ethanol (for UV), formed clear yellowish solutions. Only UV absorber AQ4 formed opaque solution. From the Figure 68 it is evident that UV absorbers AQ1, AQ2 and AQ3 have very similar composition, due to the peak position. The absorbance spectrum of AQ4 absorber is in accordance with the opaque yellowish solution, which absorbs in

ultraviolet and also in visible spectrum. Because of the absorber opaque quality, further work with it was discontinued.

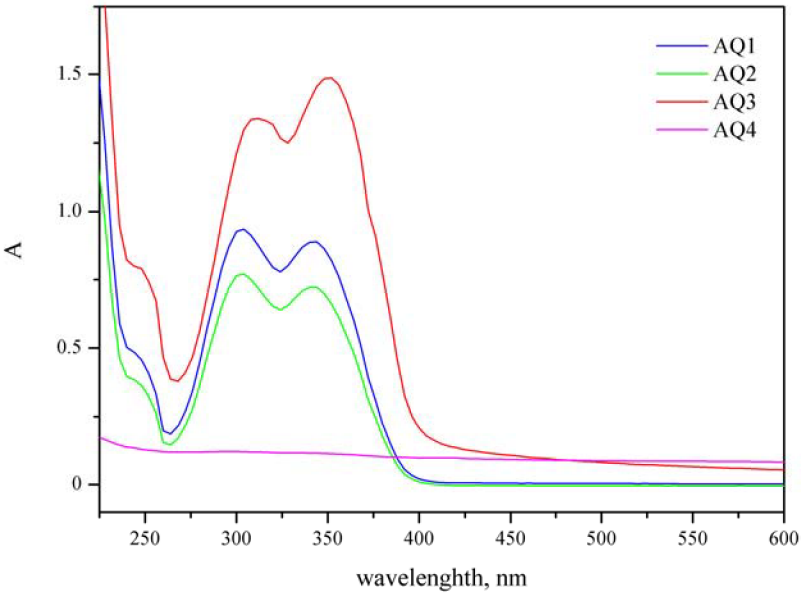

Figure 68 *Absorbance spectra of UV EVERSORB absorbers diluted in ethanol for UV*

4.3 Surface characterisation

4.3.1 Used printing medium characterisation

Reflectance spectra and CIE L*

Reflectance spectra of both inkjet papers didn't reach past reflectance value of 100%. But they posses peak in 425 nm region that suggest presence of OBA's.

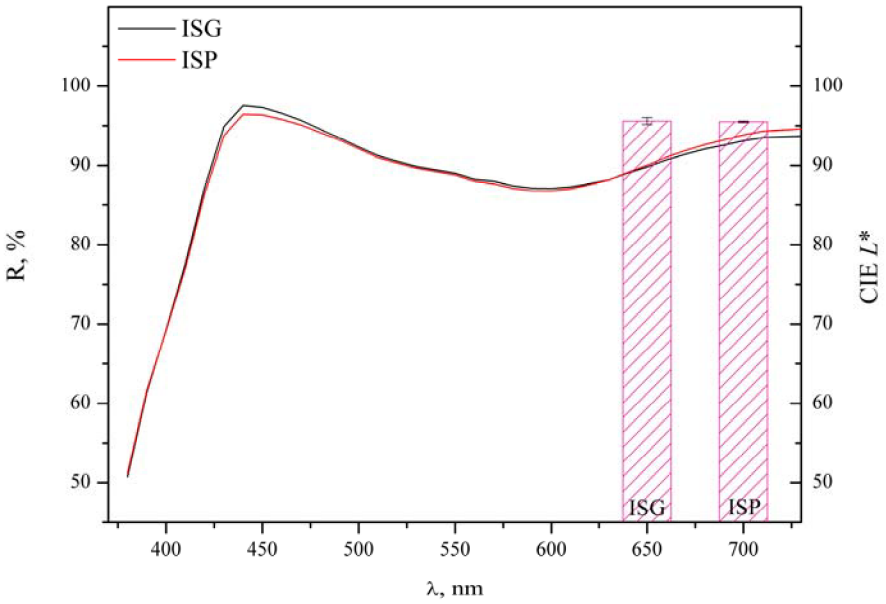

Figure 69 *Reflectance spectra of ISG and ISP inkjet papers and their lightness (CIE L*)*

pH

By measuring the pH of the used inkjet papers Ilford Galerie Smooth Pearl and Ilford Galerie Smooth Gloss by flat membrane electrode, it was ascertained that they are slightly acidic.

Table 12 *Measured pH values of used printing medium*

paper substrate / *measurement nr.*	*Ilford Smooth Pearl*	*Ilford Smooth Gloss*
1	6.06	5.95
2	6.00	5.92
3	5.89	5.84
4	5.47	5.64
5	5.62	5.74
average pH value	**5.8**	**5.8**
standard deviation	**0.3**	**0.1**

4.3.2 Viscosity

Varnish dynamic viscosity is 839.87 mPa·s, and its machine calculated measurement deviation is 1.78 %. The measurement lasted for 86.34 s.

The applied shear stress on the non-Newtonian varnish liquid showed that the varnish can accommodate the increase until some point. After a threshold of 63.1 s^{-1} is reached, the mechanical degradation occurs and with that comes radical decrease of viscosity. The radical drop of viscosity is probably caused by the breaking of hydrogen bonds. And it is presumed that there will be partial relaxation after the stress is removed.

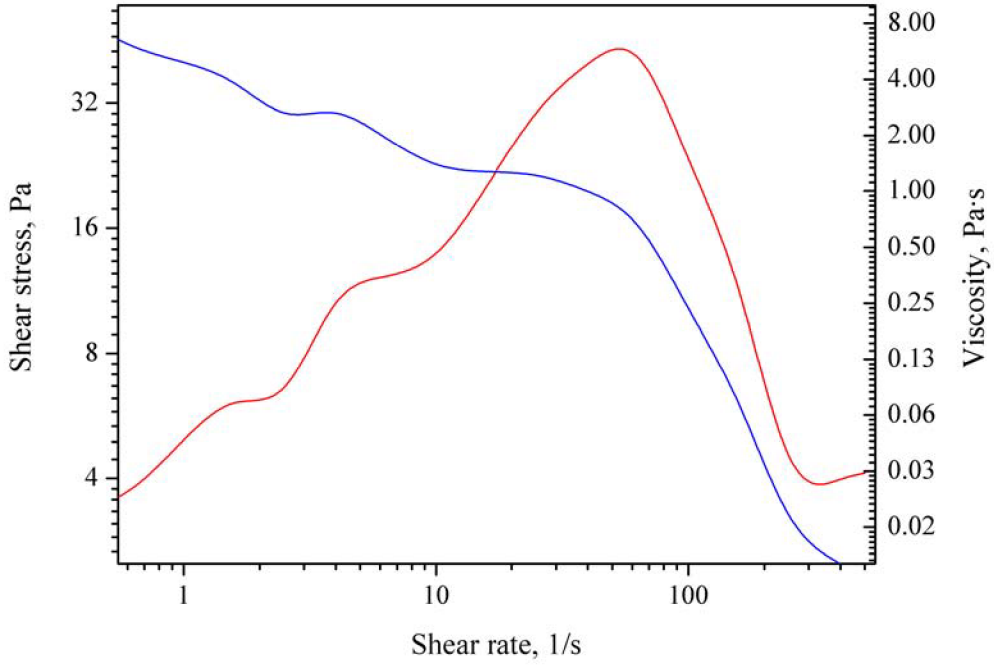

Figure 70 *The dependence of shear stress and shear rate (red line) and viscosity on shear rate (blue line).*

4.3.3 Profilometry

Dry film thickness was averaged from three measurements of varnish applied on Pyrex glass substrate. The varnish average dry thickness is 12 µm, when applied with Baker bar with wet film thickness of 60 µm.

Table 13 *Overview of dry varnish layer thicknesses*

Layer type	*Average layer thickness*	*Stylus vertical deviation*
clear varnish	11 µm	±2 µm
varnish + 10 w% AQ1	12 µm	±4 µm
varnish + 10 w% AQ2	12 µm	±5 µm
varnish + 10 w% AQ3	13 µm	±3 µm

4.3.4 Gloss measurement

Gloss of printed and blank (unprinted) and varnished and unvarnished paper samples were measured.

4.3.4.1 Unprinted, varnished paper

Measured gloss values on unprinted inkjet medium, Iford Smooth Pearl, is in accordance with the type of the semigloss medium. It is clear that varnishing this type of semi-gloss microporous inkjet paper has augmented its gloss by 70%. Addition of AQ3 has augmented the gloss value by 90% During the accelerated ageing gloss of unprinted paper samples mainly remained unchanged, when standard deviation is taken into consideration.

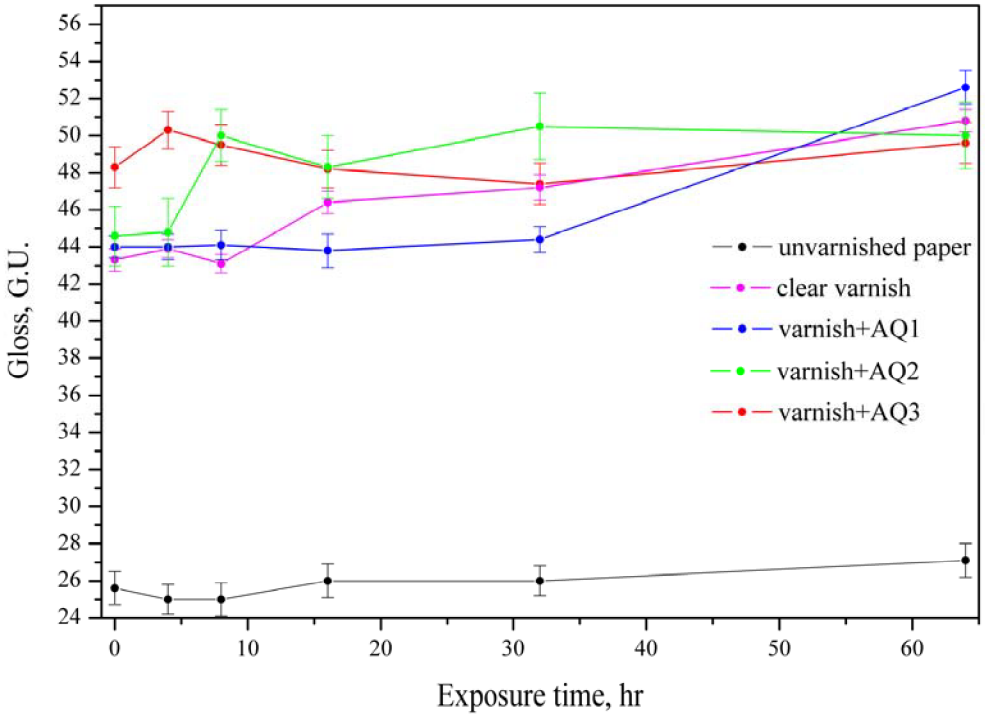

Figure 71 *Gloss values of unprinted Ilford smooth Pearl substrate during the accelerated ageing test done in Q-Sun test chamber.*

4.3.4.2 Test targets, varnished

Gloss was measured on three places on the printed target. Since the gloss is influenced by the colour of the substrate, three representative measuring positions were considered.

Claria, HP and MIS dye prints

In Figure 72, Figure 73 and Figure 74 are depicted measured gloss values of samples before and after the accelerated lightfastness test. The results show that after the test the gloss value have mostly changed. The possitive change in gloss, meaning risen value, is thought to be due to either colour change, since gloss is influenced by it and also by the effect of elevated temperature which might have smoothened the surface.

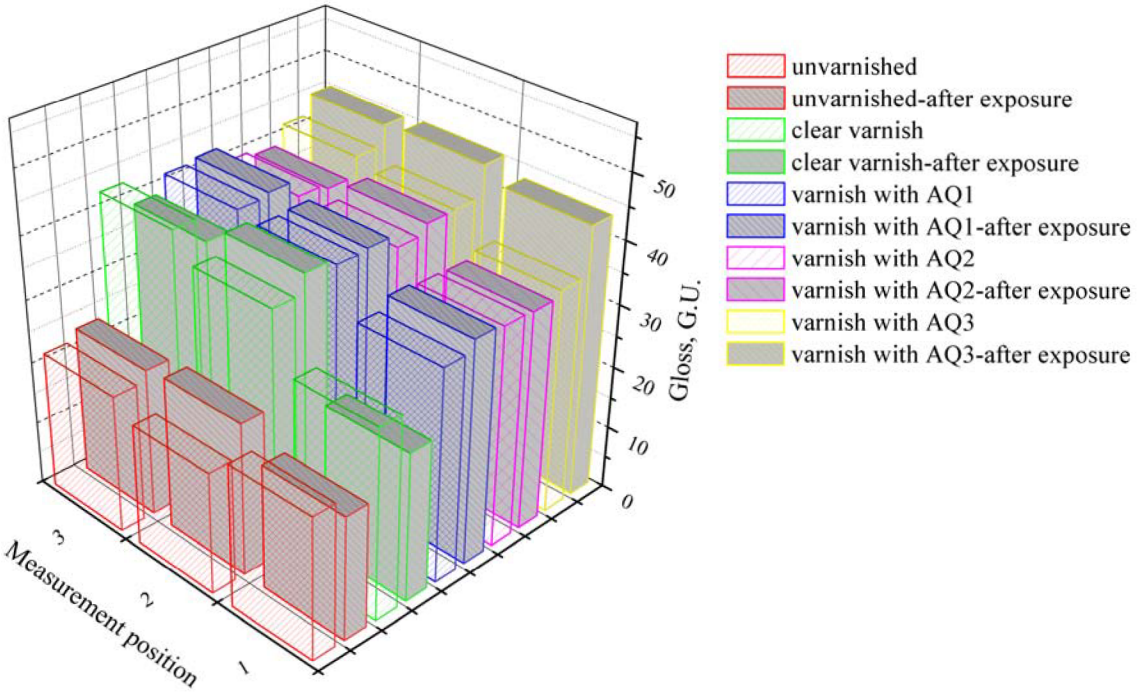

Figure 72 *Gloss measurement evaluation for Claria ink samples on Ilford Smooth Pearl paper*

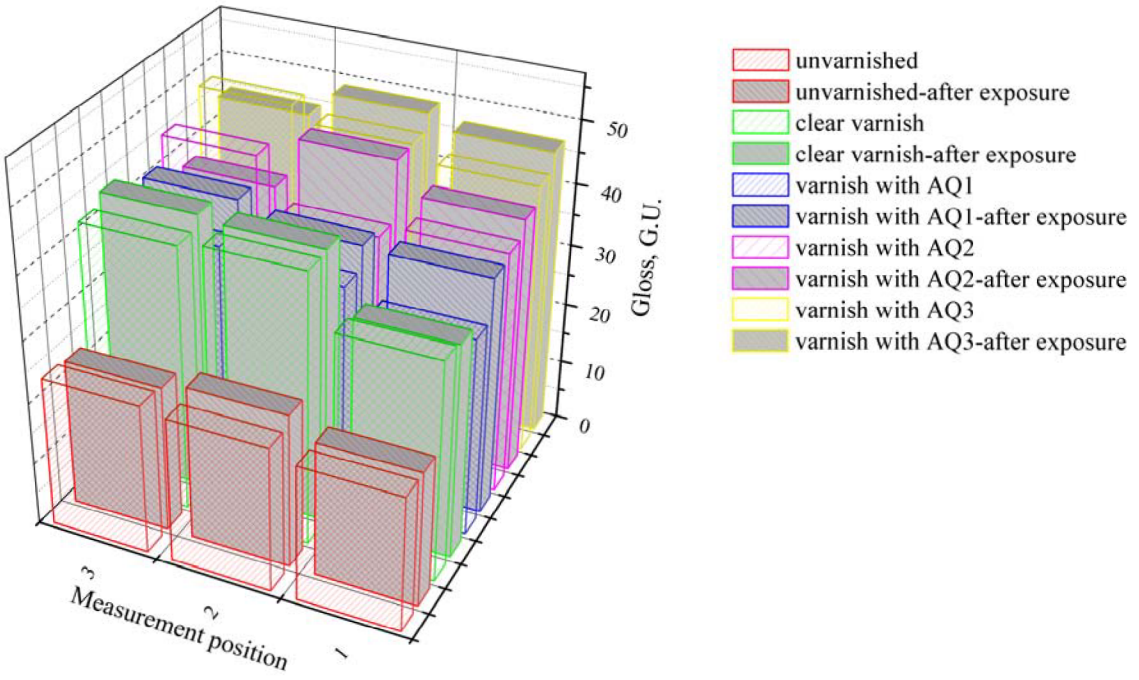

Figure 73 *Gloss measurement evaluation for HP ink samples on Ilford Smooth Pearl paper*

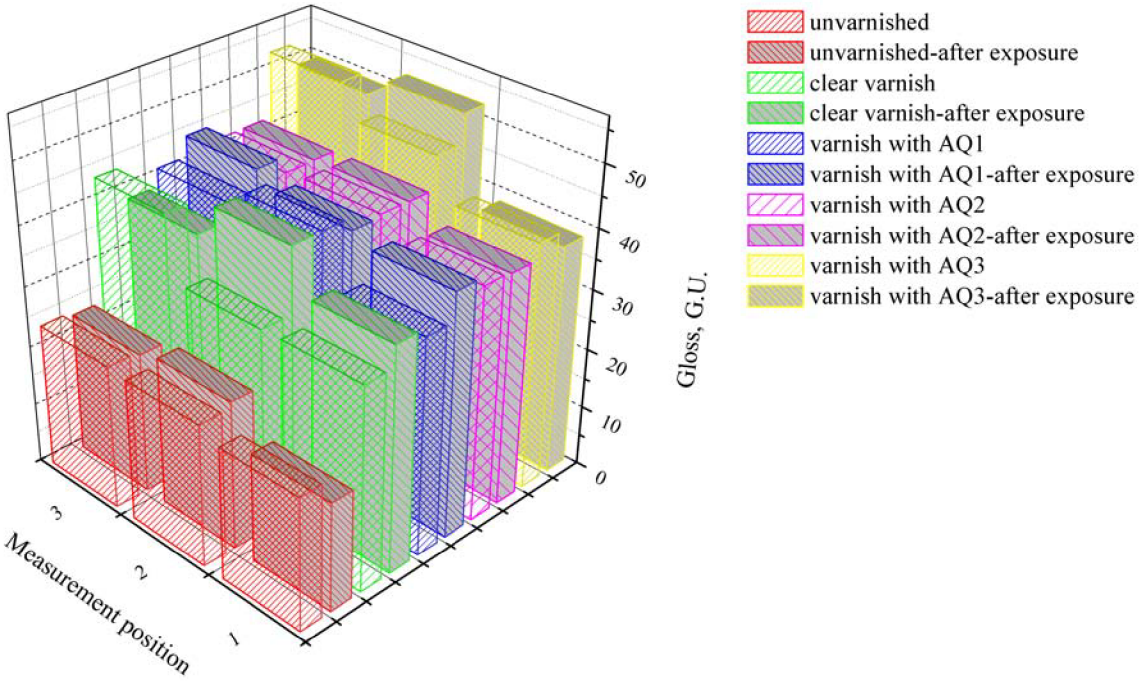

Figure 74 *Gloss measurement evaluation for MIS Dye ink samples on Ilford Smooth Pearl paper*

4.3.5 Colour change after varnish application

Unprinted paper (Table 14) and eight patches representing important colours (Table 15) on i-1.5 test target (Figure 49) were measured to determine the colour change after varnish application. Values of ΔL^*, Δa^*, Δb^* have been color-coded according to change in the colour space CIE $L^*a^*b^*$ (Figure 75) for better orientation in data values.

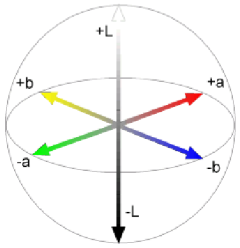

Figure 75 *CIE* L*a*b* *and also a color-coding legend*[121]

When unprinted paper was coated with clear varnish and varnishes with UV absorbers it has darkened and shifted its colour balance into blue-green.

Table 14 *A summary of colour change values after varnishing unprinted paper*

	clear varnish	*clear varnish+AQ1*	*clear varnish+AQ2*	*clear varnish+AQ3*
Δ*E*	5.5	7.5	7.6	7.8
Δ*L**	-2.2	-2.4	-2.5	-2.5
Δ*a**	-1.1	-1.6	-1.7	-1.8
Δ*b**	4.9	6.9	7.0	7.2

On Claria targets (Table 15) after varnishing the print lightness have mainly lowered, however the biggest difference was observable on off-white patch. Varnishing has also slightly shifted colour

balance to green. Varnish with AQ1 addition has moved the colour balance mainly to yellow-green; AQ3 on the other hand has shifted balance yellow-green and green-blue.

Table 15 *A summary of colour change values after varnishing on Claria test targets*

	Δ*L*	Δ*a**	Δ*b**	Δ*E* AQ1	Δ*L*	Δ*a**	Δ*b**	Δ*E* AQ2	Δ*L*	Δ*a**	Δ*b**	Δ*E* AQ3
red	−0.3	−0.6	1.9	2.0	0.4	−12.7	−0.4	12.8	−0.8	−0.4	−0.4	1.0
black	0.4	0.1	0.0	0.4	−0.2	0.2	0.6	0.7	0.3	−0.2	0.1	0.4
green	0.1	−2.0	1.3	2.3	−4.3	1.9	−3.0	5.5	−0.7	−0.7	−0.1	1.0
hot pink	−1.3	−1.4	−2.1	2.8	−6.5	−7.4	−4.9	11.0	−2.2	−2.8	−1.9	4.0
off white	−2.4	−0.1	2.5	3.4	−11.8	0.0	2.3	12.1	−4.6	−0.4	2.5	5.2
yellow	1.0	−1.2	0.2	1.6	1.5	−1.8	−2.3	3.3	1.7	−1.7	−0.8	2.6
grey	0.7	−5.9	0.4	5.9	−4.5	−2.9	−4.4	6.9	−0.9	−2.6	−5.2	5.9
blue	0.8	1.1	−2.6	2.9	−0.5	−3.4	1.8	3.9	0.3	−3.3	1.7	3.7

Coating HP test targets with varnish with addition of AQ1 has augmented the lightness and mainly shifted the colour balance to yellow and red.

Table 16 *A summary of colour change values after varnishing on HP test targets*

	Δ*L*	Δ*a**	Δ*b**	Δ*E* AQ1	Δ*L*	Δ*a**	Δ*b**	Δ*E* AQ2	Δ*L*	Δ*a**	Δ*b**	Δ*E* AQ3
red	3.0	8.5	1.7	9.2	−2.6	3.4	−1.6	4.6	−2.4	2.8	−4.2	5.5
black	3.9	2.1	1.4	4.6	0.1	2.9	0.0	2.9	0.6	0.4	−2.2	2.4
green	4.7	−6.4	−1.3	8.1	0.0	−1.0	−1.0	1.4	−1.9	0.6	−5.3	5.6
hot pink	1.5	−2.9	13.3	13.7	1.1	−3.2	8.6	9.2	1.3	−0.9	4.0	4.3
off white	6.6	1.0	3.4	7.5	−2.8	0.6	4.4	5.3	−1.8	1.2	2.9	3.6
yellow	3.5	−3.5	0.9	5.0	2.0	5.9	3.2	7.0	1.2	0.4	−2.7	2.9
grey	2.3	0.9	−2.6	3.6	−4.2	3.5	−6.2	8.3	−4.3	6.0	−8.0	10.9
blue	3.9	0.0	−3.0	4.9	−0.5	−2.7	5.8	6.4	−0.6	−3.2	5.3	6.2

Lightness values of MIS Dye test targets have mainly lowered with the application of varnish with UV absorbers, the only augmentation have been on red patches and yellow one. Mostly the balance have shifted on *b** axis to yellow and on *a** to green.

Table 17 *A summary of colour change values after varnishing on MIS Dye test targets*

	Δ*L*	Δ*a**	Δ*b**	Δ*E* AQ1	Δ*L*	Δ*a**	Δ*b**	Δ*E* AQ2	Δ*L*	Δ*a**	Δ*b**	Δ*E* AQ3
red	1.0	−0.1	1.1	1.5	1.7	−1.7	2.3	3.4	1.8	−1.6	2.4	3.4
black	−1.7	−2.4	4.1	5.0	−0.3	−2.7	1.2	2.9	−0.5	−2.6	1.1	2.8
green	−5.1	−2.0	−8.1	9.7	−3.6	−0.1	−10.2	10.8	−5.7	−1.3	−9.3	11.0
hot pink	−5.5	−0.2	3.0	6.3	−4.2	−2.0	1.6	4.9	−5.9	0.1	3.6	6.9
off white	−4.3	−0.3	1.2	4.5	−2.9	−0.3	1.9	3.5	−3.5	−0.2	1.3	3.7
yellow	2.6	2.6	4.8	6.0	−2.6	2.4	2.9	4.5	−1.2	2.2	−0.6	2.6
grey	−8.8	0.2	−15.4	17.8	−6.3	−0.5	−11.6	13.3	−4.8	0.5	−9.2	10.4
blue	−3.2	1.9	−0.2	3.7	−3.3	−0.2	0.9	3.4	−4.5	1.8	1.8	5.1

4.4 Fastness tests results

The results are in both fastness tests arranged in the same manner for HP, MIS Dye and Claria (in this exact order), first are results of commercial varnishes, then unvarnished print, clear varnish and 5 and 10 w% addition of each UV absorber.

4.4.1 Accelerated lightfastness test

4.4.1.1 Light conditions

Samples were exposed in Q-Sun test chamber with parameters summarized in Table 11 to the radiation simulating the daylight. In Table 18 are measured illuminance values corresponding to set irradiances on Q-Sun xenon test chamber.

Table 18 *Spectral irradiance setting intensities on Q-Sun xenon test chamber and its corresponding irradiance and illuminance intensities measured with optometer X1$_1$. Values in bold correspond to the recommended setting in ASTM F2366 standard.*

Spectral irradiance, W·m^{-2} at 340 nm	***Irradiance UV-A, W·m^{-2}***	***Illuminance, klx***
0.25	15.55	38.7
0.30	18.11	47.6
0.35	**21.79**	**55.2**
0.40	24.13	58.5
0.45	28.07	66.2

For calculation of exposure doses and equivalent lifetime was used averaged value of illuminance (Table 19). Exposure doses were calculated as a product of either average illuminance or irradiance (measured with optometerX1$_1$) and time. Values of exposure doses for particular test steps and their equivalent lifetime are in Table 20. Equivalent lifetime has been calculated according to the equation 21.

Table 19 *Irradiance and illuminance values measured with optometer X1$_1$, for 0.35 W·m^{-2} at 340 nm irradiance intensity on Q-Sun xenon test chamber*

	Irradiance UV-A, W·m^{-2}	***Illuminance, klx***
measurement	**kW·m^{-2}**	**klx**
1	20.46	55.5
2	21.08	55.7
3	21.60	57.0
4	21.22	57.1
5	21.02	52.8
6	20.76	56.4
average	**21.0**	**55.8**
SD	0.39	1.59

Table 20 *Values of time and their corresponding exposure doses and equivalent lifetime in Q-Sun test chamber*

Time, h	***Exposure dose, klx·h***	***Equivalent lifetime, months***
4	223	1.4
8	446	2.8
16	892	5.5
32	1784	11.0
48	2676	16.5
64	3568	22.0
80	4460	27.5
96	5352	33.0
112	6244	38.5
128	7136	44.0
144	8028	49.6
160	8920	55.1
176	9812	60.6
192	10704	66.1
208	11596	71.6
224	12488	77.1
240	13380	82.6
256	14272	88.1
272	15164	93.6
288	16056	99.1
304	16948	104.6

4.4.1.2 Commercial varnishes

HP

Inkjet print made on printer HP 500 PS with HP dye-based ink set on ISP paper, varnished with three commercial light protective varnishes Hahnemühle, Tetenal and Herma. The least stable is print protected with Herma varnish; it has reached the test endpoint criterion after 48 hours (2676 klx·h). Print varnished with Hahnemühle varnish reached the test threshold in 64 hours (3568 klx·h). And print varnished with Tetenal has reached the endpoint in 64 klx·h. The unvarnished sample (Figure 79) reached endpoint criterion after 1784 klx·h.

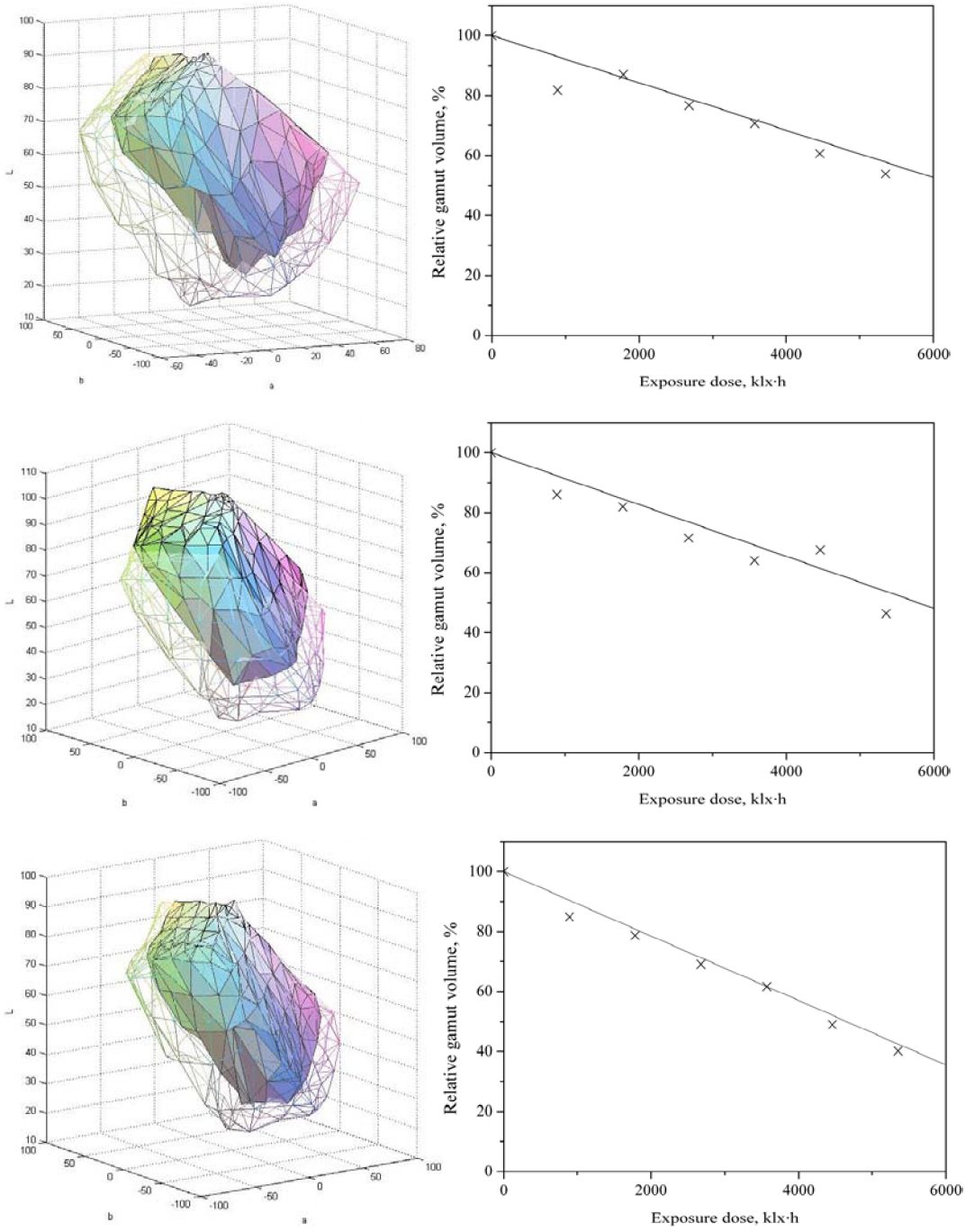

Figure 76 *Change in relative gamut volume of inkjet prints made with printer HP 500PS and HP dye-based ink set on ISP paper after accelerated lightfastness test done in Q-Sun xenon test chamber – sprayed with Hahnemühle(front row), Tetenal (middle row), Herma (bottom row) varnishes.*

MIS DYE

Inkjet print made on printer Epson Stylus Photo P50 with MIS Associates MIS Dye dye-based ink set on ISP paper, varnished with three commercial light protective varnishes Hahnemühle, Tetenal and Herma. The least stable have been print varnished with Tetenal varnish, it has lost 30% of its relative gamut volume in 80 hours of exposure (4460 klx·h). Print varnished with Tetenal have reached the endpoint criterion in 112 hours of exposure (6240 klx·h) and Hahnemühle-varnished one in 192 hours (10704 klx·h).

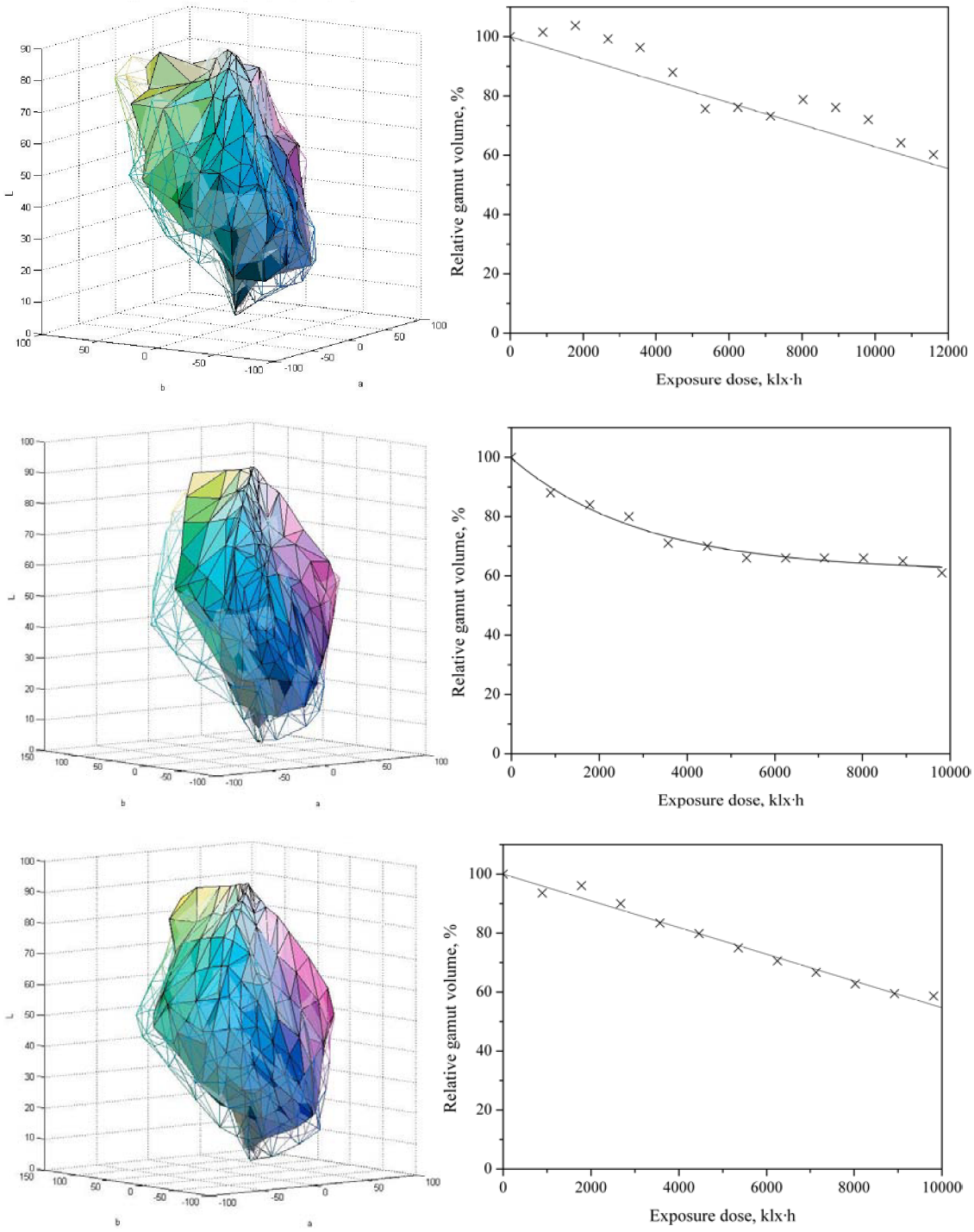

Figure 77 *Change in relative gamut volume of inkjet prints made with printer Epson Stylus Photo P50 and MIS Dye dye-based MIS Associates ink set on ISP paper after accelerated lightfastness test done in Q-Sun xenon test chamber – sprayed with Hahnemühle(front row), Tetenal (middle row), Herma (bottom row) varnishes.*

Claria

Inkjet print made on printer Epson Stylus Photo P50 with Epson Claria dye-based ink set on ISP paper, varnished with three commercial light protective varnishes Hahnemühle, Tetenal and Herma. Claria inks proved to be the most stable, from the tested ones. In comparison with unvarnished test target (Figure 87), which had after exposure dose 13380 klx·h (240 hours) retained 82% of its original relative gamut volume; the application of protective varnishes had improved lightfastness. Prints varnished with Herma and Tetenal varnish, both have retained 88% of original relative gamut volume after 240 hours. Sample with Hahnemühle has after the same exposure dose retained 94%.

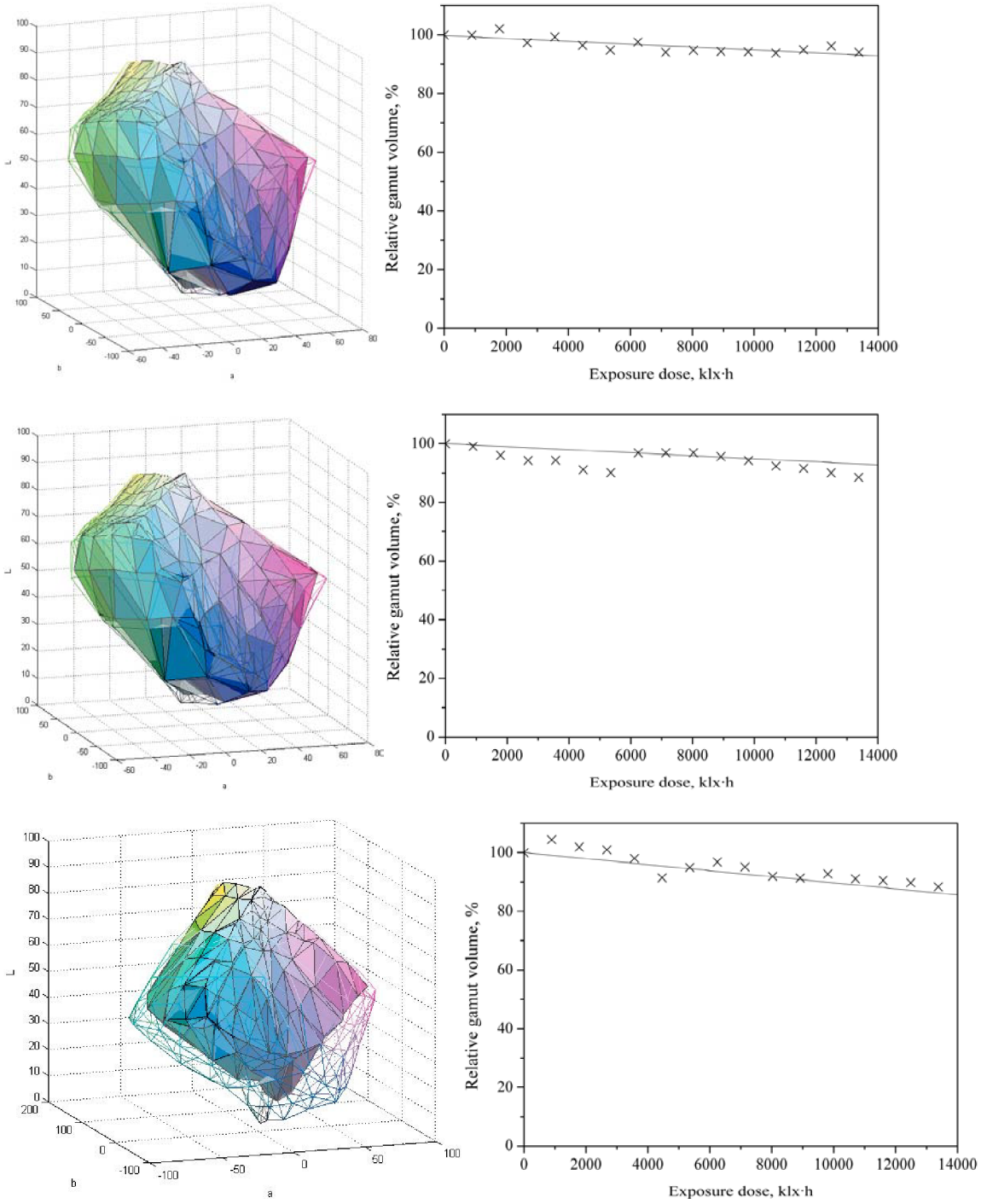

Figure 78 *Change in relative gamut volume of inkjet prints made with printer Epson Stylus Photo P50 and dye-based Epson Claria inks on ISP paper after accelerated lightfastness test done in Q-Sun xenon test chamber – sprayed with Hahnemühle (front row), Tetenal (middle row), Herma (bottom row) varnishes.*

4.4.1.3 Prepared varnish composition

HP

This type of printer substrate and ink combination doesn't belong among the stable ones. The unprotected print have reached the threshold value of 70% of gamut volume loss after 32 hours of exposure, which corresponds to 1784 klx·h. From the graph depicting plot of gamut volume loss and exposure dose (Figure 79-top right) the degradation shows exponential decay, so it can be assumed that the degradation process adheres to the kinetics of the first order.

The print protected by the prepared composition has degraded in the same manner and the threshold value was reached also after 32 hours of exposure (1784 klx·h). But the process of degradation is less pronounced, has slower course. It can be seen also on the gamut visualizations on Figure 79-left, where the gamut of protected print has shrunken down symmetrically and doesn't have split in around L axis.

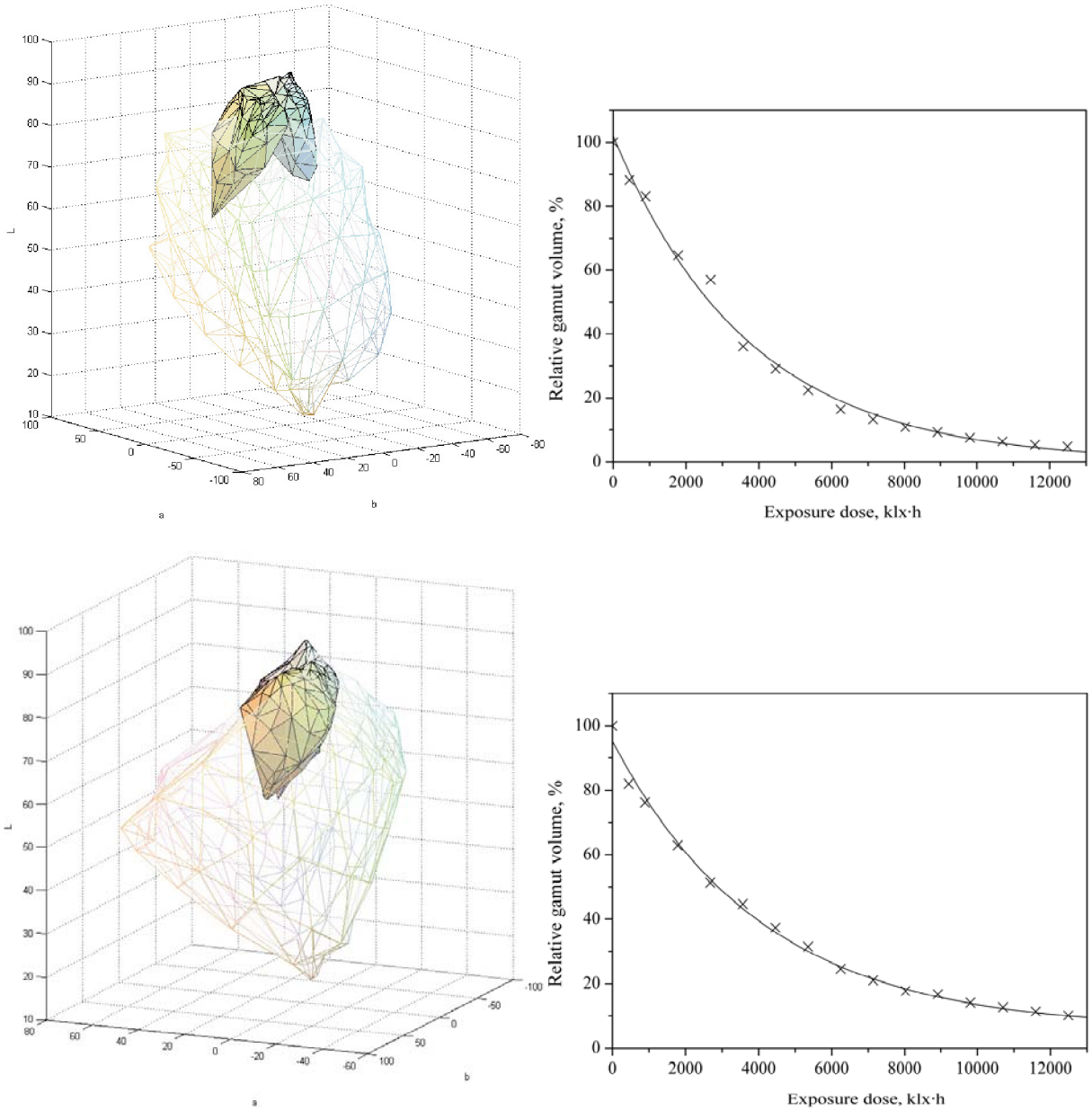

Figure 79 *Change in relative gamut volume of inkjet prints made with printer HP 500PS and HP dye-based ink set on ISP paper after accelerated lightfastness test done in Q-Sun xenon test chamber – unvarnished (first row), prepared composition – clear varnish (second row)*

Addition of UV absorber changed the progression of the degradation process. The addition of 5 weight percent didn't augment the light stability; the threshold has been reached after 32 hours of exposure, but the degradation progress have changed. After quite rapid gamut volume loss in the first two exposure steps, the decrease continued more or less linearly.

The double amount, 10 weight percent addition, shows that there is influence on the stability. The threshold value has been reached after 96 hours of exposure, which equals to exposure dose of 5352 klx·h. Also the progress has changed a little, instead of exponential or linear it's more step like.

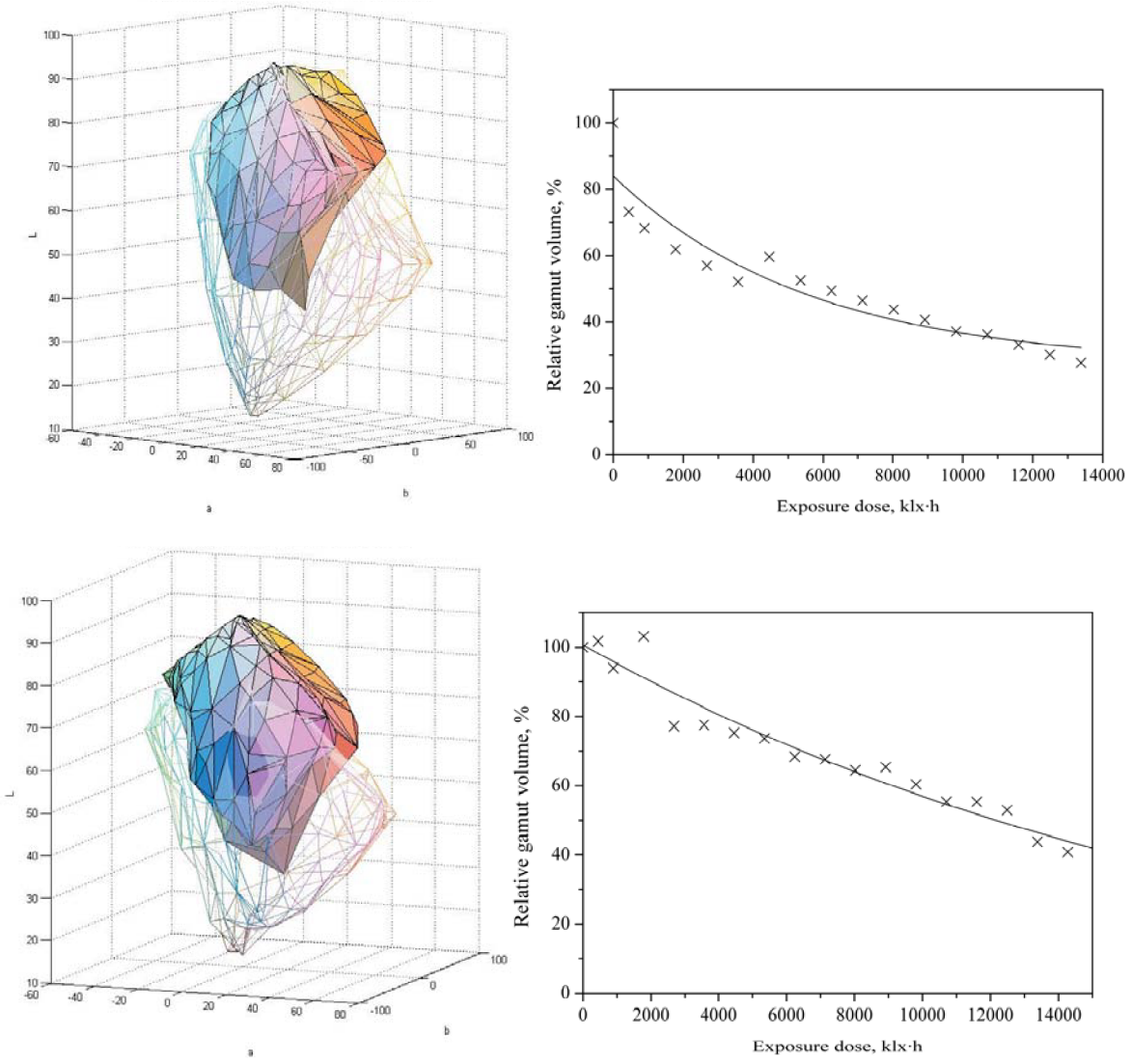

Figure 80 *Change in relative gamut volume of inkjet prints made with printer HP 500PS and HP dye-based ink set on ISP paper after accelerated lightfastness test done in Q-Sun xenon test chamber; varnish with 5w% addition of AQ1(first row), varnish with 10w% addition of AQ1 (second row)*

In case of 5 weight percent addition of UV absorber AQ2 the threshold has been reached after 64 hours of exposure. The progress of the degradation is still similar to exponential decay, thus first order kinetics. But the step like progress is slightly recognizable.

Step like progress is more pronounced in case of 10 percent weight addition of UV absorber AQ2. The threshold has been achieved in 64 hours as well.

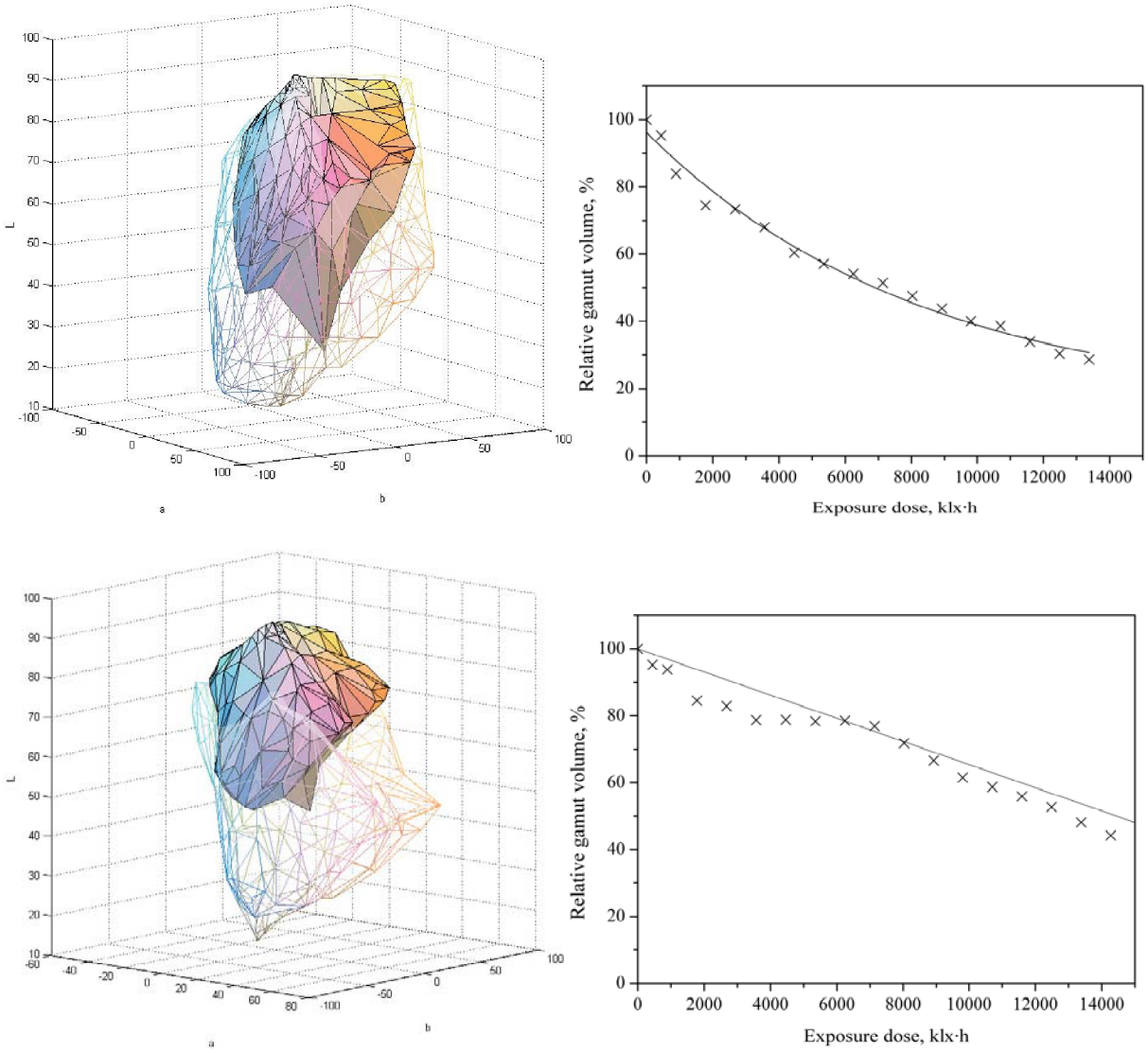

Figure 81 *Change in relative gamut volume of inkjet prints made with printer HP 500PS and HP dye-based ink set on ISP paper after accelerated lightfastness test done in Q-Sun xenon test chamber; varnish with 5w% addition of AQ2 (first row), varnish with 10w% addition of AQ2 (second row)*

Influence of the addition of UV absorber AQ3 is not so much visible on the degradation curves of both 5 and 10 weight percent as well as on the light protection. Both test targets varnished with composition with 5w% AQ3 has reached the treshold value of 30% gamut loss in 80 hours of exposure, which is equal to 4460 klx·h exposure dose.

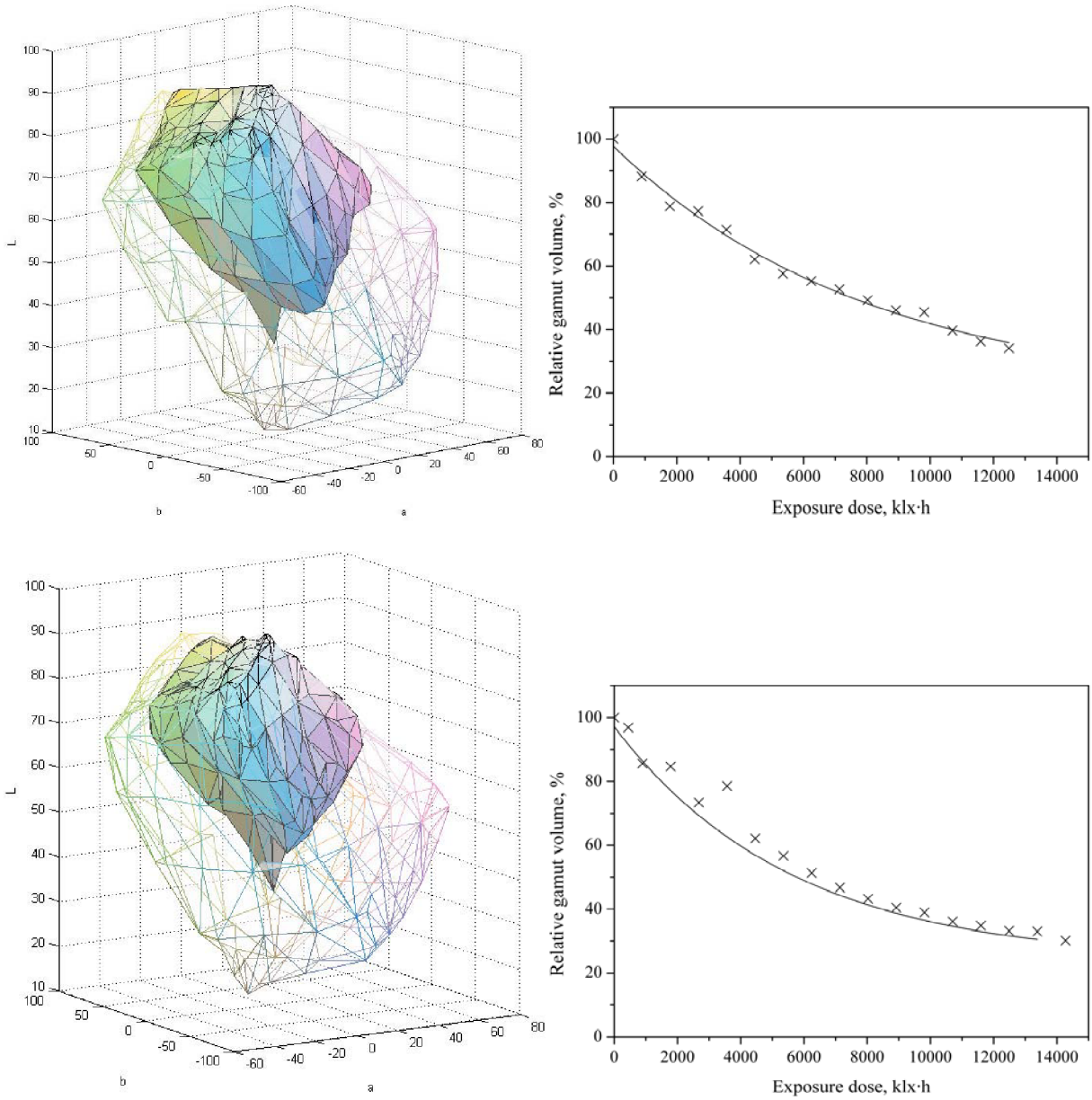

Figure 82 *Change in relative gamut volume of inkjet prints made with printer HP 500PS and HP dye-based ink set on ISP paper after accelerated lightfastness test done in Q-Sun xenon test chamber; varnish with 5w% addition of AQ3 (first row), varnish with 10w% addition of AQ3 (second row)*

MIS Dye

The unprotected MIS Dye print has reached the threshold after 32 hours of exposure (1784 klx·h). With such exponential decay curve, it can be assumed that the degradation process goes by the first order kinetics. Clear varnish protected print resembles with decay more linear decrease of the gamut volume. The 30% gamut volume loss has been reached after 128 hours of exposure (7136 klx·h).

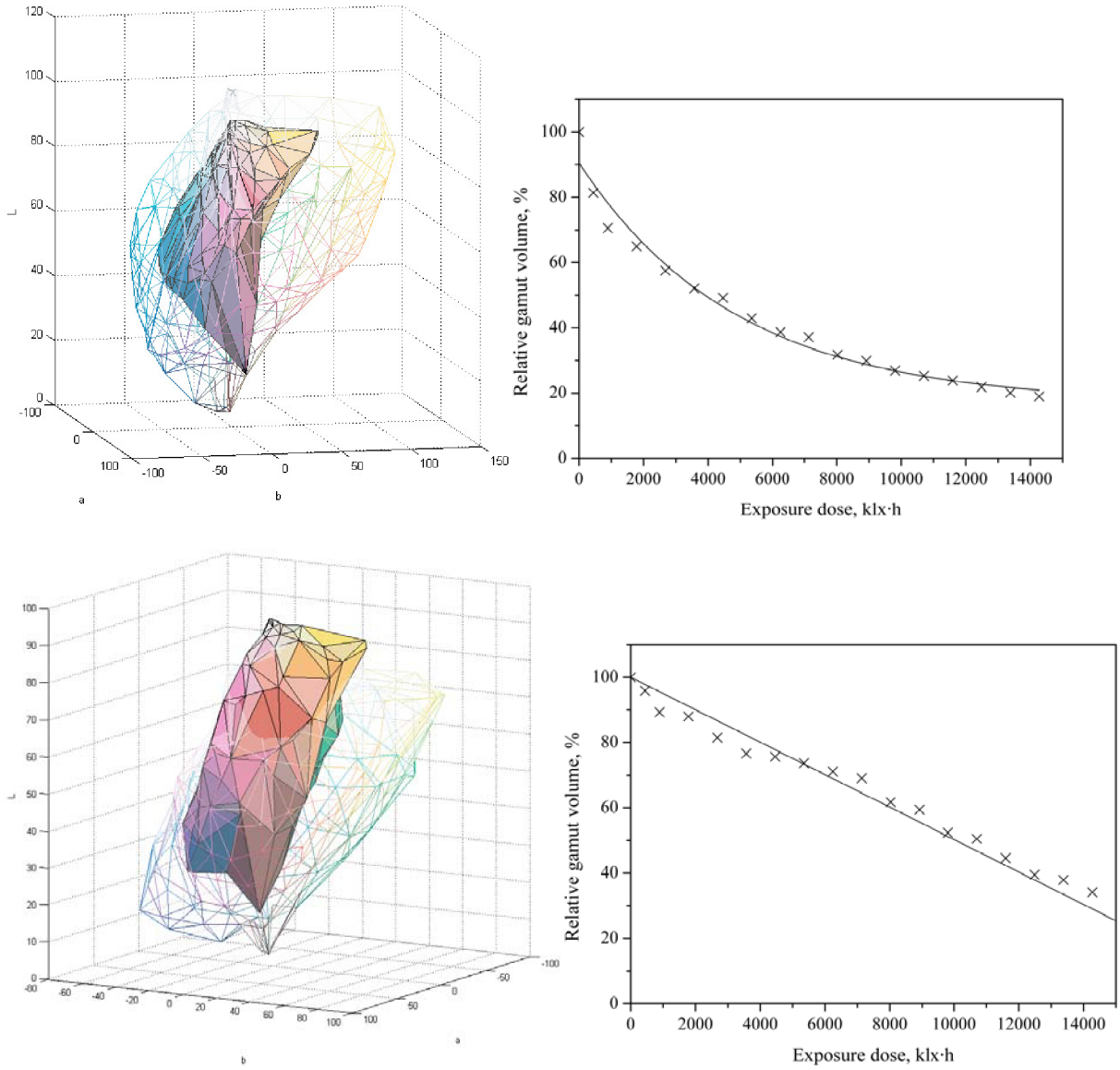

Figure 83 *Change in relative gamut volume of inkjet prints made with Epson Stylus Photo P50 printer and MIS Dye dye-based ink set on ISP paper after accelerated lightfastness test done in Q-Sun xenon test chamber; unvarnished (first row); prepared composition clear varnish (second row)*

With the addition of UV absorbers into the varnish has changed the degradation progress. In case of 5w% addition of AQ1 the curve of first order degradation is after first three exposure doses more or less linear. The sample has reached the endpoint criterion value of 70% gamut volume loss in 112 hours (6244 klx·h).

In case of 10w% addition of AQ1 absorber the difference in shape of degradation process curve is even more pronounced and exponential has been replaced by more step-like shape. And the print has faded under the acceptable criterion in 160 hours of exposure (8920 klx·h).

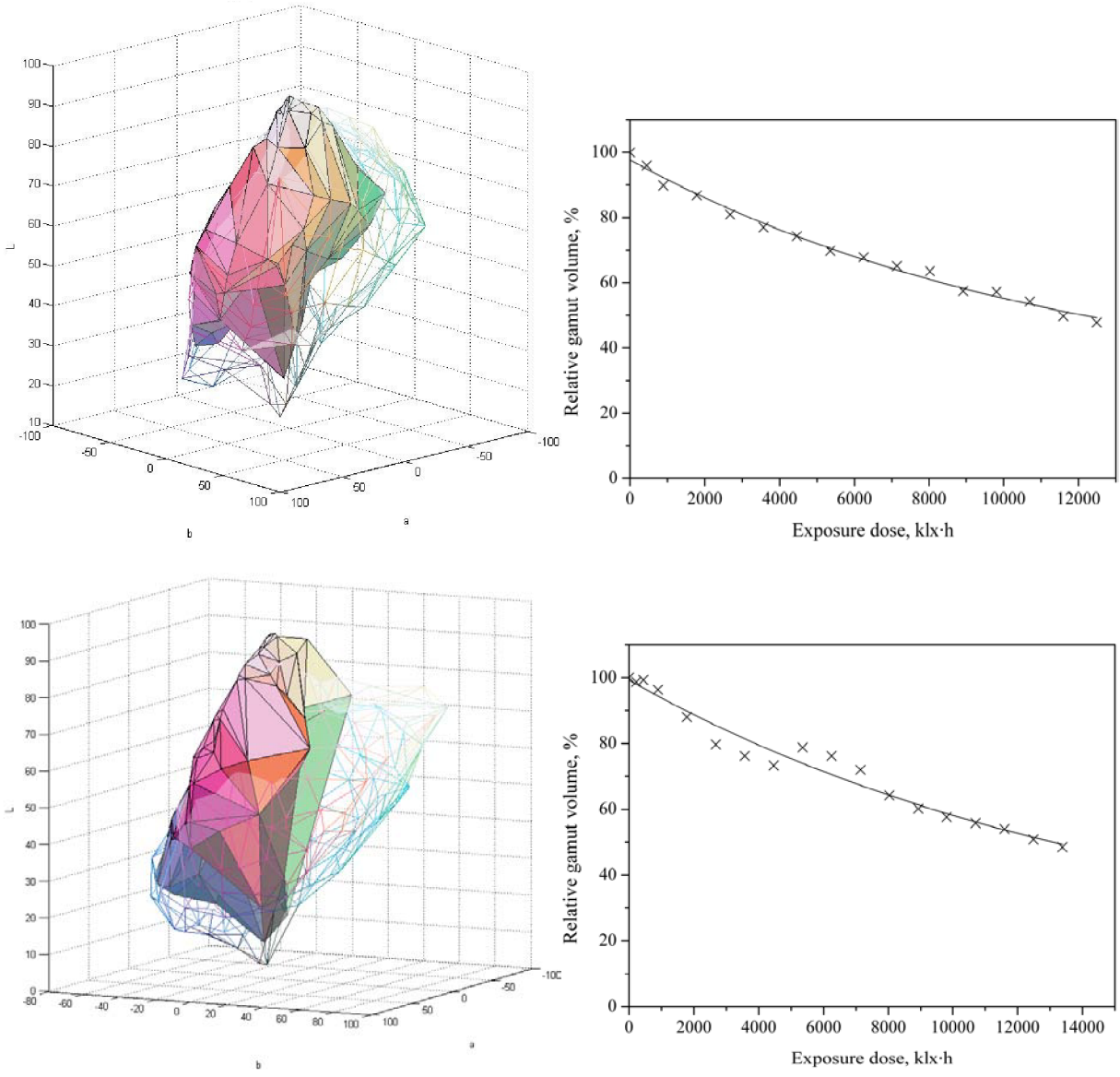

Figure 84 *Change in relative gamut volume of inkjet prints made with Epson Stylus Photo P50 printer and MIS Dye dye-based ink set on ISP paper after accelerated lightfastness test done in Q-Sun xenon test chamber; varnish with 5w% addition of AQ1 (first row), varnish with 10w% addition of AQ1 (second row)*

As well as previous sample with addition of 5w% UV absorber the degradation has been still exponential in the first part of the curve, so it can be assumed that the inks degrade with first order kinetics. When the amount of UV absorber is doubled, the change in the change is no longer following the exponential degradation of the first order kinetics. In first case of 5% UV absorber addition, the print reached 30% gamut volume loss in 64 hours (3568 klx·h), but when its amount is doubled the threshold is achieved after 160 hours of exposure (8920 klx·h).

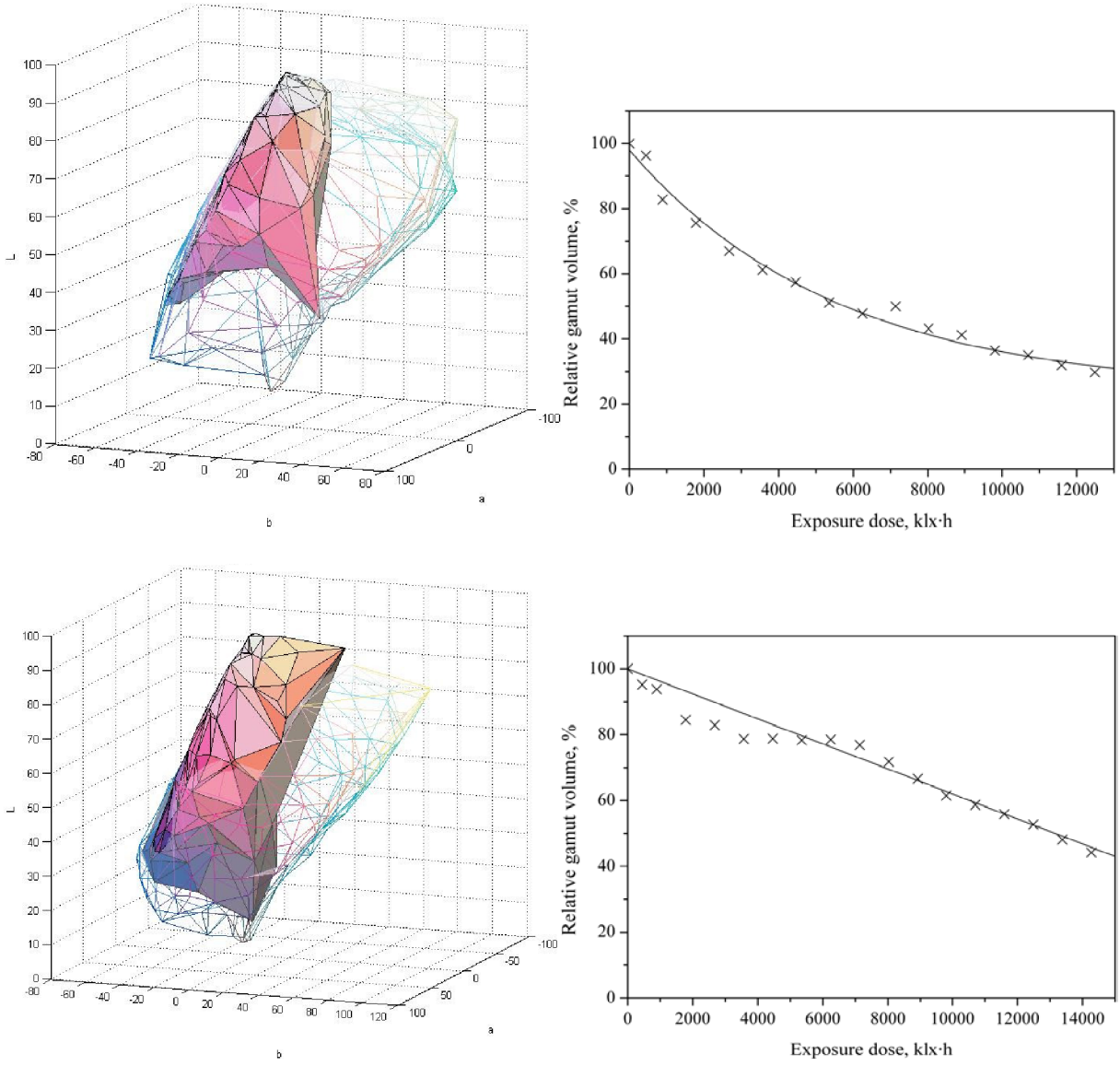

Figure 85 *Change in relative gamut volume of inkjet prints made with Epson Stylus Photo P50 printer and MIS Dye dye-based ink set on ISP paper after accelerated lightfastness test done in Q-Sun xenon test chamber; varnish with 5w% addition of AQ2 (first row), varnish with 10w% addition of AQ2 (second row)*

In case of prints protected with UV absorber AQ3, in both cases the degradation progressed in exponencial manner. In case of 5w% addition ov AQ3 the treshold has been achieved after 80 hours of exposure (4460 klx·h) and in case of 10w% after 96 hours (5352 klx·h).

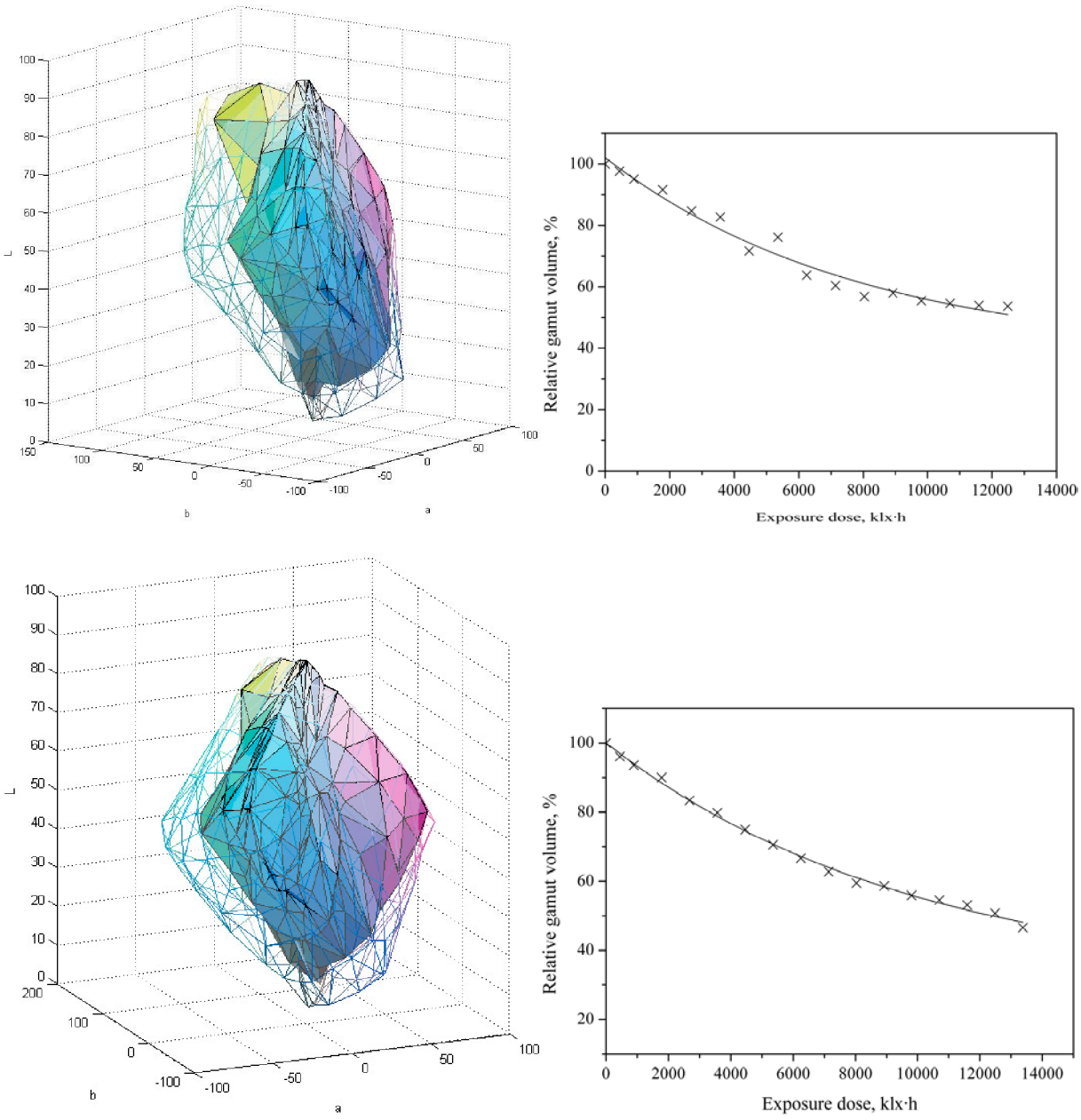

Figure 86 *Change in relative gamut volume of inkjet prints made with Epson Stylus Photo P50 printer and MIS Dye dye-based ink set on ISP paper after accelerated lightfastness test done in Q-Sun xenon test chamber; varnish with 5w% addition of AQ3 (first row), varnish with 10w% addition of AQ3 (second row)*

Claria

Claria inks belong among very stable ones, even if the are dye-based inks. The stability of unprotected sample is shown in the Figure 87, where after 304 hours of exposure the print is quite stable and the gamut volume ia at 78% of relative gamut volume.

With the application of clear varnish, the stability has been enhanced and after 304 hours of exposure (16948 klx·h) the print still retained 83% of its original gamut volume (Figure 87-bottom row). In Figure 88 and Figure 89**,** there are degration curves for prints varnished with composition and 5w% and 10w% addition of UV absorbers AQ1, AQ2, AQ3. With all three uv absorbers the degradation was greater with the higer addition of UV absorber.

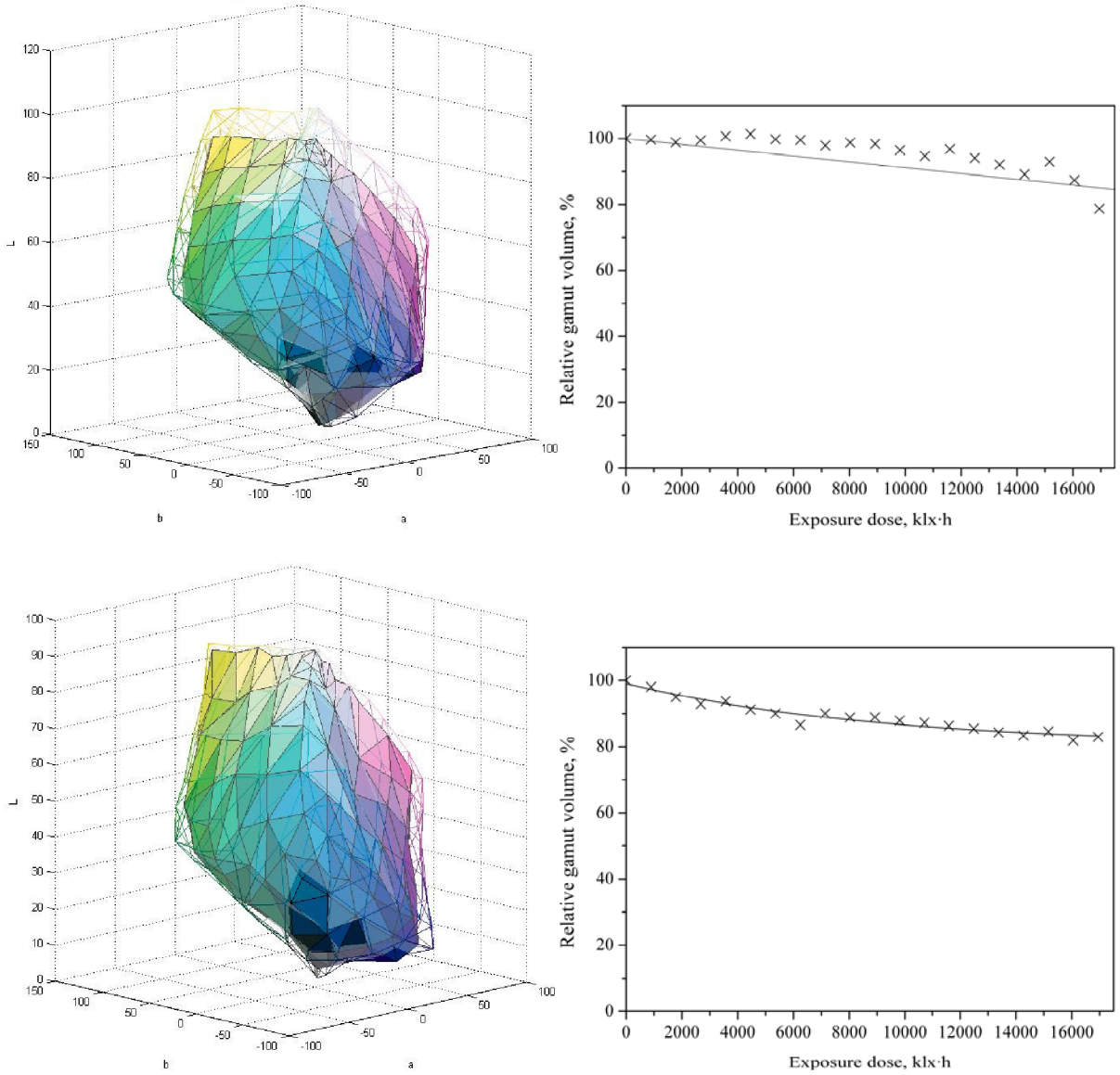

Figure 87 *Change in relative gamut volume of inkjet prints made with Epson Stylus Photo P50 printer and Epson Claria dye-based ink set on ISP paper after accelerated lightfastness test done in Q-Sun xenon test chamber; unvarnished (first row), prepared composition-clear varnish (second row)*

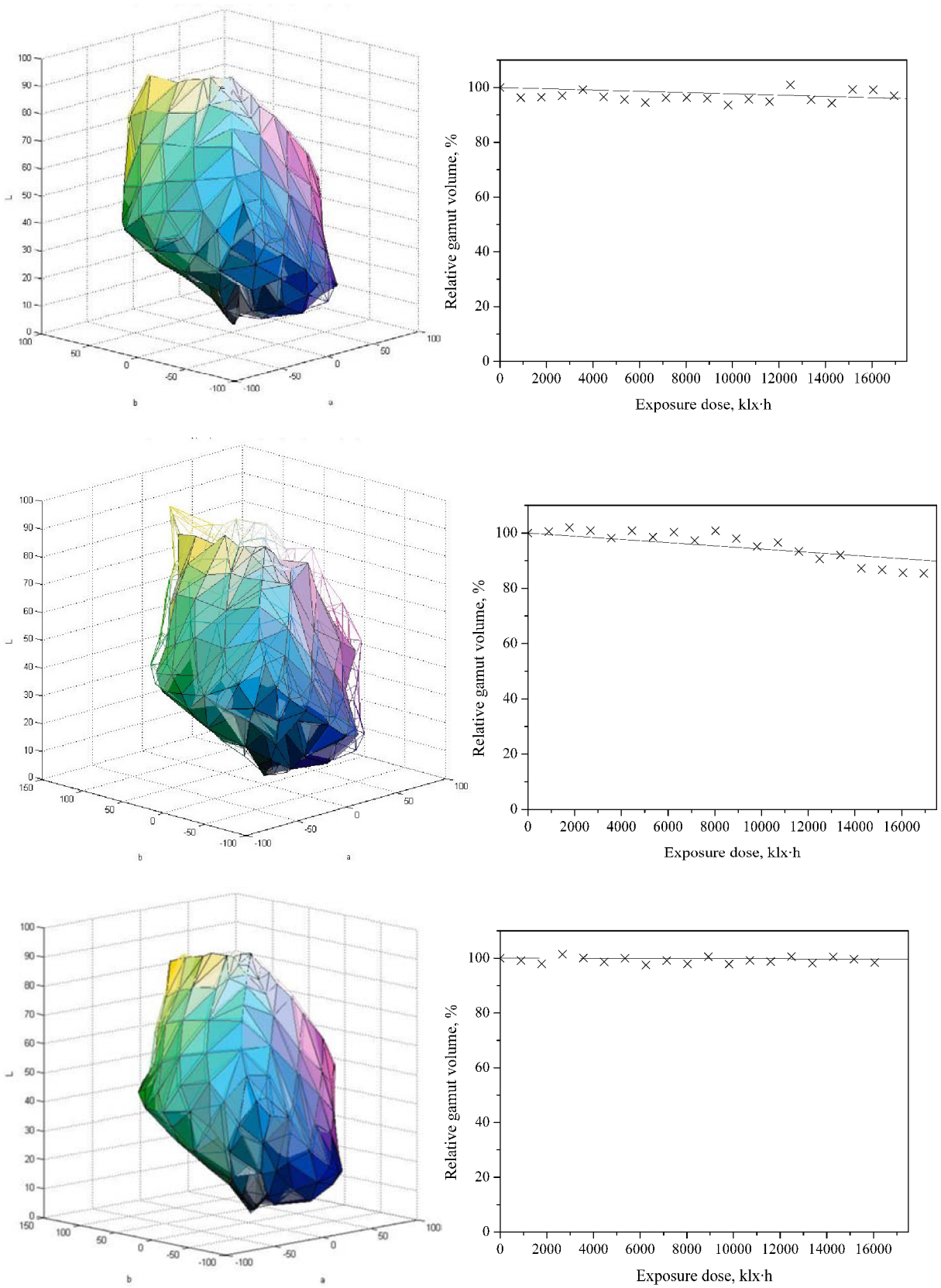

Figure 88 *Change in relative gamut volume of inkjet prints made with Epson Stylus Photo P50 printer and Epson Claria dye-based ink set on ISP paper after accelerated lightfastness test done in Q-Sun xenon test chamber; varnish with 5w% addition of AQ1 (first row), varnish with 10w% addition of AQ1 (second row) and 5w% addition of AQ2 (third row)*

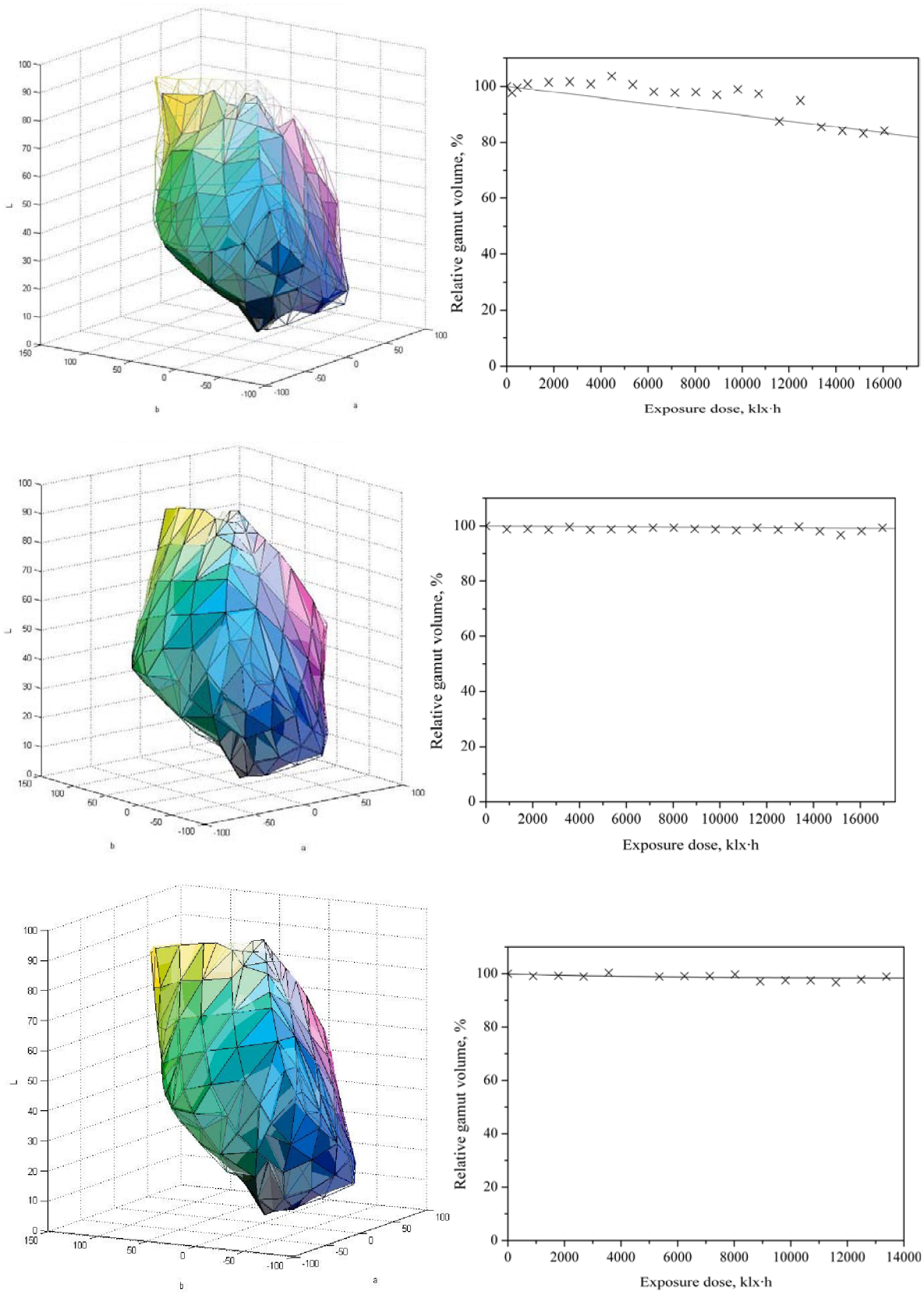

Figure 89 *Change in relative gamut volume of inkjet prints made with Epson Stylus Photo P50 printer and Epson Claria dye-based ink set on ISP paper after accelerated lightfastness test done in Q-Sun xenon test chamber; varnish with 10w% addition of AQ2 (first row), varnish with 5w% addition of AQ3 (second row) and 10w% addition of AQ3 (third row)*

4.4.2 Accelerated lightfastness test-Summary

In next three figures (Figure 90, Figure 91 and Figure 92) there are summaries of exposure doses that took or would take to 30% relative gamut volume loss. This exposure dose has been recalculated to equivalent lifetime in months.

Unvarnished and varnished with clear varnish HP print has faded very quickly and reached the endpoint criterion of 30% relative gamut volume in 10 hours of exposure, which is approximately 4 months of exposure in real conditions. From the commercial varnishes the best result has achieved the Hahnemühle protective varnish in 32 hours of exposure (11 months) has lost 30% of relative gamut volume. Tetenal varnished print has achieved the endpoint criterion in 28 hours (10 months) and Herma varnish in 16 hours (6 months).

From prints protected with prepared composition with UV absorber additions, the best results have shown print with 10w% AQ1. Other two AQ2 and AQ3 have produced similar protection (57–65 hours; 20–23 months of exposure in real conditions).

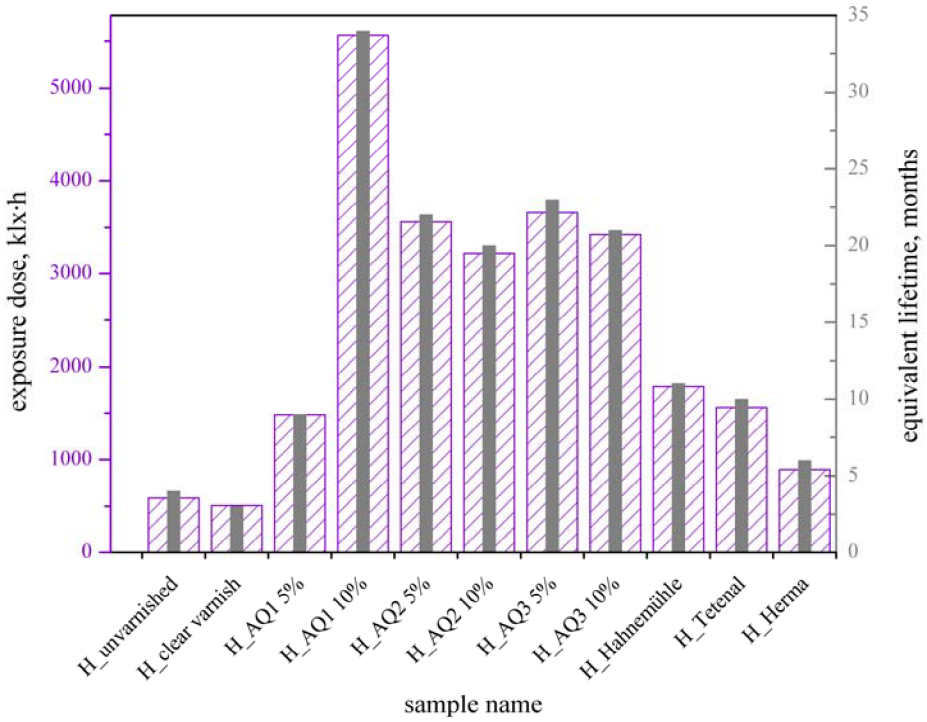

Figure 90 *Exposure dose needed to achieve 30% relative gamut volume loss for inkjet prints made on HP 500 PS printer, HP dye-based ink set and ISP paper.*

Unvarnished MIS Dye print would have take approx. 11 months before it would loose 30% of its relative gamut volume. From Figure 91 it is clear that any form of varnishing prolongs the equivalet lifetime. Comparable results and high protection provided clear varnish varnish with 10w% of AQ1 and AQ2 and also Hahnemuhle print as well.

Interpretation of certain Epson Claria prints results made on ISG substrate should be approached with caution (Figure 91). Prints protected with 5w% of AQ2, 5 and 10w% of AQ3 shown throughout the test duration extreme lightfastness, but it cannot be expected to continue with this behaviour further on. Even thou the calculated equivalent lifetime is exceedingly optimistic, it is assumed that the reciprocity law has failed and the real–time degradation will proceed in different manner.

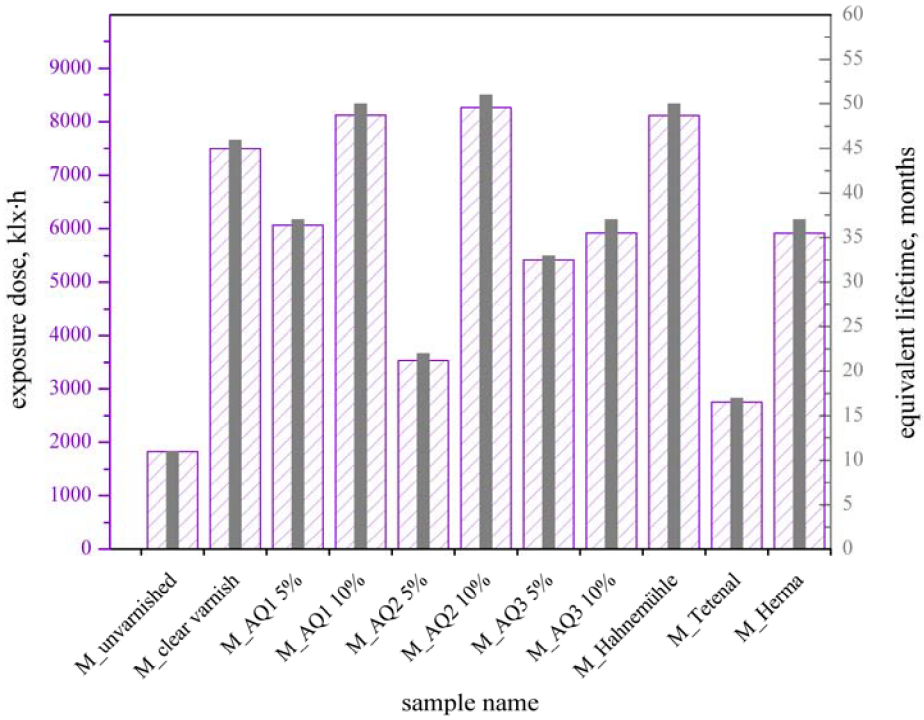

Figure 91 *Exposure dose needed to achieve 30% relative gamut volume loss for inkjet prints made on Epson Stylus Photo P50 printer, MIS Dye dye-based ink set and ISP paper.*

Negative value of exposure dose needed to reach threshold value at print protected with 5w% of AQ1 is caused by almost steady level of its relative gamut volume (Figure 88). It has oscillated around relative gamut volume of 100%, it has rather increased, thus the negative value.

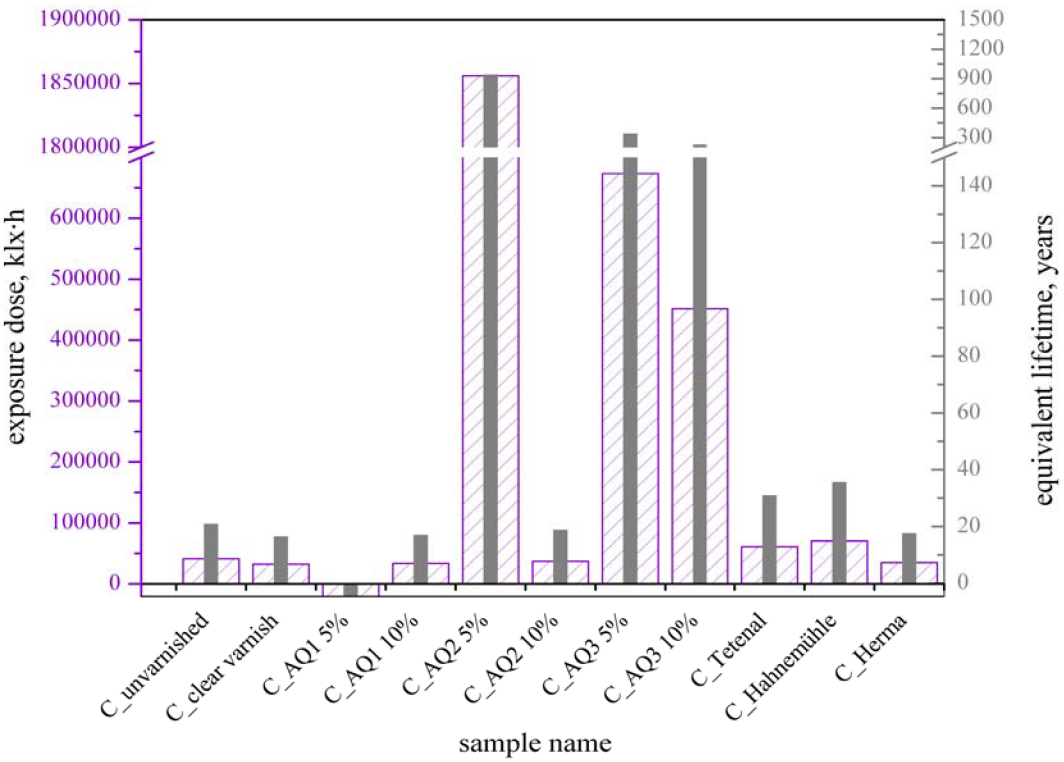

Figure 92 *Exposure dose needed to achieve 30% relative gamut volume loss for inkjet prints made on Epson Stylus Photo P50 printer, Epson Claria dye-based ink set and ISP paper.*

4.4.3 Ozone fastness test

4.4.3.1 Ozone absorption spectra and an exposure dose calculation

Concentration of generated ozone was determined by spectrophotometrical method. From measured absorbance value at 254 nm an ozone concentration is calculated from Lambert-Beers law.

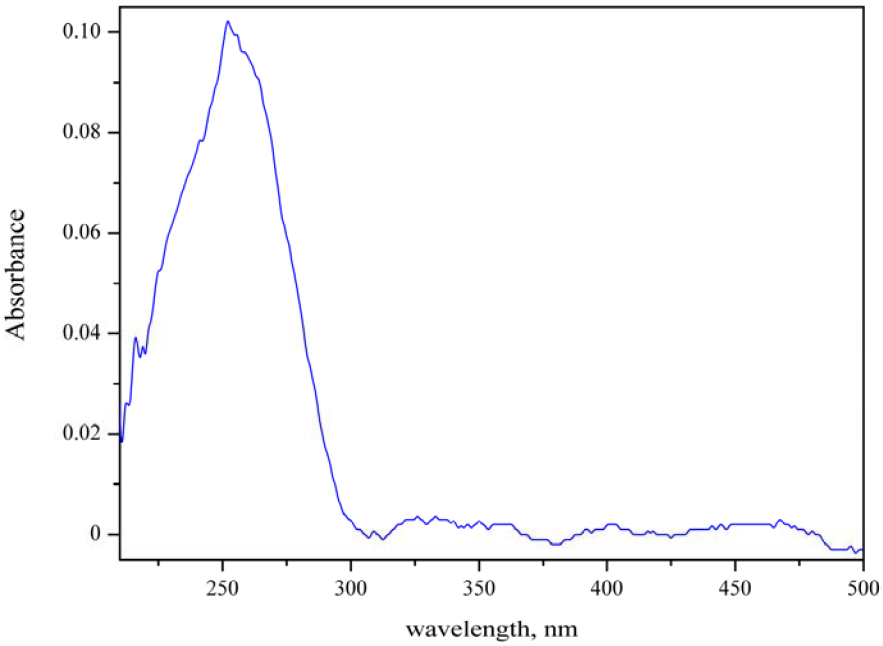

Figure 93 *Absorbance spectrum of reaction gas with ozone measured with Ocean Optics Red Tide spectrometer*

$$c = \frac{A}{\varepsilon \cdot l} = \frac{0.1}{3000(\text{at } 254 \text{ nm}) \cdot 10} = 3{,}333 \cdot 10^{-6}\text{mol}\cdot\text{dm}^3 \quad (23)$$

From the ozone concentration an exposure dose in ppm·h was calculated from ideal gas law, where ozone behaviour was considered ideal was calculated the volume of the ozone in the reaction chamber.

$$V = \frac{n \cdot R \cdot T}{p} = \frac{3.333 \cdot 10^{-6} \cdot 8.314 \cdot 298.15}{101325} = 8.15 \cdot 10^{-8}\text{m}^3 \quad (24)$$

Ozone concentration in the test chamber for previously mentioned setting (Ch. 3.6.2) is 81.5 ppm per hour. An overview of exposure steps and their equivalent ozone exposure doses is in Table 21. Also accelerated ozone doses were recalculated to equivalent days of exposure.

Where an average daily ozone dose is 480 ppb·h per day, which means that average yearly exposure is 175 ppm·h.[122] Ozone exposure doses were divided by the average yearly dose to gain equivalent years of exposure (Table 21).

Table 21 *Summary of exposure steps, their corresponding ozone doses in ppm·h and calculated equivalent years of exposure.*

number of hours	***ozone exposure dose, ppm·h***	***equivalent years of exposure***
0	0	0
1.5	122	0.7
3	245	1.4
4.5	367	2.1
6	489	2.8
7.5	611	3.5
9	734	4.2
12	978	5.6
15	1223	7.0
18	1467	8.4
21	1712	9.8
24	1956	11.2
27	2201	12.6
30	2445	14.0
33	2690	15.4
36	2934	16.8
39	3179	18.2
42	3423	19.6
48	3912	22.4
54	4401	25.1
60	4890	27.9
66	5379	30.7
72	5868	33.5
84	6846	39.1

4.4.3.2 Ozone distribution test

Cyan dye, most sensitive to the ozone induced fading, has been exposed to 81.5 ppm of ozone per hour. Heat map in the Figure 94 shows uniform ΔE distribution. Variability of ΔE varies from 0.09 to 0.89, and since it doesn't show any pattern, the ozone distribution in the test chamber can be considered as uniform.

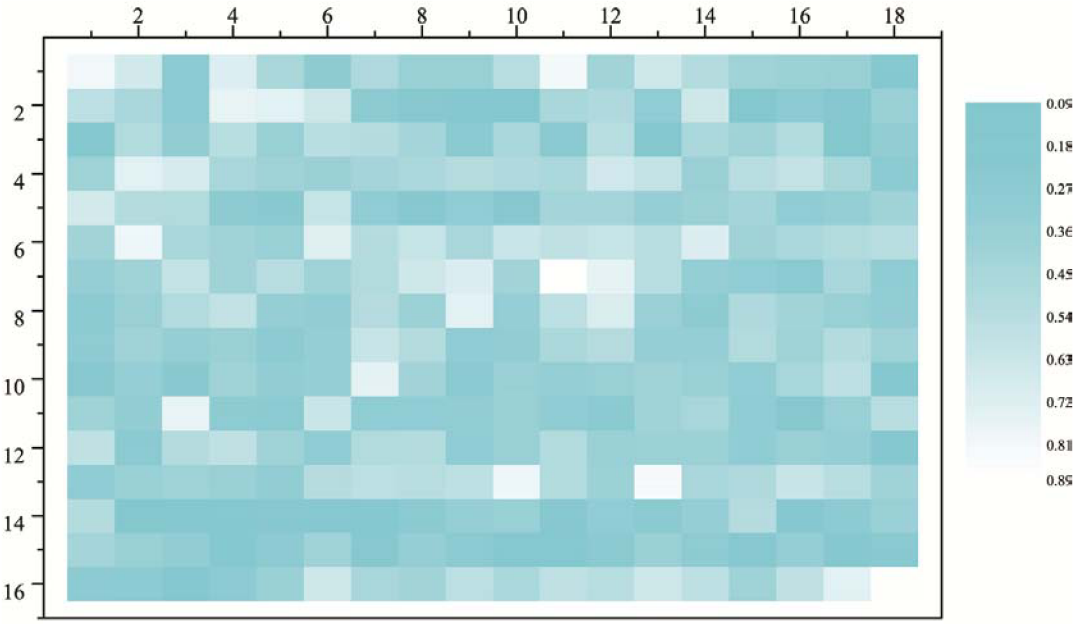

Figure 94 *Heat map of ΔE of the cyan test target; scale on the left shows values of ΔE from the lowest (cyan) to the highest (white).*

4.4.3.3 Commercial varnishes

HP

In next figure (Figure 95) there is depicted degradation in ozone test chamber of HP 500 PS prints varnished with commercial protective varnishes – Hahnemühle, Tetenal and Herma. From the comparison among previously mentioned and unvarnished HP print (Figure 98) it is clear that varnishing with spray protective varnishes, creates barrier that definitely prolongs the longevity of the prints when they are exposed to ozone. The unprotected print has lost almost 90% of the gamut volume in 1.5 hours of exposure (224 ppm·h) and those varnished with commercial varnishes Tetenal and Hahnemühle have reached the endpoint test criterion of 30% gamut volume loss, when exposed to the same exposure dose of 224 ppm of O_3 in 1.5 hours. The test target vanished with Herma protective varnish has lost 30% of gamut volume after 4.5 hours (367 ppm·h) of ozone exposure.

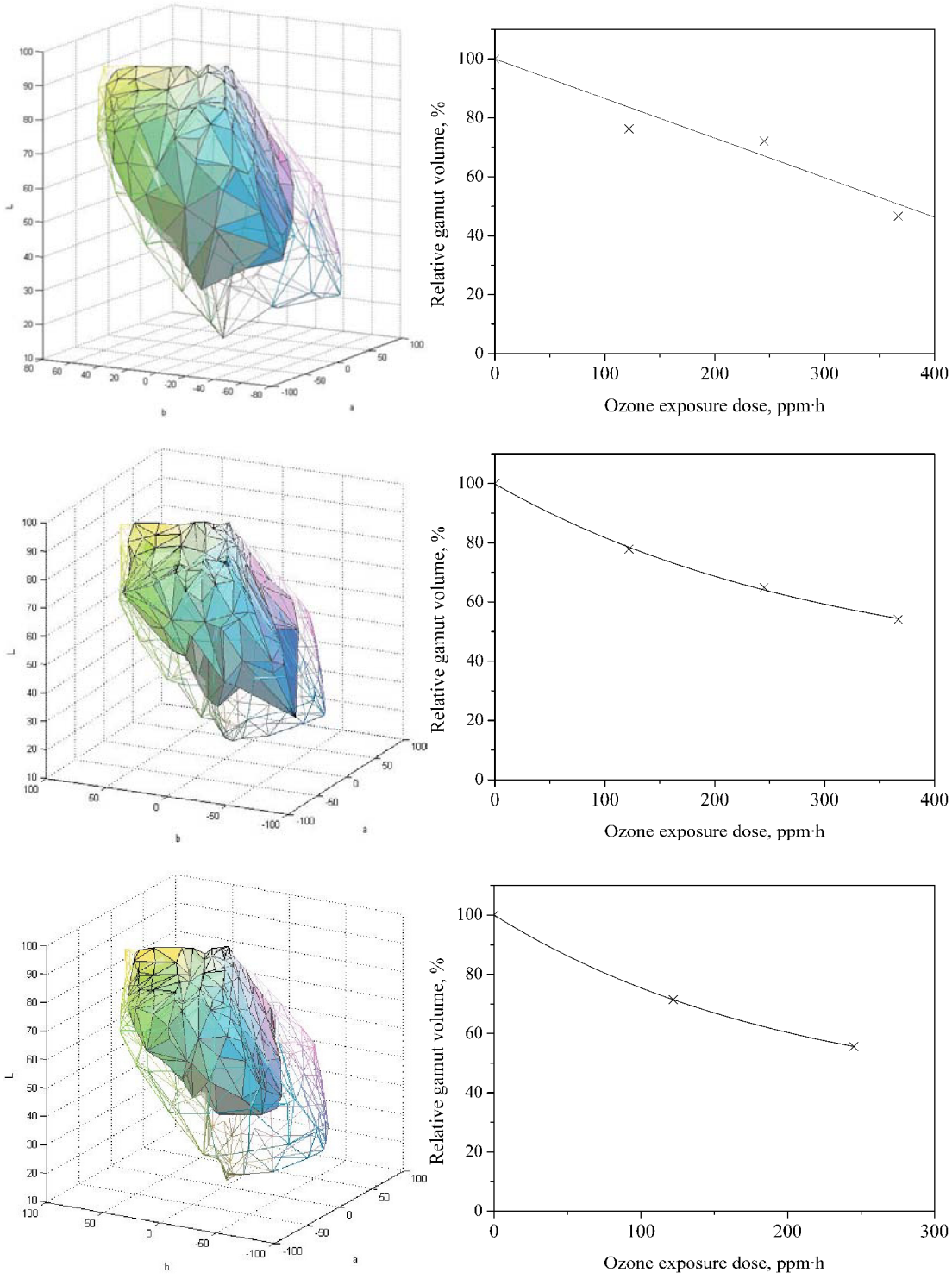

Figure 95 *Change in relative gamut volume of inkjet prints made with printer HP 500PS and HP dye-based ink set on ISP paper after exposure in ozone chamber – varnished with Hahnemühle (front row), Tetenal gloss varnish (middle row), Herma (bottom row) protective varnishes.*

MIS DYE

Degradation in ozone chamber of prints made with Epson Stylus P50 printer with MIS Associates Inc. dye-based ink set varnished with commercial protective varnishes – Hahnemühle, Tetenal and Herma – can be seen on Figure 96. When compared to the unvarnished sample (Figure 101), applied varnishes have provided barrier and protection against ozone, thus augmenting the exposure dose needed to achieve endpoint criterion. All three samples have faded in 4.5 hours of exposure, which is 367 ppm·h O_3.

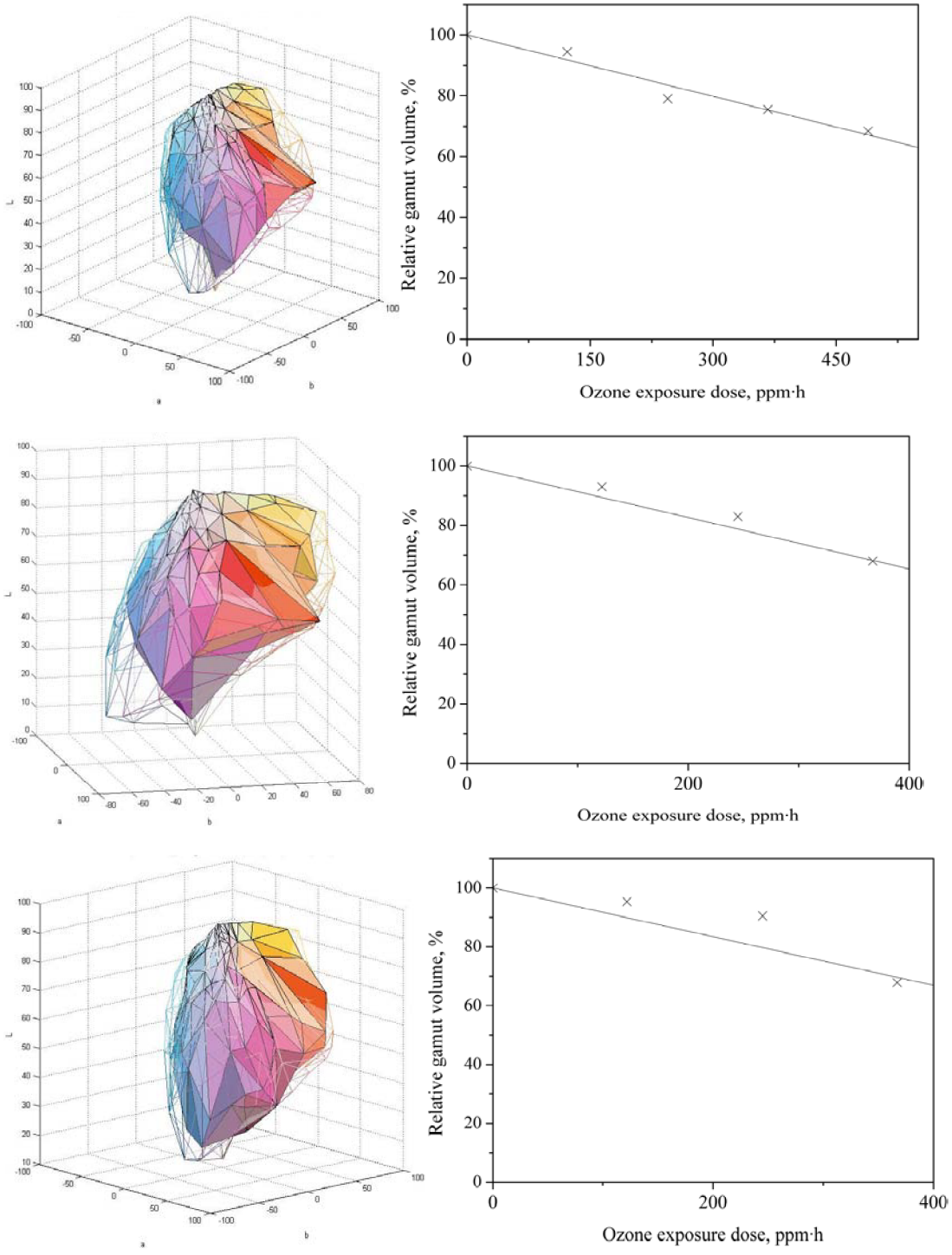

Figure 96 *Change in relative gamut volume of inkjet prints made with printer Epson Stylus Photo P50 and MIS Associates Inc. dye-based ink set on ISP paper after exposure in ozone chamber – varnished with Hahnemühle (front row), Tetenal gloss varnish (middle row), Herma (bottom row) protective varnishes.*

Claria

Degradation in ozone chamber of prints made with Epson Stylus P50 printer with Epson Claria dye-based ink set varnished with commercial protective varnishes – Hahnemühle, Tetenal and Herma– can be seen on the 0. From the comparison of protected prints previously mentioned and unvarnished Claria print (Figure 104)–it is clear that varnishing with either commercial varnish didn't improve gasfastness, but the opposite.

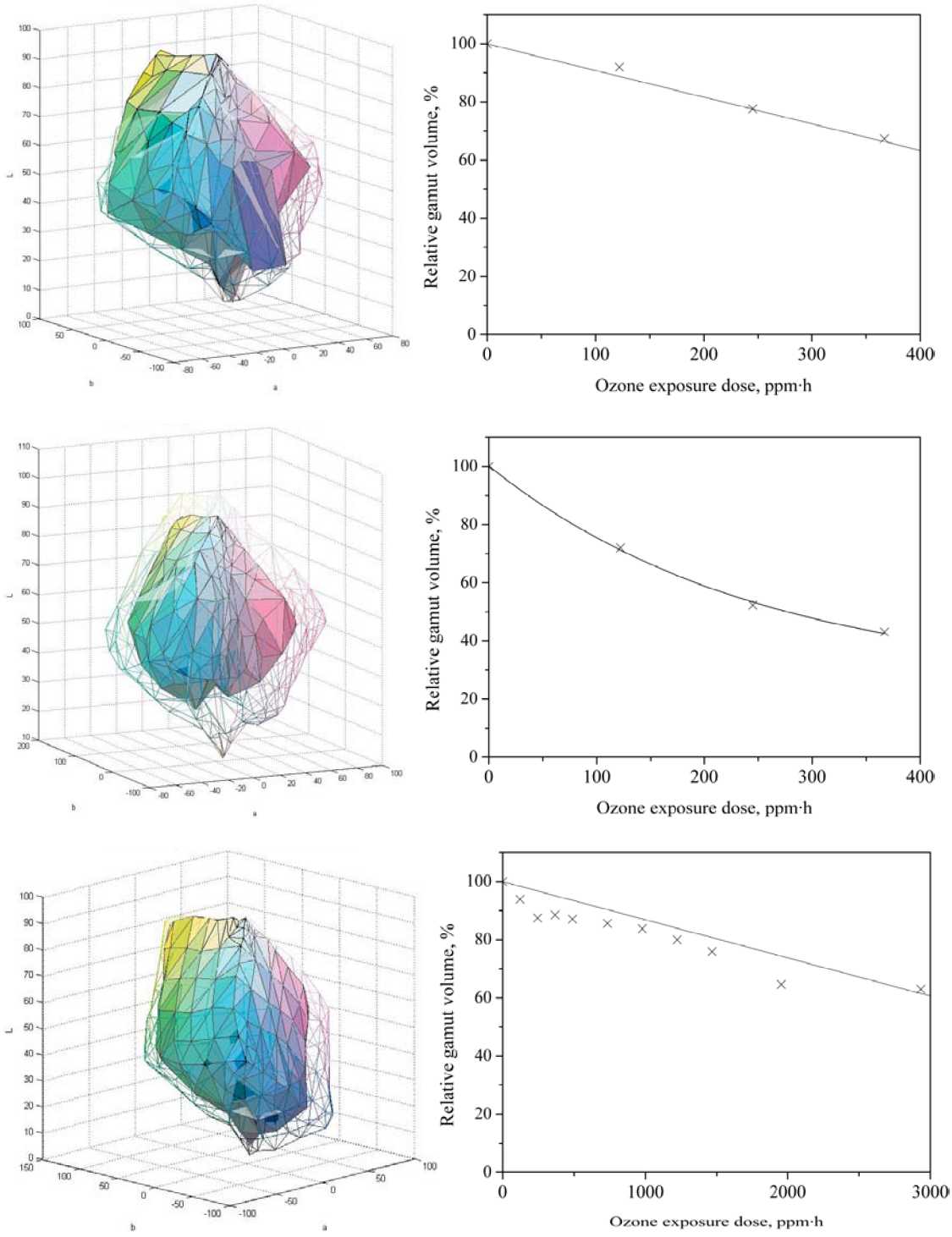

Figure 97 *Change in relative gamut volume of inkjet prints made with printer Epson Photo Stylus P50 and Epson Claria dye-based ink set on ISP paper after exposure in ozone chamber – varnished with Hahnemühle (front row), Tetenal gloss varnish (middle row), Herma (bottom row) protective varnishes.*

4.4.3.4 Prepared varnish composition

HP

Prints prepared with Hewlett-Packard 500 PS printer and HP dye-based ink set on ISP paper doesn't belong among the stable ones. Unprotected print has lost almost 90% of its original relative gamut volume (Figure 98) after 1.5 hour exposure in the ozone test chamber, which is equal to exposure dose of 122 ppm·h. Varnishing definitely helps prolong the fastness of the print. With application of the clear varnish, the 30% relative gamut volume loss has not been achieved, before the end of the test.

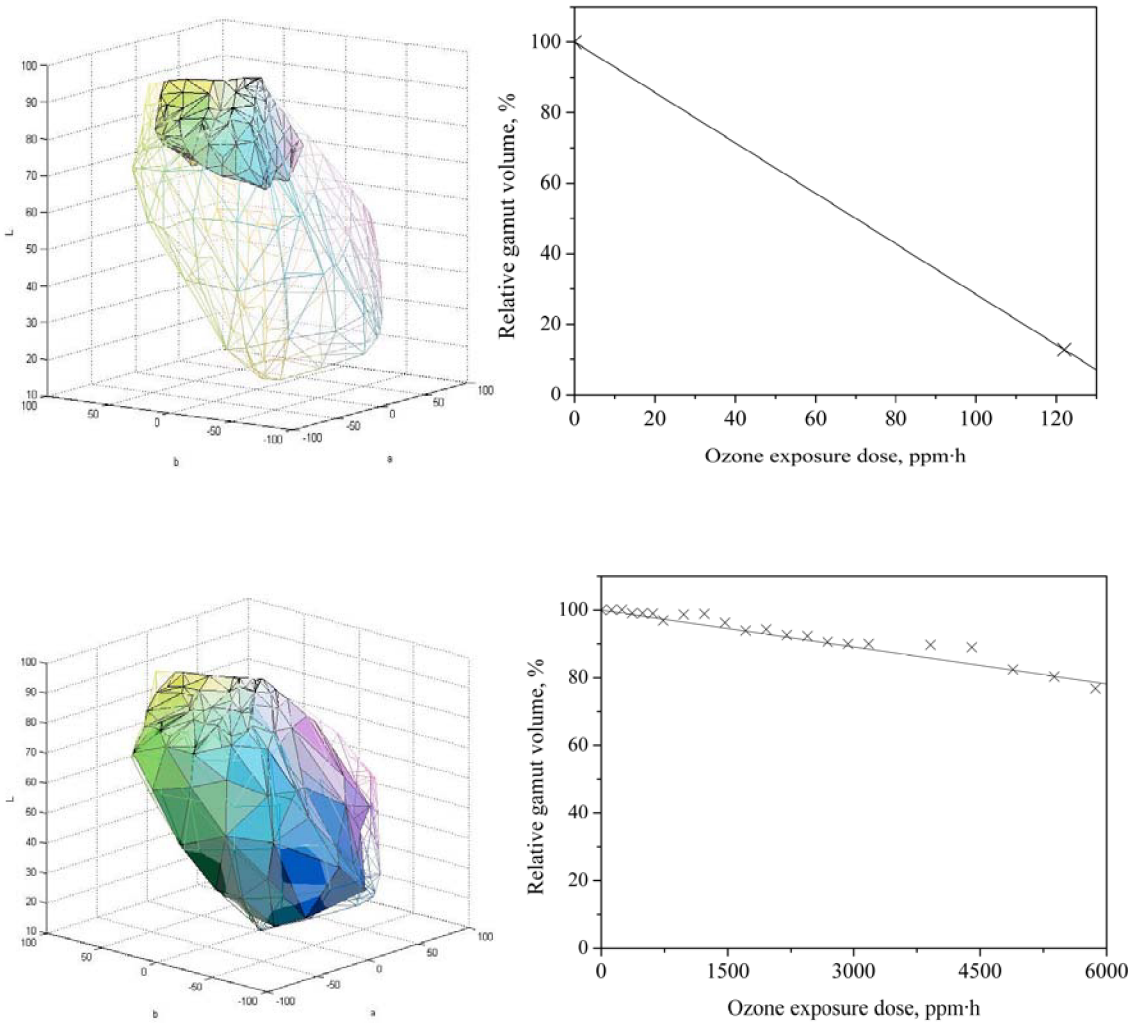

Figure 98 *Change in relative gamut volume of inkjet prints made with printer HP 500PS and HP dye-based ink set on ISP paper after exposure in ozone chamber – unvarnished (first row), prepared composition – clear varnish (second row).*

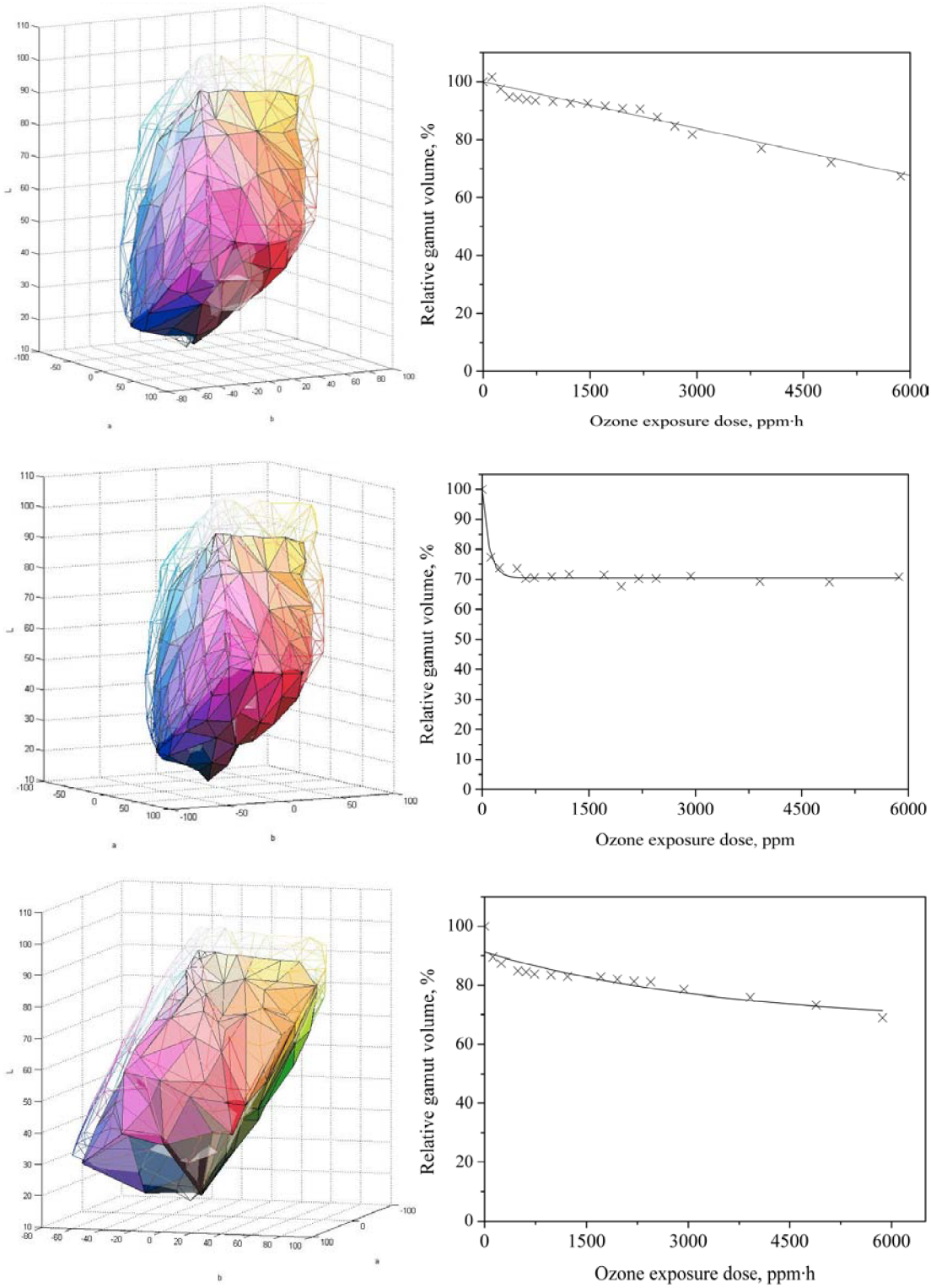

Figure 99 *Change in relative gamut volume of inkjet prints made with printer HP 500PS and HP dye-based ink set on ISP paper after exposure in ozone chamber – varnish with addition of 5w% (first row), 10w% (second row) of AQ1 and 5w% AQ2 (third row).*

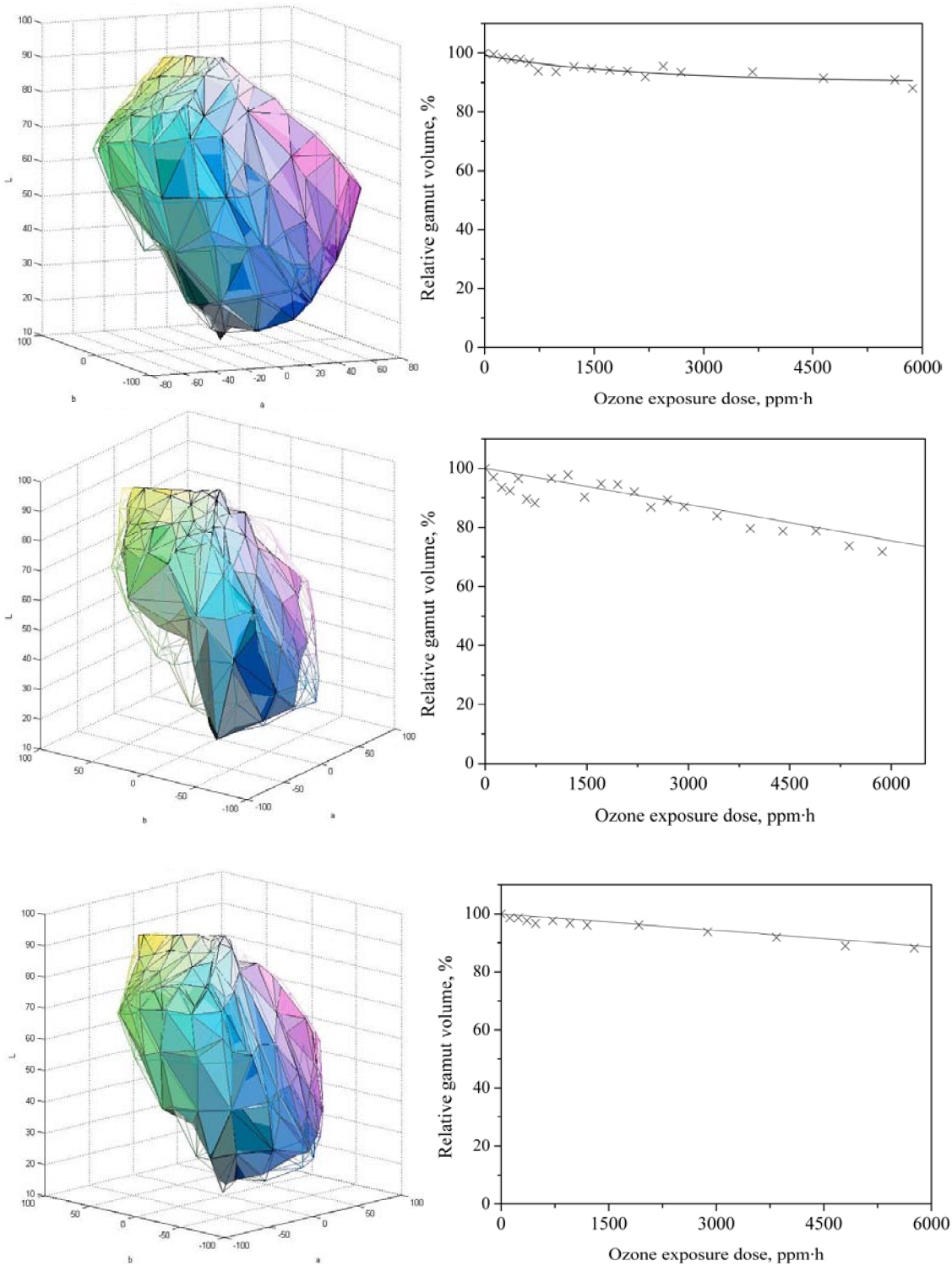

Figure 100 *Change in relative gamut volume of inkjet prints made with printer HP 500PS and HP dye-based ink set on ISP paper after exposure in ozone chamber – varnish with addition of 10w% AQ2 (first row), 5w% (second row) and 10w% (third row) of AQ3.*

MIS Dye

Prints made on Epson P50 printer with MIS Associates dye-based ink set on ISP receiving layer, when unvarnished, lost 40% of relative gamut volume during the first exposure step (122 ppm·h). And after 7.5 hours of exposition to ozone, and total dose of 611 ppm·h, it has retained only 30% of the starting relative gamut volume. The degradation process corresponds with first order reaction kinetics- an exponential decay. When a clear varnish is applied on MIS dye print, the gasfastness ameliorates and after 72 hours of exposition to ozone and total dose of 5868 ppm·h, the print didn't reach the endpoint criterion. It has retained 76% of its original relative gamut volume. The degradation progress does retain exponential progress.

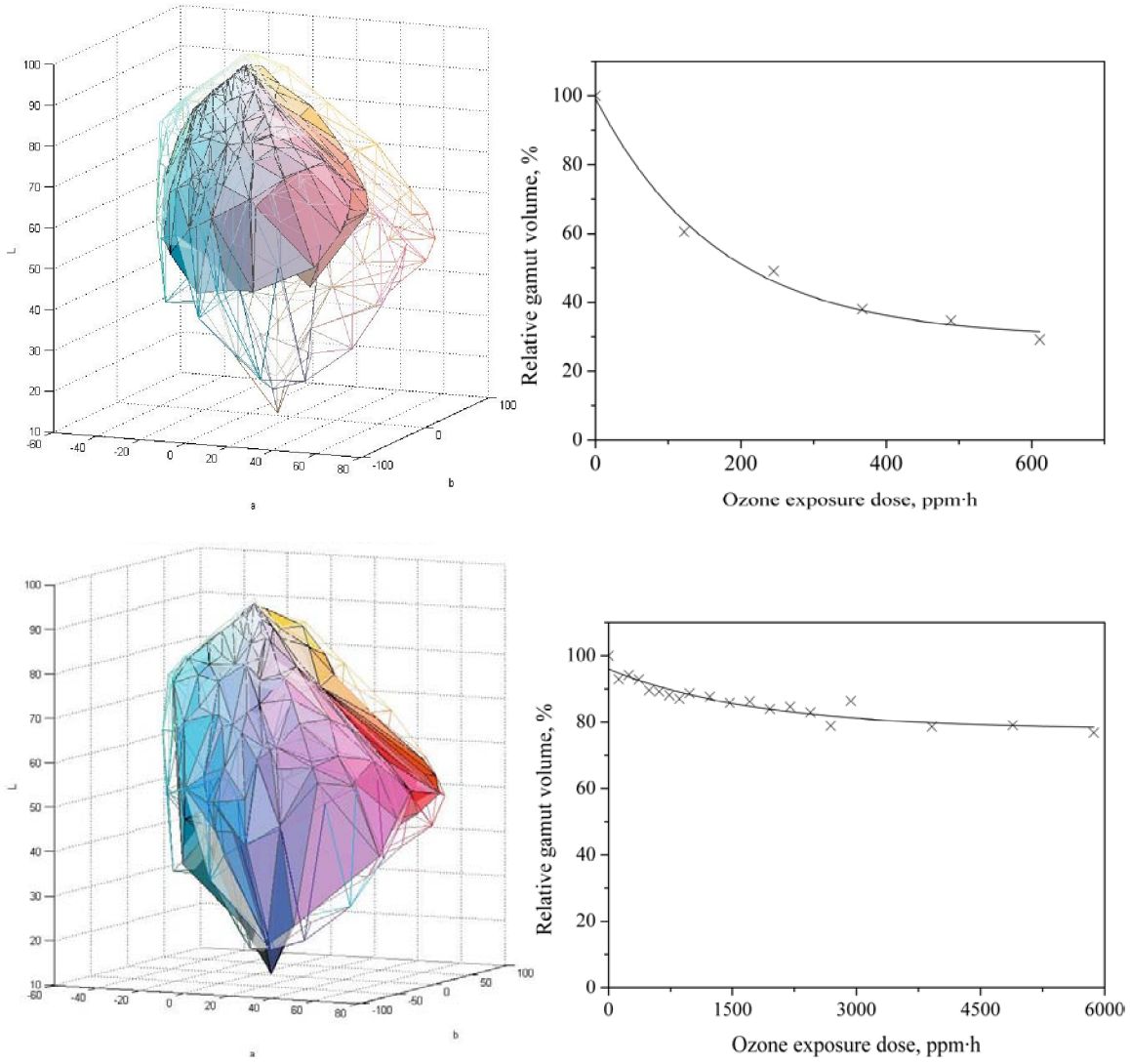

Figure 101 *Change in relative gamut volume of inkjet prints made with Epson Stylus Photo P50 printer and MIS Associates dye-based MIS Dye ink set on ISP paper after exposure in ozone chamber – unvarnished (first row), prepared composition – clear varnish (second row)*

Prints made on Epson P50 printer with MIS Associates dye-based ink set on ISP receiving layer varnished with composition and UV absorber AQ1 5 and 10w% addition (Figure 102) have not lost 30% of its relative gamut volume, during the test. After the test end, 72 hours and total exposure dose of 5868 ppm·h, the prints have retained more than 80% of original relative gamut volume. Both prints had lost its gamut volume more or less in steps continuously.

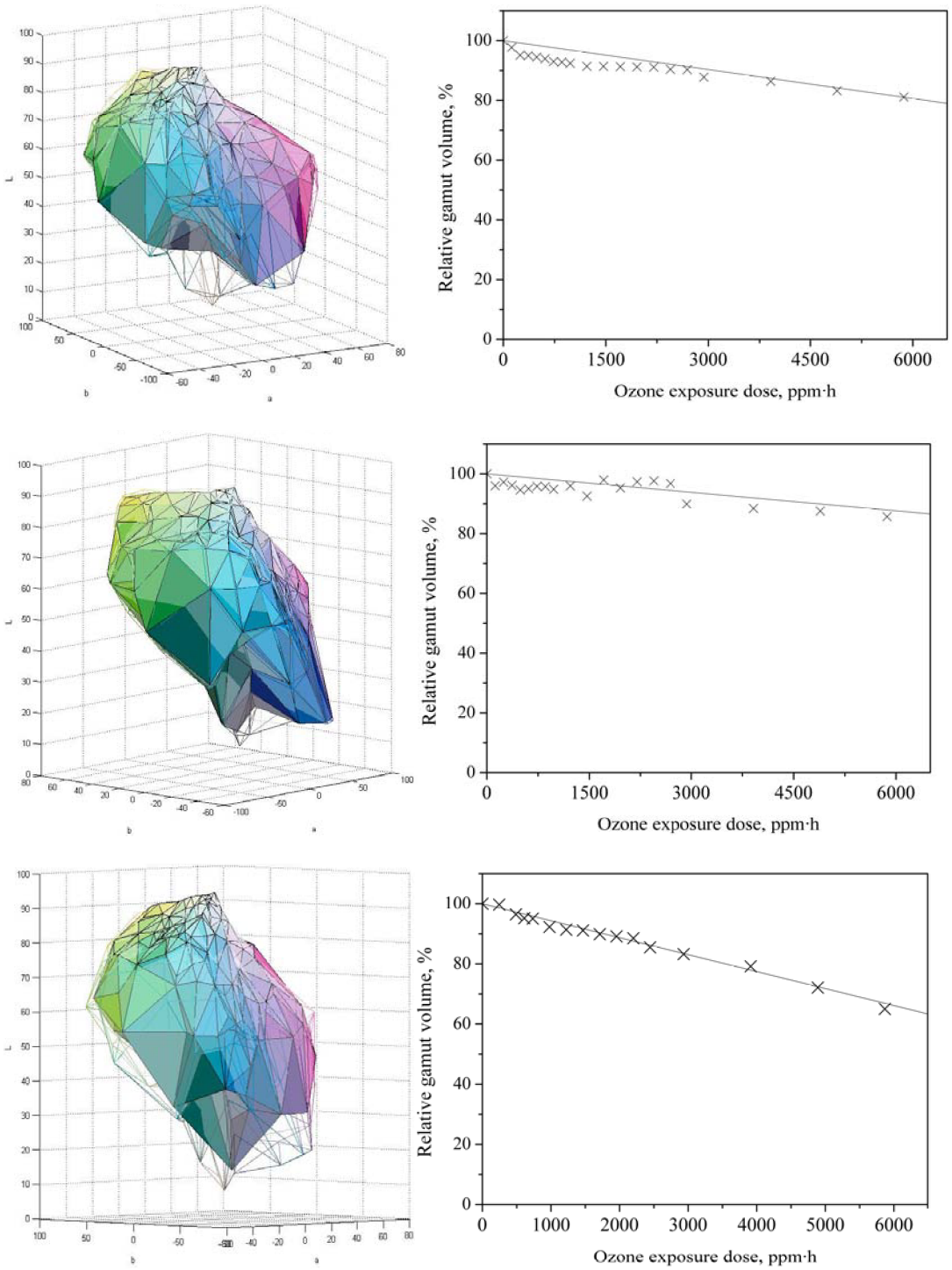

Figure 102 *Change in relative gamut volume of inkjet prints made with Epson Stylus Photo P50 printer and MIS Associates dye-based MIS Dye ink set on ISP paper after exposure in ozone chamber – varnish with addition of 5w% (first row), 10w% (second row) of AQ1 and 5w% AQ2 (third row)*

Prints made on Epson P50 printer with MIS Associates dye-based ink set on ISP receiving layer varnished with composition and UV absorber AQ2 5 and 10w% addition have faded continuously (Figure 102, Figure 103). In case of 5 w% addition of AQ2, the print reached the criterion after 75 hours (5868 ppm·h), it has faded by 35%. And in case of 10 w% AQ2 addition, the print did not reach the threshold during the test duration. But when the degradation regressions are compared, the print with 5 w% addition degrades in almost linear manner, on the other hand print with 10w% addition still retains exponential curve.

Prints made on Epson P50 printer with MIS Associates dye-based ink set on ISP receiving layer varnished with composition and UV absorber AQ3 5 w% and 10 w% addition have similar degradation progress (Figure 103). The print varnished with 5 w% addition of AQ3 composition has reached the threshold in 48 hours of ozone exposure (3912 ppm·h). Print varnished with 10 w% addition of AQ3 composition have not reached threshold during the test duration.

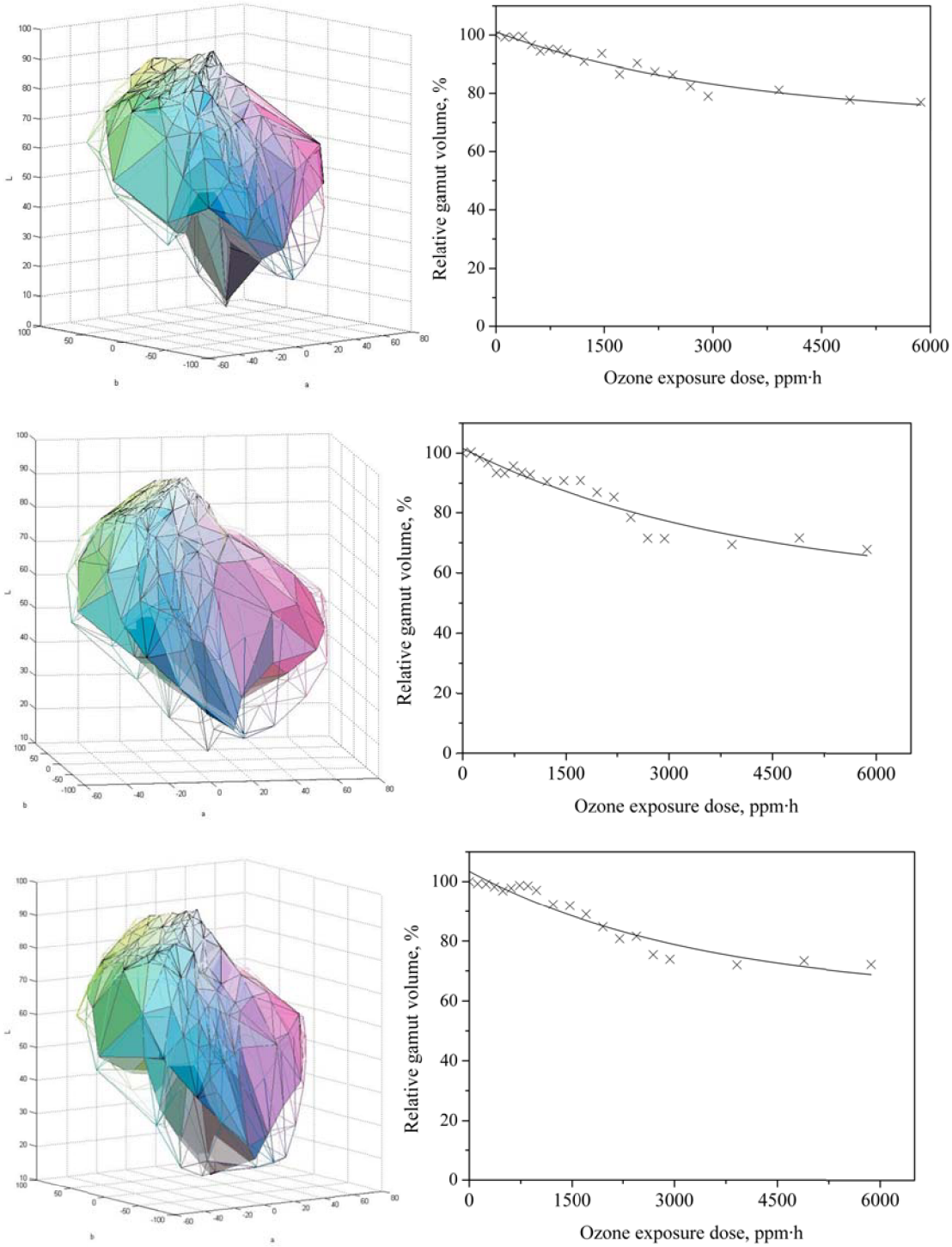

Figure 103 *Change in relative gamut volume of inkjet prints made with Epson Stylus Photo P50 printer and MIS Associates dye-based MIS Dye ink set on ISP paper after exposure in ozone chamber – varnish with addition of 10 w% (first row) of AQ2, 5 w% (second row) and 10 w% AQ3 (third row)*

Claria

Prints made on Epson P50 printer with Epson Claria dye-based ink set on ISP receiving layer unvarnished and varnished with prepared composition have been tested on gasfastness in ozone chamber. For the results see Figure 104. Unprotected Claria print has faded, and reached the threshold in 21 hours of exposure. Which equals exposure dose of 1712 ppm·h. When the print was varnished with clear composition, the gasfastness improved radically and after the test was ended, after 72 hours (5868 ppm·h exp. dose) the print lost only 10% of its original relative gamut volume.

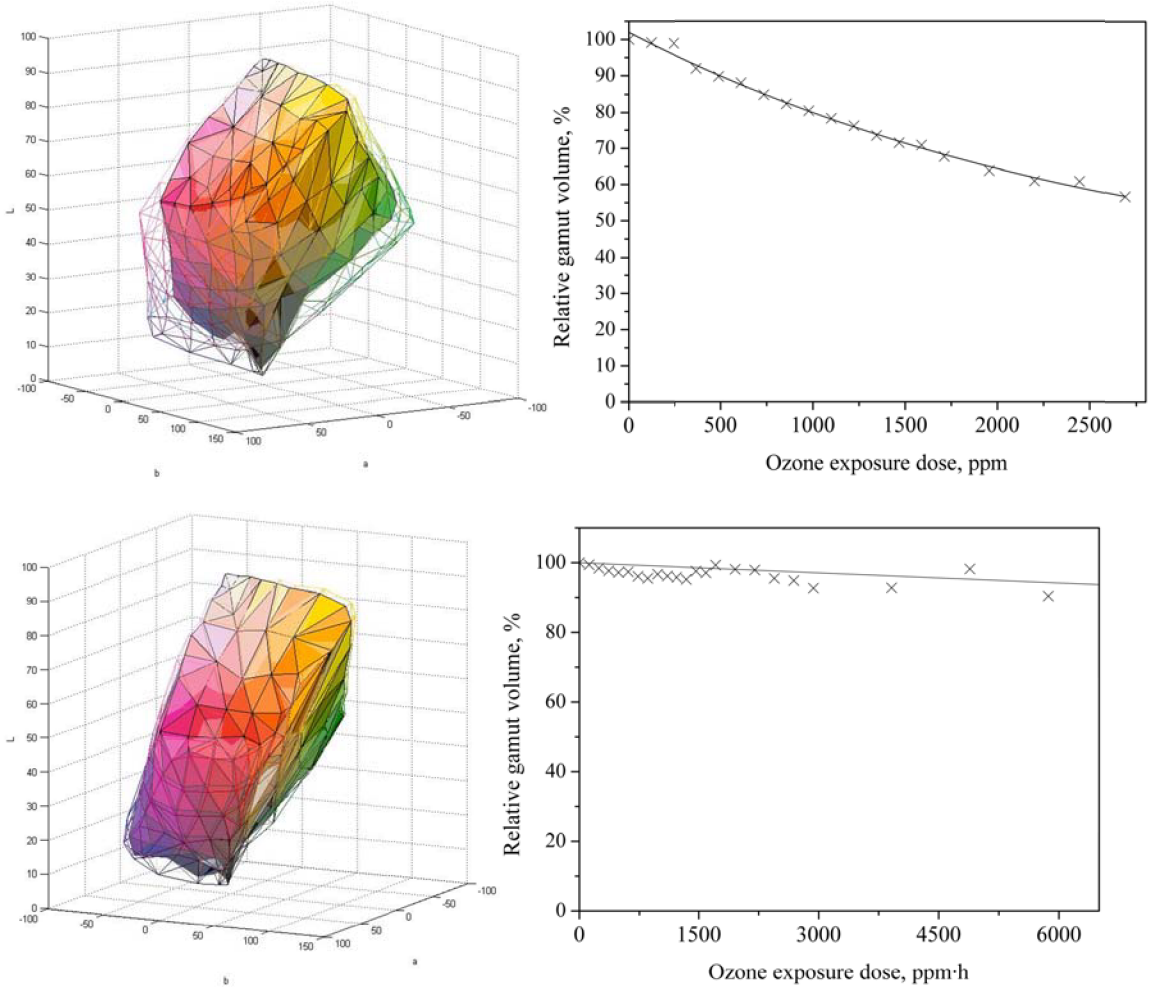

Figure 104 *Change in relative gamut volume of inkjet prints made with Epson Stylus Photo P50 printer and Epson Claria dye-based ink set on ISP paper after exposure in ozone chamber – unvarnished (first row), prepared composition – clear varnish (second row)*

On the next two pages (Figure 105, Figure 106) are the results of gasfastness test for prints varnished with composition with addition 5 w% and 10 w% of UV absorbers AQ1, AQ2 and AQ3. In all six cases the print remained very stable during the test and after 72 hours and exposure dose of 5868 ppm·h O_3, the prints did not lose 10% of their relative gamut volume.

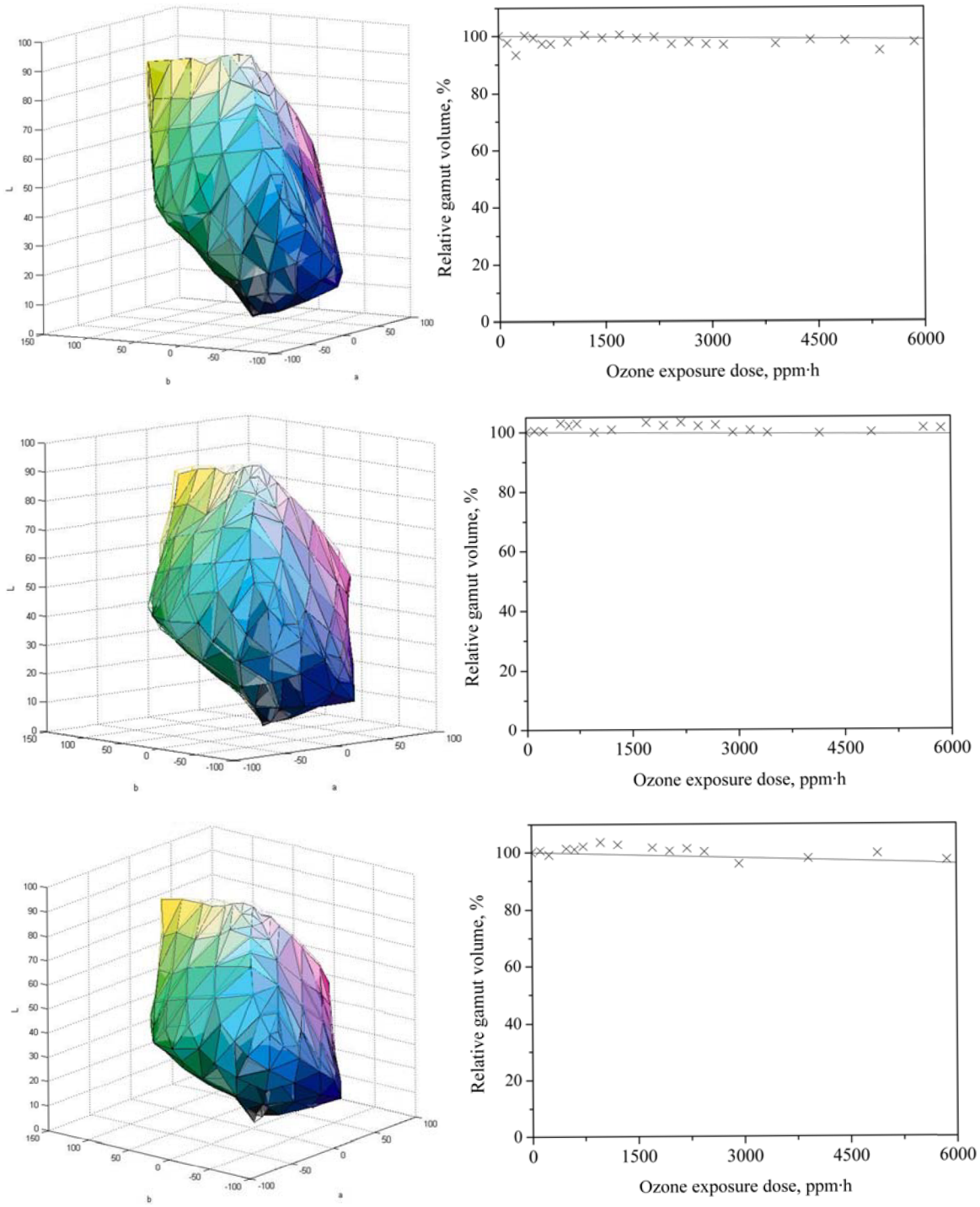

Figure 105 *Change in relative gamut volume of inkjet prints made with Epson Stylus Photo P50 printer and Epson Claria dye-based ink set on ISP paper after exposure in ozone chamber –varnish with addition of 5 w% (first row), 10 w% (second row) of AQ1 and 5 w% of AQ2 (third row).*

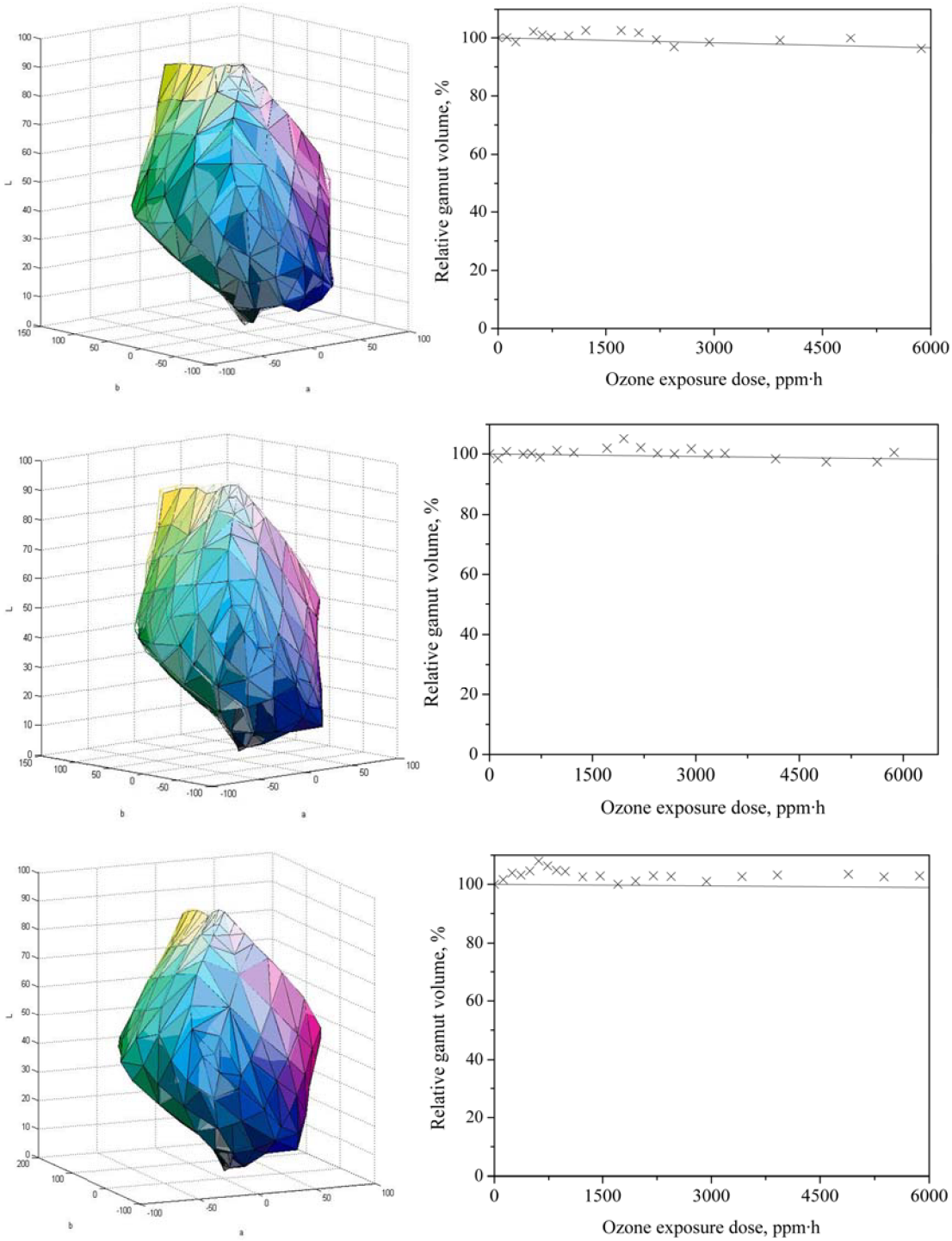

Figure 106 *Change in relative gamut volume of inkjet prints made with Epson Stylus Photo P50 printer and Epson Claria dye-based ink set on ISP paper after exposure in ozone chamber–varnish with addition of 10 w% (first row) of AQ2, 5 w%(second row) and 10 w% (third row) of AQ3.*

4.4.4 Ozone fastness test-Summary

In general the results of gas-fading test of sprayed–on comercial varnishes are not very conclusive, because of the application method. Even thou it was done to the highest standard, and with great caution, it can never be applied as precicely as with rod or bar.

Unprotected HP (Figure 107) sample have lost in 1.5 hour of exposure (122 ppm·h) lost almost 80% of its relative gamut volume. So it can be considered as very sensitive to ozone. Varnishing have improved equivalent lifetime four to six times in case of commercial varnishes and in case of prepared composition equivalent lifetime is at least 60 times longer.

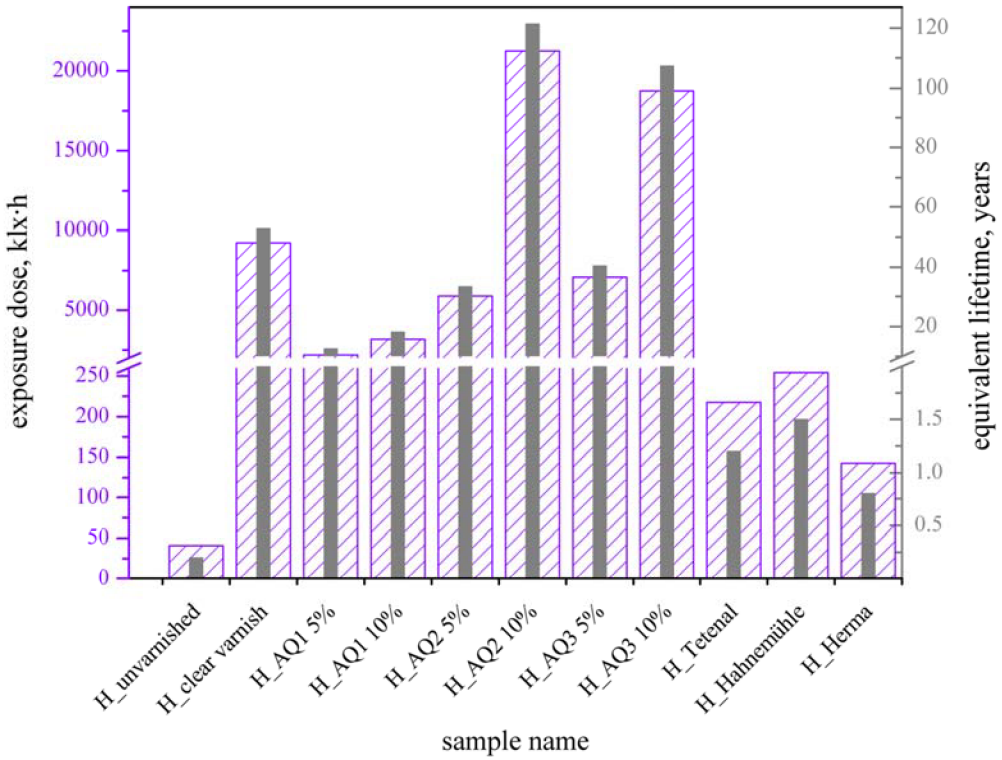

Figure 107 *Exposure dose needed to achieve 30% relative gamut volume loss for inkjet prints made on HP 500PS printer with HP dye-based ink set on ISP paper*

MIS Dye samples proofed with prepared composition have times more equivalent lifetime value, than unvarnished sample or samples varnished with commercial varnishes. But fom results it it clear that sprayed–on commercial varnishes create barrier on top of print and provide some sort of protection.

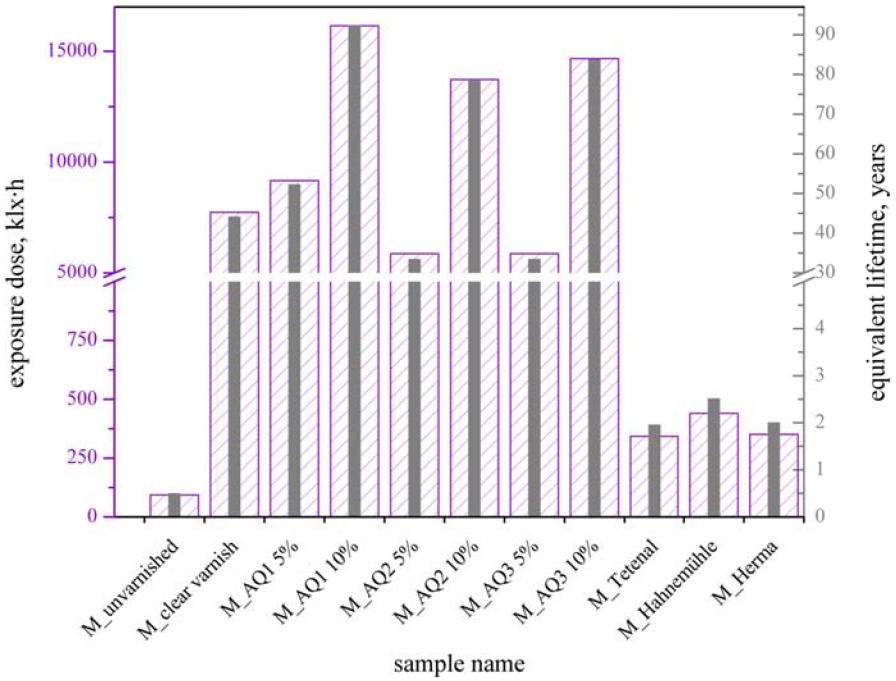

Figure 108 *Exposure dose needed to achieve 30% relative gamut volume loss for inkjet prints made on Epson Stylus Photo P50 printer, MIS Associates Inc. dye-based ink set and ISP paper*

As with Claria prints (Figure 109), providing layer of prepared composition has ameliorated the persistance against gas by at least 150times. Commercial varnishes Tetenal and Hahnemühle have very short life span, up to two years before they loose 30% of their relative gamut volume.

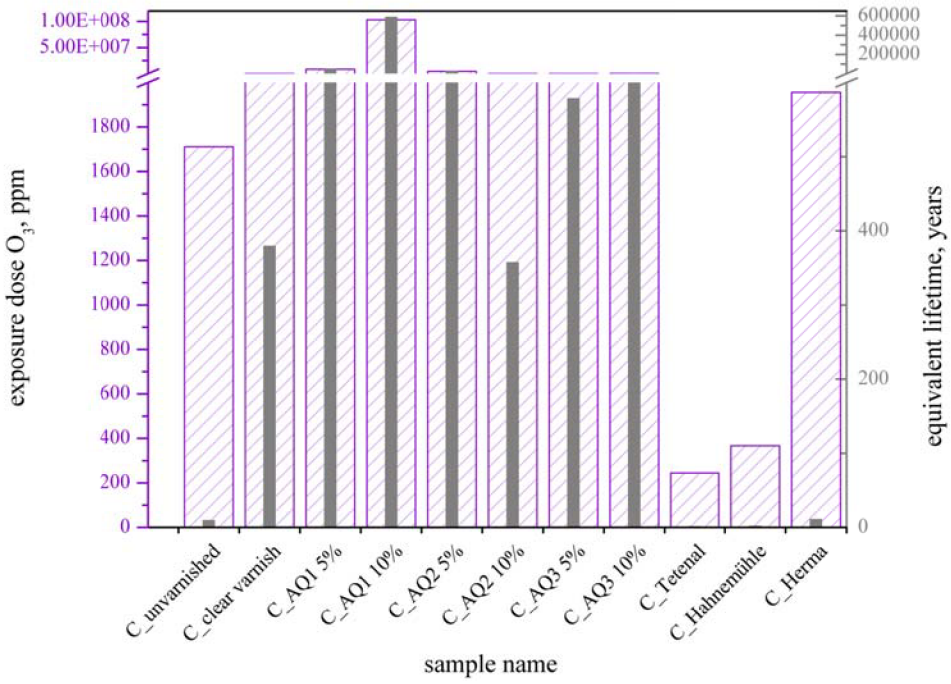

Figure 109 *Exposure dose needed to achieve 30% relative gamut volume loss for inkjet prints made on Epson Stylus Photo P50 printer, Epson Claria dye-based ink set and ISP paper*

4.4.5 Water vapour permeability test

Figure 110, Table 22 and 0 sum up the results of water vapour permeability test (Ch. 3.6.2.2). The medium itself has proved to be quite transmissive since the silicagel weight augmented by 0.677 g after the test. With the application of either varnish, commercial or prepared composition, some sort of barrier was formed and water vapour permeability of the medium has significantly decreased.

The applied amount of commercial varnishes was comparable (Table 22), but the application method needs to be taken into account. They were sprayed on and thus varnish layer needn't have to be fully homogeneous, which is indicated by the augmented standard deviation value. But the same uncertainty of the varnish distribution has to be taken into account when applied on the actual photographs/prints.

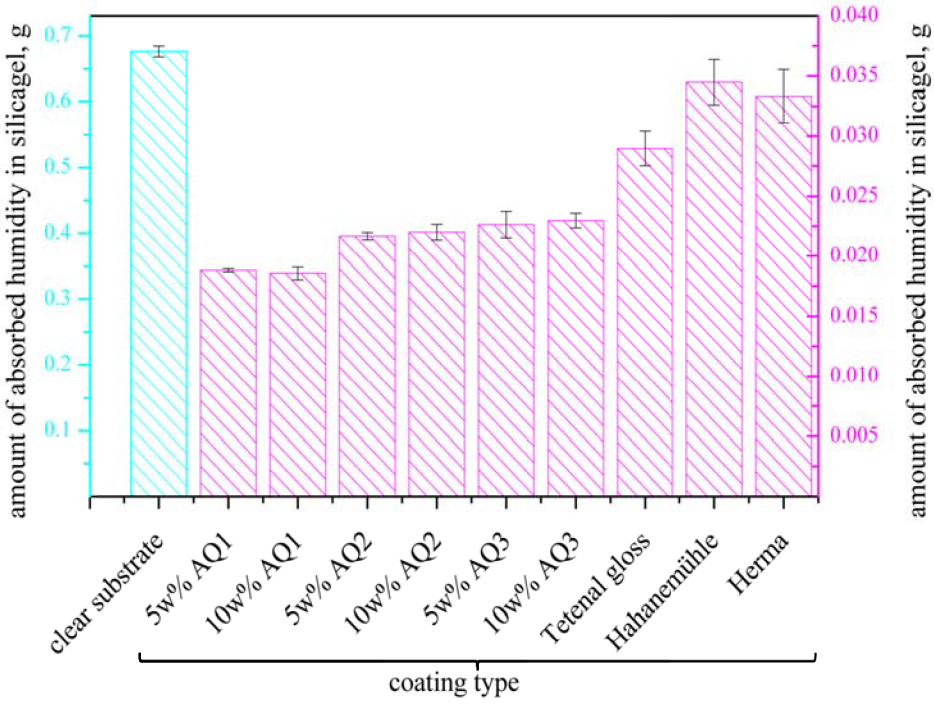

Figure 110 *The results of water vapour permeability test*

Table 22 *Amount of permeated water vapour absorbed in silicagel (values in table are in grams) for the samples coated with commercial varnishes*

coating / *measurement nr.*	*clear substrate*	*Tetenal gloss*	*Hahnemühle*	*Herma*
1	0.6844	3.04×10^{-2}	3.24×10^{-2}	3.15×10^{-2}
2	0.6770	2.90×10^{-2}	3.51×10^{-2}	3.58×10^{-2}
3	0.6680	2.75×10^{-2}	3.60×10^{-2}	3.27×10^{-2}
Average	**0.6765**	$\mathbf{2.90\times10^{-2}}$	$\mathbf{3.45\times10^{-2}}$	$\mathbf{3.33\times10^{-2}}$
St. deviation	8.2×10^{-3}	14.5×10^{-4}	18.7×10^{-4}	22.2×10^{-4}
applied amount of varnish	-	6.3×10^{-3}	5.8×10^{-3}	6.1×10^{-3}

On the other hand, varnish layer made by Mayer rod seem to form quite uniform barrier (Table 23), so the test of analysis of variance has been done for all seven groups.

Table 23 *Amount of permeated water vapour absorbed in silicagel (values in table are in grams) for the samples varnished with prepared varnish composition.*

coating / *meas. nr.*	*clear substrate*	*5w%AQ1*	*10w%AQ1*	*5w%AQ2*	*10w%AQ2*	*5w%AQ3*	*10w%AQ3*
1	0.6844	1.90×10^{-2}	1.91×10^{-2}	2.14×10^{-2}	2.19×10^{-2}	2.15×10^{-2}	2.23×10^{-2}
2	0.6770	1.88×10^{-2}	1.80×10^{-2}	2.20×10^{-2}	2.14×10^{-2}	2.37×10^{-2}	2.35×10^{-2}
3	0.6680	1.87×10^{-2}	1.86×10^{-2}	2.16×10^{-2}	2.27×10^{-2}	2.27×10^{-2}	2.31×10^{-2}
Average	**0.6765**	$\mathbf{1.88\times10^{-2}}$	$\mathbf{1.88\times10^{-2}}$	$\mathbf{2.17\times10^{-2}}$	$\mathbf{2.20\times10^{-2}}$	$\mathbf{2.26\times10^{-2}}$	$\mathbf{2.30\times10^{-2}}$
St. dev.	8.2×10^{-3}	1.5×10^{-4}	5.5×10^{-4}	3.1×10^{-4}	6.6×10^{-4}	11.0×10^{-4}	6.1×10^{-4}

Null hypothesis for first ANOVA test is that all groups have equal means. And alternative hypothesis, that one of the sample means is different from another. F value for all seven groups is 18385.2 with (6;14) degrees of freedom and $F_{crit.}$ is 2.85.[123] Which means that null hypothesis is right and at least one from the group is different (clear substrate). Second ANOVA test has been done only with data from coated samples, 6 groups. The hypotheses are the same. H_0: all groups have equal means and H_a that at least one of the means vector is different from another. The F value 24.47 with (5;11) degrees of freedom. For this set of data F is considerably lower than the previous one. F_{crit} for this data set is 3.20[123] and $F>F_{crit}$. On the significance level 0.01%, is H_a true, so there is statistical significance among the amount of permeated water vapour by each sample.

Table 24 *First ANOVA test results computed with all seven data groups*

Source	*DF*	*Sum of squares*	*Mean squares*	*F*	*Pr > F*
Model	6	1.1047	0.1841	18385.2	< 0,0001
Error	14	0.0001	0.0000		
Corrected Total	20	1.1048			

Table 25 *Second ANOVA test after elimination of clear substrate data*

Source	*DF*	*Sum of squares*	*Mean squares*	*F*	*Pr > F*
Model	5	0.0001	0.0000	24.47	< 0,0001
Error	11	0.0000	0.0000		
Corrected Total	16	0.0001			

4.4.6 Oxygen transmission rate – OTR

In Figure 111 is a summary of measured oxygen transmission rates for all used varnishes in this work. And in Table 26 is overview of amount of varnishes applied on circular samples with 12 cm in diameter. Substrate has OTR 5646±16 $cm^3 \cdot m^{-2} \cdot day^{-1} \cdot bar^{-1}$, which is considered as transmissive material. With application of commercial varnishes that were sprayed on, the varnish amount was detemined gravimetrically. From the thickest layer applied it was Hahnemühle, Tetenal and Herma varnish, which is consistent with OTR results, as the least transmissive was Hahnemühle sample, the second Tetenal and the third Herma sample. The application procedure although as precise as it was possible to be done by hand, doenst rule out possible unevenness of the applied layer, which shows in case of Herma varnished sample, that has aggravated standard deviation value.

With samples with prepared composition the amount of applied varnish should be equal as it was applied by the Mayer rod. The application of the varnish itself has provided some sort of barrier. It seems that with higher UV absorber percetage, the transmission is lowered. This matter needs to be investigated further.

Table 26 *Applied amount of varnishes*

varnish	*amount applied, g*
Tetenal gloss	0.0522
Hahnemühle	0.0567
Herma	0.0548
clear varnish	0.2370
5 w% AQ1	0.2386
10 w% AQ1	0.2425
5 w% AQ2	0.2298
10 w% AQ2	0.2369
5 w% AQ3	0.2380
10 w% AQ3	0.2534

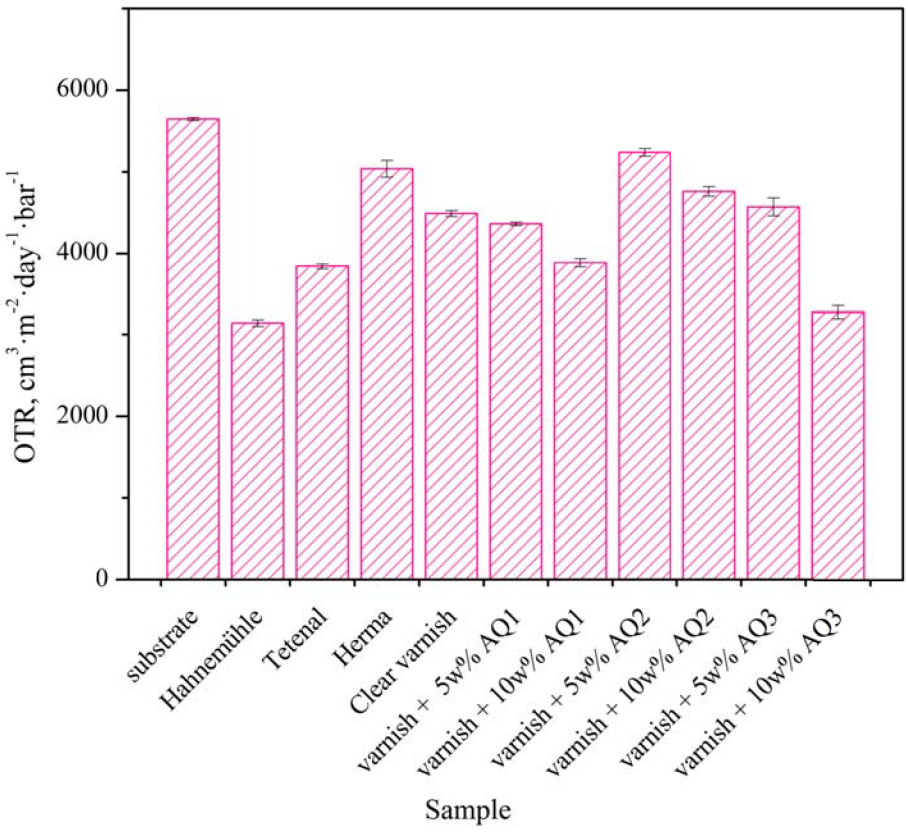

Figure 111 *Summary averaged OTR values for all used varnishes*

5 CONCLUSIONS

A protective varnish compatible with photographic media has been prepared. To ameliorate the protection against harmful UV light, three EVERSORB UV absorbers form AQ series have been added in two concentrations. As a printing medium was used microporous photo paper and on this medium was printed test target i-1 1.5 containing 288 patches. For the test were used two printers Epson Stylus Photo P50 and HP 500 PS and three dye-based ink sets Epson Claria, Hewlett Packard and MIS Associates Inc. Samples were proofed with varnish layer of clear composition and mixture and UV absorbers. For comparison also three commercial light protective photo varnishes entered the test.

Used photo paper was characterised (ch. 4.3.1) and from the measured reflectance spectra it can be assumed that it does contain OBA's, due to presence of peak in blue part of spectra. As a microporous pearl paper its gloss value corresponds to the type of semi-gloss-media. Measurement of pH with surface electrode indicates that the inert papers with microporous receiving layer are slightly acidic.

Accelerated lightfastness test has been done in Q-Sun xenon test chamber, with "daylight" filter. During the dye degradation in inkjet prints, relative gamut volume decreases. The evaluation of protective character was judged with relative gamut volume change and software VolGa. Both MIS Dye and HP prints, when unvarnished, can be considered as prints with low light stability. But Claria prints even though that are dye based have great light stability and colours with high clarity and brillance, indicated with almost double size of gamut volume. HP prints proofed with clear varnish showed any improvement, but with the addition of UV absorbers, estimated lifetime has been multiplied. From commercial varnishes the best protection has been provided by Hahnemühle protective light varnish, which according to the measured absorbance spectra should contain UV absorbers (Figure 67). Prints made with MIS Associates Inc. inks, which are alternative inks for Epson printers, showed that varnishing with prepared composition has also multiplied the exposure dose needed to achieve 30% relative gamut volume loss and by that the calculated estimated lifetime. The higher concentration of all UV absorbers brought about better lightfastness. Hahnemühle and Herma varnishes on MIS dye prints have provided the same level of protection as prepared composition with UV absorbers. When it comes to results interpretation of Epson Claria prints, they need to be approached with elevated attention. From the Figure 92 it is clear that 5w% addition of all three UV absorbers and 10w% of AQ3 significantly helps with the lightfastness and prolongs greatly estimated lifetime. However, reciprocity law failure needs to be taken into account in case of accelerated lightfastness test and it is assumed that prints will need much less time to fade, than estimated.[124]

Gasfading of inkjet prints was tested in ozone test chamber, where prints were exposed to 80 ppm O_3 per hour. In general the results of gas-fading test of sprayed–on comercial varnishes are not very conclusive, because of the application method. Even thou it was done to the highest standard, and with great caution, it is assumed that homogeneous varnish layer is not formed, thus prints protected with comercial varnishes are more prone to gasfading. Unprotected print done with HP ink set is very sensitive to ozone and faded very quickly. It has lost almost 90% of its relative gamut volume in 1.5 hours of exposure. Overal, varnishing of the HP targets with prepared varnish conposition, regardless of the UV absorber added, have prolonged its lifetime by at least 65 times. So from original 3 months to 12 years. MIS Associates inks on ISP paper are also prone to ozone induced degradation. Unprotected, they are also unstable as HP prints. By varnishing the estimated lifetime goes from 6 months to at least 30 years. Claria prints proved to be almost twenty times more resistant than the other two unvarnished prints. It has not subjected to gasfading easily and values of exposure dose needed to achieve 30% loss of relative gamut volume needed to be extrapolated, so equivalent lifetime values are very high in uncertainty.

Varnishing unprinted ISP paper has shifted its colour balance to blue and green and it has lost in lightness. On Claria targets after varnishing the print lightness have mainly lowered. Varnishing has also slightly shifted colour balance to green. Coating HP targets with varnish with addition of AQ1 has

augmented the lightness and mainly shifted the colour balance to yellow and red. Lightness values of MIS Dye test targets have mainly lowered with the application of varnish with UV absorbers, the only augmentation have been on red patches and yellow one. Mostly the balance has shifted to yellow and green.

Transmission of water vapour trough prepared varnish has been tested. With the prepared composition application, quite uniform barrier was formed, which provides similar water vapour permeability, thus comparable blocking character. The applied amount of commercial varnishes was comparable, but the application method needs to be taken into account. They were sprayed on and thus varnish layer needn't have to be fully homogeneous, which is indicated by the augmented standard deviation value.

Oxygen transmission rate was determined by carrier gas method. Used substrate had OTR 5646±16 $cm^3 \cdot m^{-2} \cdot day^{-1} \cdot bar^{-1}$, which is considered as transmissive material. With application of commercial varnishes that were sprayed on, the varnish amount was detemined gravimetrically. From the thickest layer applied it was Hahnemühle, Tetenal and Herma varnish, which is consistent with OTR results, as the least transmissive was Hahnemühle sample, the second Tetenal and the third Herma sample. The application procedure although as precise as it was possible to be done by hand, doesn't rule out possible unevenness of the applied layer, which manifests itself in form of elevated value of deviation. The application of prepared composition has provided some sort of barrier. It seems that with higher UV absorber percentage, the oxygen transmission lowers. But to make definitive conclusions, this matter needs to be investigated further.

6 LITERATURE AND SOURCES

[1] CLOTTES, Jean. *Chauvet cave*: *the art of earliest times*. Salt Lake City: University of Utah Press, c2003, 225 p. ISBN 08-748-0758-1.

[2] *The Inkjet Print as Objet D'Art* [online]. 1995-2012 [cit. 2012-07-25]. Dostupné z: http://www.luminous-landscape.com/tutorials/handmade.shtml

[3] KIPPHAN, Helmut. *Handbook of print media*: *technologies and production methods*. New York: Springer, 2001, xx, 1207 p. ISBN 35-406-7326-1.

[4] DZIK, Petr a Michal VESELÝ. Problematika archivní stálosti inkoustového tisku. In: 8. POLYGRAFICKÝ SEMINÁŘ, 8.19. *Sborník přednášek*. Pardubice: Univerzita Pardubice, Fakulta chemicko-technologická, Katedra polygrafie a fotofyziky, 2007, 70–76. ISBN 978-80-7194-991-6.

[5] DZIK, Petr a Michal VESELÝ. Inkoustový tisk-současnýs tav, možnosti a trendy. In: 8. POLYGRAFICKÝ SEMINÁŘ, 8.19. *Sborník přednášek*. Pardubice: Univerzita Pardubice, Fakulta chemicko-technologická, Katedra polygrafie a fotofyziky, 2007, s. 81-87. ISBN 978-807-1949-916.

[6] ROMANO, Frank J. *Inkjet!*: *history, technology, markets, and applications*. 1st ed. Pittsburgh: Digital printing Council, 2008, ix, 316 s. ISBN 978-0-88362-623-8.

[7] THE IMAGING RESOURCE.*A Guide to Digital Printers* [online]. 2012. vyd. 2012 [cit. 2014-09-26]. Dostupné z: http://www.imaging-resource.com/ARTS/GSPRINT/GSPRINT.HTM

[8] THE IMAGE PERMANENCE INSTITUTE.*Modern Photo Papers* [online]. 2008. vyd. 2008 [cit. 2014-09-26]. Dostupné z: www.imagepermanenceinstitute.org/shol_sub/modernphotopapers.pdf

[9] LORDI, James. *Paper/plastic laminate and method for making same* [patent]. US 6,926,986, B2. Uděleno Aug. 9, 2005.

[10] MCCORMICK-GOODHART, Mark a Henry WILHELM. Humidity-Induced Colour Changes and Ink Migration Effects in Inkjet Photographs in Real- World Environmental Conditions .In: YUASA, General chair: Howard Mizes. Publications chair: Mashiho. *Final program and proceedings of IS*: *October 15 - 20, 2000, the Westin Bayshore Hotel, Vancouver, B.C., Canada*. Springfield, Va: IS, 2000, s. 74-77. ISBN 0-89208-230-5.

[11] ILFORD IMAGING EUROPE GMBH. *Press releases* [online]. 2013 [cit. 2015-05-18]. Dostupné z: http://www.ilford.com/about-us/press/ilford-introduces-new-240gsm-glossy-paper-everyday-

[12] SEN, Radha. *Microporous inkjet recording material* [patent].patent, US 20070116904 A1.Uděleno 24.5.2007.

[13] WILHELM, Henry. How Long Will They Last? An Overview of the Light-Fading Stability of Inkjet Prints and Traditional Color Photographs. In: ENGLISH ..]., [sponsored by:] Society for Imaging Science. *Final program and advance printing of paper summaries*: *February 20*. Springfield, La.: IS: IS, 2002, s. 32-37. ISBN 0-89208-237-2.

[14] BURLEY, J, John YOUNGQUIST a Julian EVANS. *Encyclopedia of forest sciences*.1st ed. Oxford: Elsevier, 2004, 4 v. ISBN 01-214-5160-7.

[15] *American inkjet corporation* [online]. 2007 [cit. 2014-06-16]. Dostupné z: http://www.americaninkjet.com/ecosolventink.html

[16] WILHELM, Henry. A 15-Year History of Digital Printing Technology and Print Permanence in the Evolution of Digital Fine Art Photography. In: STELTER, ISJ. *Final program and proceedings*: *September 17 - 22, 2006, Denver, Colorado*. Springfield, Va: IS, 2006, s. 308-315. ISBN

[17] FRYBERG, Mario. Dyes forInk Jet Printing. *Review of progress in coloration and related topics*: *revision A*. Upper Saddle River: Prentice Hall, c1994, Volume35, s. 1-30. ISSN 0557-9325.

[18] MOFFATT, John R. a Matthew THORNBERRY. *Protection of printed images from gas fade by incorporation of polyphenylenesulfide in print medium* [patent]. patent, EP 1 518 703 A1. Udelené30.3.2005.

[19] DOLL, P., F. SHI, S. KELLY a W. WNEK. The Problem of Catalytic Fading With Ink-Jet Inks. In: KOROL, General chair: David Dreyfuss. Publications chair: Steve. *Final program and proceedings of IS*: *October 18 -23, 1998, Westin HarbourCastle Hotel, Toronto, Ontario, Canada*. Springfield, Va: Society forImaging Science and Technology, 1998, 118–121. ISBN 0-89208-212-7.

[20] STEIGER, Rolf., Pierre-Alain BRUGGER. Photochemical Studies on the Lightfastness of Ink-Jet Systems. In: KOROL, General chair: David Dreyfuss. Publications chair: Steve. *Final program and proceedings of IS*: *October 18 -23, 1998, Westin Harbour Castle Hotel, Toronto, Ontario, Canada*. Springfield, Va: Society forImaging Science and Technology, 1998, 114–117. ISBN 0-89208-212-7

[21] Indoor Pollutant Gas Concentration and the Effect on Image Stability. In: IOANNIDIS, General chair: Andronique. *Final program and proceedings of IS: October 31 - November 5, 2004*. Springfield, Va: IS, 2004, s. 748-752. ISBN 0892082534.

[22] FRYBERG, Mario. Dyes for Ink Jet Printing. *Review of progress in coloration and related topics*: *revision A*. Upper Saddle River: Prentice Hall, c1994, Volume35, s. 1-30. ISSN 0557-9325

[23] LAVERY, A. The environmental stability of digital photo papers. *The imaging science journal*. 2002, Volume 50, Issue 3, s. 125-132. ISSN 1368-2199.

[24] KANAZAWA, Yukihiko, SEOKA, Shinzou KISHIMOTO a Naotsugu MURO. Indoor Pollutant Gas Concentration and the Effect on Image Stability. In: IOANNIDIS, General chair: Andronique. *Final program and proceedings of IS*: *October 31 - November 5, 2004, Little America Hotel and Towers, Salt Lake City, Utah*. Springfield, Va: IS, 2004, 748–752. ISBN 0-89208-253-4.

[25] GEISENBERG, J., K. SAITMACHER, MACHOLDT a H. MENZEL. Stability of Ink Jet Prints to Gas Fading – New Developments. In: NG, General chair: Yee S. *Final program and proceedings of IS*: *September 28 - October 3, 2003, Hyatt Regency Hotel, New Orleans, Louisiana*. Springfield, Va: IS, 2003, 394–395. ISBN 0-89208-247-X.

[26] FUJIE, Yoshihiko. Development of High Durability Cyan and Magenta Dyes for Ink Jet Printing System. *FUJIFILM RESEARCH & DEVELOPMENT* [online]. 2009, č. 54 [cit. 2014-05-07].Dostupné z: http://www.fujifilm.com/about/research/report/054/pdf/index/ff_rd054_007_en.pdf

[27] DIAMOND, Arthur S a David S WEISS. *Handbook of imaging materials*.2nd ed., rev. and expanded. New York: Marcel Dekker, c2002, x, 676 p. Optical engineering (Marcel Dekker, Inc.), v. 74. ISBN 08-247-8903-2.

[28] KITAMURA, Kazuhiko, Yasuhiro OKI, Hidemasa KANADA a Hiroko HAYASHI. A Study of Fading Property Indoors Without Glass Frame from an Ozone Accelerated Test. In: NG, General chair: Yee S. Final program and proceedings of IS: September 28 - October 3, 2003, Hyatt Regency Hotel, New Orleans, Louisiana. Springfield, Va: IS, 2003, 415–419. ISBN 0-89208-247-X.

[29] DR. MILLER, Nils. Inket prints: Here to stay. In: *Hewlett Packard* [online]. 2004 [cit. 2015-02-04].Dostupné z:

http://www.hp.com/products1/printpermanence/pdfs/Lightfastness_white_paper_update_final.pdf

[30] MCCORMICK-GOODHART, Mark a Henry WILHELM. New test Methods for Evaluating the Humidity – Fastness of Inkjet Prints. In: *JAPAN HARDCOPY*. 2005. vyd. Japan: The Imaging Society of Japan, 2005, s. 95-98. ISSN 0916-8087.

[31] WILHELM, Henry a Mark MCCORMICK-GOODHART. The Influence of Relative Humidity on Short Term Color Drift in InkJet Prints. In: WEISS ..., General chair: David S.... *Final program and proceedings of IS*: *September 30 - October 5, 2001, Marriott Harbor Beach Resort*. Springfield, Va: IS, 2001, s. 179-185. ISBN 0-89208-234-8ISSN 0-89208-234-8.

[32] DOLL, P. a F. SHI. The Problem of Catalytic Fading with Ink-Jet Inks. In: KOROL, General chair: David Dreyfuss. Publications chair: Steve. *Final program and proceedings of IS*: *October 18 -23, 1998, Westin Harbour Castle Hotel, Toronto, Ontario, Canada*. Springfield, Va: Society for Imaging Science and Technology, 1998, s. 118-121. ISSN 0-89208-212-7.

[33] LAVEDRINE, B. a F. ROBERT. Evaluation of Dark Stability of Reversal Colour Films using Arrhenius' Law. *The imaging science journal*.1988, roč.1988, č. 36.ISSN 1368-2199.

[34] BARD, Charleton C. a George W. LARSON. Predicting Long-Term Dark Storage Dye Stability Characteristics of Color Photographic Products from Short-Term Tests. *Journal of applied photographic engineering*.1980, roč. 1980, č. 2, s. 42-45. ISSN 0098-7298.

[35] ARRHENIUS, S.A. *Zeitschrift für physikalische Chemie*. 1889, roč. 1889, č. 4, s. 226. ISSN 0942-9352.

[36] WILHELM, Henry. Light-Induced and Thermally Induced Yellowish Stain Formation in Inkjet Prints and Traditional Chromogenic Color Photographs. In: *JAPAN HARDCOPY*. 2003. vyd. Japan: The Imaging Society of Japan, 2003, s. 213-216. ISSN 0916-8087.

[37] SCHANDA, János. *Colorimetry*: *understanding the CIE system*. Hoboken, N.J.: Wiley-Interscience, c2007, xxix, 459 p. ISBN 04-700-4904-9.

[38] *Additive mixture: mixture of primary colours, effects of additive synthesis and subtractive synthesis* [online]. 1994, 2012 [cit. 2012-09-05].Dostupné z: http://media-2.web.britannica.com/eb-media/12/7712-004-D7CE5860.jpg

[39] FRASER, Bruce, Chris MURPHY a Fred BUNTING. *Správa barev*: *průvodce profesionála v grafice a pre-pressu*.Vyd.1. Překlad Milan Daněk. Brno: Computer Press, 2003, 521 s. ISBN 80-722-6943-7.

[40] KUEHNI, Rolf G. *Color Vision & Technology*. 2008. vyd. USA: AATCC, 2008.

[41] *Spectral variations in natural light* [online]. 2009, 2009 [cit. 2012-09-06]. Dostupné z: http://www.handprint.com/HP/WCL/IMG/surfintens.gif

[42] RENSSELAER POLYTECHNIC INSTITUTE, Troy, NY12180USA. *Lighting research centre*: *How can full-spectrum light sources be compared?*[online]. 2003-2005, 2012 [cit. 2012-09-18]. Dostupné z: http://www.lrc.rpi.edu/programs/nlpip/lightinganswers/fullspectrum/comparisons.asp

[43] SHEVELL, Steven K. *The science ofcolor*.2nd ed. United States: Optical Society of America, 2003, ix, 339 p. ISBN 04-445-1251-9.

[44] MALACARA, Daniel. *Color vision and colorimetry*: *theory and applications*. Bellingham, WA: SPIE Press, c2002, vii, 164 p. ISBN 08-194-4228-3.

[45] HUNT, R. *The reproduction of colour*.5th ed. London: Fountain Press England, 1995, 814 s. ISBN 08-634-3381-2.

[46] HUNT, R.W.G. *Measuring colour*. 3rd ed. Kingston-upon-Thames: Fountain, 1998. ISBN 08-634-3387-1.

[47] GIORGIANNI, Edward J. *Digital Color Management*

[48] MADDEN, Thomas E. *Digital color management*. S.l.: Addison-WesleyPublishingCompany, 1998, 576 s. ISBN 02-016-3426-0.

[49] KAPLANOVÁ, Marie. *Moderní polygrafie*. Praha: Svaz polygrafických podnikatelů, 2010, 391 s. ISBN 978-80-254-4230-2.

[50] Panák, J., Čeppan, M., Dvonka, V. et al.: *Polygrafické minimum*. 3. vydání, Bratislava: Typoset, 2008. 264 p. ISBN 978-80-970069-0-7

[51] Panák, J., Čeppan, M., Dvonka, V. a kol.: *Polygrafické minimum*. 1. vydání, Bratislava: Typoset, 2000. 256 s. ISBN 80-967811-2-X

[52] Color differences and tolerances; Commercial colour acceptability. *Datacolor* [online]. 2013 [cit. 2015-05-18]. Dostupné z: http://industrial.datacolor.com/support/wp-content/uploads/2013/01/Color-Differences-Tolerances.pdf

[53] SHARMA, Abhay. *Understanding color management*.CliftonPark: Thomson/Delmar Learning, 2004, xvii, 362 s. ISBN 14-018-1447-6.

[54] SHARMA, Gaurav. *Digital color imaging handbook*. Boca Raton, FL: CRC Press, c2003, 797 p. ISBN 08-493-0900-X.

[55] Veselý, M., Králová, I., Dzik, P., Zita, J.: *Vnímaní barev a jejich měření.* VUT v Brně, Chemická fakulta, Ústav fyzikální a spotřební chemie

[56] ENGELDRUM, Peter G. *Psychometric scaling*: *a toolkit for imaging systems development*. Winchester, Mass.: Imcotek Press, c2000, xv, 185 p. ISBN 09-678-7060-7.

[57] WILHELM, Henry Gilmer a Carol BROWER. *The permanence and care of color photographs*: *traditional and digital color prints, color negatives, slides, and motion pictures*. 1st ed. Grinnell, Iowa, U.S.A.: Preservation Pub. Co., c1993, ix, 744 p. ISBN 09-115-1501-1.

[58] WILHELM, Henry. How Long Will They Last? Part II – An Overview of the Light-Fading Stability of Inkjet Prints and Traditional Color Photographs. In: ENGLISH ..]., [sponsored by:] Society for Imaging Science. *Final program and advance printing of paper summaries*: *February 20*. Springfield, La.: IS: IS, 2002, s. 37. ISBN 0-89208-237-2.

[59] WILHELM, Henry. Yellowing stain Formation in Inkjet Prints and Traditional Silver-Halide Photographs. In: NG, General chair: Yee S. *Final program and proceedings of IS*: *September 28 - October 3, 2003, Hyatt Regency Hotel, New Orleans, Louisiana*. Springfield, Va: IS, 2003, s. 444-449. ISBN 0-89208-247-X. Dostupné z: CANON.Printers - PIXMA [online]. 2010. vyd. 2010 [cit. 2012-09-26]. Dostupné z: http://www.canon.cz/For_Home/Product_Finder/Multifunctionals/Inkjet/PIXMA_MG6150/index.aspx

[60] McCormick-Goodhart M., Wilhelm H.: Progress Towards a New Test Method Based on CIELAB Colorimetry for Evaluating the Image Stability of Photographs. *Proceedings of IS&T's 13th International Symposium on Photofinishing Technologies*, pp. 25–30. Las Vegas 2004. ISBN 0-89208-249-6.

[61] ISO 18909 *Photography – Processed photographic colour films and paper prints and paper prints – Methods for measuring image stability*, 2006, Switzerland

[62] Oldfield D.J., Pino G; Assessment of the Current Light Fade Endpoint Metrics Used in the

Determination of Print Life – Part II; *IS&T's Archiving Conference,* p. 36-42, 2004. ISBN 0-89208-251-8

[63] Shibahara Yoshihiko, Makoto Machina: Endpoint Criteria for Print Life Estimation ;*IS&T's NIP20 International Conference on Digital Printing Technologies,* p. 673-679, Salt Lake City 2004. ISBN 0-89208-253-4

[64] WILHELM IMAGING RESEARCH. *A New Test Method Based on CIELAB Colorimetry for Evaluating the Permanence of Pictorial Image* [online]. 16 June 2003. 2003 [cit. 2012-09-26]. Dostupné z: http://www.wilhelm-research.com/pdf/WIR_CIELAB_TEST_2003_07_25.pdf

[65] WILHELM, Henry a Kabenla ARMAH. Improved Test Method for Evaluating the Permanence of Digitally-Printed Photographs. In: *Proceedings Imaging conference Japan 2009*. June 10-12, 2009: The Imaging Society of Japan, 2009, s. 213. ISSN 1881-9958.

[66] KANG, Henry R. *Computational color technology*. Bellingham, Wash.: SPIE Press, c2006, xix, 511 p. ISBN 978-081-9461-193.

[67] MCCORMICK- GOODHART, Mark a Henry WILHELM. Progress Towards a New Test Method Based on CIELAB Colorimetry for Evaluating the Image stability of Photographs. In: TECHNOLOGY ..., Sponsored by Society for Imaging Science. *Final program and advanced printing of paper summaries*: *co-located with the PMA Show; February 8 and 9, 2004, The Riviera Hotel, Las Vegas, Nevada*. Springfield, Va.: Society for Imaging Science: Society for Imaging Science, 2004, s. 25-30. ISBN 0-89208-249-6. Dostupné z: http://www.wilhelm-research.com/

[68] ISO 18909:2006E.*Photography*: *Processed photographic colour films and paper prints – Methods for measuring image stability*. 2006. vyd. Switzerland: International Organization for Standardization, 2006.

[69] CP-3901.*JEITA CP-3901*: *Digital Color Photo Print Stability Evaluation*. 9/2010. Japan: Japan Electronics and Information Technology Industries Association, 2010.

[70] F2366-05(2008). *International Standard Practice for Determining Relative Lightfastness of Ink Jet Prints Exposed to Windows Filtered Daylight Using a Xenon Arc Light Apparatus*. 2008. vyd. USA: ASTM International, 100 Barr Harbor Drive, PO Box C700, West Conshohocken, PA, 19428-2959 USA, 2008.

[71] RASMUSSEN, Adam, Veronika CHOVANCOVA a Dan FLEMING III. Light Fastness of Pigment-based and Dye-based Inkjet Inks. In: *Proceedings of the 57th TAGA Annual Technical Conference*. April 2005. Toronto, Ontario, 2005, s. 34-44. Dostupné z: http://www.wmich.edu/pci/faculty/Publication/fleming/AdamR%20Paper%20for%20TAGA.pdf

[72] DZIK, Petr a FURST,Tomas. Gamut Volume as a Tool for Image Permanence Determination: Recent Advances Using the Quick-hull Algorithm. In: 10[TH] SEMINAR IN GRAPHIC ARTS, 19th - 21th September 2011. *Conference proceedings*. Pardubice: University of Pardubice, Department of Graphic Arts and Photophysics, 2011, s. 45-52. ISBN 978-80-7395-420- 8.

[73] ISO 18941:2011. *Imaging materials – Colour reflection prints -- Test method for ozone gas fading stability*. 2011. vyd. Switzerland: International Organization for Standardization, 2011.

[74] ISO 18946:2011. *Imaging materials -- Reflection colour photographic prints -- Method for testing humidity fastness*. 2011. vyd. Switzerland: International Organization for Standardization, 2011.

[75] *YASUDA SEIKI SEISAKUSHO, LTD.* [online]. 2007 [cit. 2013-01-22]. Dostupné z: http://www.yasuda-seiki.co.jp/e/products/img/401.jpg

[76] ČSN 77 0332. *Stanovení propustnosti tenkých plošných materiálů pro vodní páru gravimetrickou*

metodou. ČR: Nakladatelství ČNI, 1980.

[77] DIN 53380-3. *Testing of plastics – Determination of gas transmission rate - Part 3: Oxygen-specific carrier gas method for testing of plastic films and plastics mouldings.*Deutschland, 1998.

[78] ROECKELEIN, Jon E. *Elsevier's dictionary of psychological theories*.1st ed. Boston: Elsevier, 2006, p. cm. ISBN 04-445-1750-2.

[79] ROHATGI-MUKHERJEE, K.K. *Fundamentals of photochemistry*. Rev. ed. New Delhi: Wiley, 1978. ISBN 08-522-6784-3.

[80] WILHELM, Henry a Mark MCCORMICK-GOODHART. Reciprocity Behavior in the Light Stability Testing of Inkjet Photographs. In: WEISS ..., General chair: David S....*Final program and proceedings of IS*: *September 30 - October 5, 2001, Marriott Harbor Beach Resort*. Springfield, Va: IS, 2001, s. 197-202. ISBN 0-89208-234-8.

[81] WLHELM, Henry. A Review of Accelerated Test Methods for Predicting the Image Life of Digitally printed Photographs - Part II. In: IOANNIDIS, General chair: Andronique. *Final program and proceedings of IS*: *October 31 - November 5, 2004, Little America Hotel and Towers, Salt Lake City, Utah*. Springfield, Va: IS, 2004, s. 664-669. ISBN 0-89208-253-4.

[82] Epson. 2005. *Print Permanence* [online]. [cit. 2015-05-12]. Dostupné z: https://ftp.epson.com/webfiles/whitepprlow.pdf

[83] Berger, M., Wilhelm, H.: *Comparison of different methods for Estimating the Sensitivity of Inkjet Images to Gas Fading*. *Final program and proceedings of IS&T's NIP 19th International Conference on Digital Printing Technologies: October 31 - November 5, 2004, Little America Hotel and Towers, Salt Lake City, Utah*. Springfield, p.:740–745, Va: IS, 2004. ISBN 08-920-8253-4.

[84] *Kitamura, K. Oki, Y., Kanada, H., Hayashi, H.,: A Study of Fading Property Indoors Without Glass Frame from an Ozone Accelerated Test. Final program and proceedings of IS&T's NIP 19th International Conference on Digital Printing Technologies: October 31 - November 5, 2004, Little America Hotel and Towers, Salt Lake City, Utah*. Springfield, p. 415–419, Va: IS, 2004. ISBN 08-920-8253-4.

[85] Miyazawa, K., Suda, Y.: Uncertainty in Evaluation of Accelerated Ozone Fading Tests of Inkjet Prints. *Proceedings of IS&T's NIP 20th International conference on digital printing technologies*, pp. 720–723. Salt Lake City 2004. ISBN 0-89208-253-4.

[86] Reber, J, Hofman, R.: Correlation of ozone test chamber data with real life permanence of inkjet prints. *Proceedings of IS&T's NIP 22nd International Conference on Digital Printing Technologies*, pp. 231–234, Denver 2006. ISBN 0-89208-263-1.

[87] *Aplikovaná molekulová spektroskopia*. Editor Viktor Milata. Bratislava: Státnítechnickáuniversita, 2008, 600 s. ISBN 978-802-2729-604.

[88] AHNE, Bernd. *Practical Handbook on Image Processing for Scientific and Technical Applications*. 2nd ed. Hoboken: Taylor, 2004. ISBN 08-493-9030-3

[89] EDITOR-IN-CHIEF, Robert A. *Encyclopedia of analytical chemistry*. [Online ed.]. Hoboken, N.J.: John Wiley, 200u. ISBN 978-047-0027-318.

[90] SMITH, Ewen a Geoffrey DENT. *Modern Raman spectroscopy: a practical approach*. Chichester: John Wiley, 2005, 210 s. ISBN 04-714-9794-0.

[91] RASTOGI, Pramod K a Erwin HACK. *Optical methods for solid mechanics: a full-field approach*. Weinheim: Wiley-VCH, 2012, xvi, 433 p. ISBN 35-274-1111-9.

[92] GROSS, Edited by Herbert.*Handbook ofOpticalSystems.*Weinheim: WILEY-VCH VerlagGmbH, 2005, 690 s. ISBN 3-527-40378-72.

[93] KORRES, By Spyridon.*On-LineTopographicMeasurementsofLubricatedMetallicSlidingSurfaces.* Karlsruhe: KIT ScientificPublishing, 2013.

[94] BYK-GARDNER GMBH. *Gloss Measurement* [online]. 2014 [cit. 2015-03-16].Dostupné z: http://www.byk.com/fileadmin/byk/support/instruments/theory/appearance/en/Intro_Gloss.pdf

[95] PEIPONEN, K, Risto MYLLYLÄaAleksandrVasil'evich PRIEZZHEV. *Opticalmeasurementtechniques: innovationsforindustry and thelifesciences*. Berlin: Springer, 2009, 155 p. Springerseries in opticalsciences, v. 136. ISBN 3540719261.

[96] WILHELM, Henry Gilmer a Carol BROWER. *The permanence and care of color photographs*: *traditional and digital color prints, color negatives, slides, and motion pictures*. 1st ed. Grinnell, Iowa, U.S.A.: Preservation Pub. Co., c1993, ix, 744 p. ISBN 09-115-1501-1.

[97] LAVÉDRINE, Bertrand, Jean-Paul GANDOLFO a Sibylle MONOD. *A guide to the preventive conservation of photograph collections*. Los Angeles: Getty Conservation Institute, c2003, xvi, 286 p. ISBN 08-923-6701-6

[98] ČEJKA, Dušan.Novémožnostitiskovýchstrojůspolečnosti KBA-Grafitec. In: 7. POLYGRAFICKÝ SEMINÁŘ, *Sborníkpřednášek*. Pardubice: Univerzita Pardubice, Fakultachemicko-technologická, Katedrapolygrafie a fotofyziky, 2005, s. 126-121. ISBN 80-7194-793-8.

[99] *Water-insoluble protective coatings for photographic materials* [patent]. Patent, 3,322,555.Uděleno 30.5.1967.

[100] Photodegradation and photostabilizationofpolymers, especially polystyrene: review. *SpringerOpenjournal* [online].2013, roč.2013, č. 2 [cit. 2014-05-29].Dostupné z: http://www.springerplus.com/content/pdf/2193-1801-2-398.pdf

[101] LAPČÍK, Lubomír. *Fotochemicképrocesy*. 1. vyd. Bratislava: Alfa, 1989, 418 s. ISBN 80-050-0049-9.

[102] SCHULZ, Ulrich. *Accelerated testing: nature and artificial weathering in the coatings industry*. Hannover, Germany: Vincentz Network, 2009. ISBN 38-663-0908-2.

[103] ÁVÁR, L. a K. BECHTOLD. Studies on the interaction of photoreactive light stabilizers and UV-absorbers. *Progress in Organic Coatings*. 1999, vol. 35, 1-4, s. 11-17. DOI: 10.1016/S0300-9440(99)00031-4.

[104] STOYE, Dieter. *Paints, coatings, and solvents*. 1st ed. New York: VCH, 1993, xvii, 409 p. ISBN 15-608-1809-3.

[105] LTD, Thomas Brock; Michael Groteklaes; Peter Mischke. Ed. by Ulrich Zorll. Transl. by HeatherYesson and. *European coatings handbook*. Hannover: Vincentz, 2000. ISBN 38-787-0559-X.

[106] SCOTT, edited by Gerald. *Mechanisms of Polymer Degradation and Stabilisation*. Dordrecht: Springer Netherlands, 1991. ISBN 978-940-1138-383.

[107] *Weathering of polymers*. Oxford: Pergamon, 1992. ISBN 00-804-1960-7.

[108] STEP, E. N. a N. J. TURRO. Mechanism of Polymer Stabilization by Hindered-Amine Light Stabilizers (HALS). Model Investigations of the Interaction of Peroxy Radicals with HALS Amines and Amino-Ethers. *Macromolecules*. Washington: American Chemical Society, 1994, č. 27.

[109] Elcometer. *Elcometer inspection equipment* [online]. © Elcometer Limited 2013 [cit. 2015-02-20]. Dostupné z: http://www.elcometer.com/en/laboratory/film-application/film-applicators-and-bar-coaters/productmanager?prod=60

[110] EASTMAN CHEMICAL COMPANY. *Eastman™: Cellulose Acetate Propionate (CAP-482-0.5)* [online]. 2014 [cit. 2014-05-23]. Dostupné z: http://www.eastman.com/Products/Pages/ProductHome.aspx?Product=71001221

[111] Product Data Sheet: Eastman™ Triacetin. *Eastman Chemical Company* [online]. 2001 [cit. 2014-05-23]. Dostupné z: http://ws.eastman.com/ProductCatalogApps/PageControllers/ProdDatasheet_PC.aspx?Product=71001147&sCategoryName=Generic

[112] *Cellulose acetate propionate* [patent]. patent, US 5,977,347 A. Uděleno 2. 11. 1999.

[113] SIGMA ALDRICH. *Cellulose acetate propionate* [online]. 2014 [cit. 2014-05-23]. Dostupné z: http://www.sigmaaldrich.com/catalog/product/aldrich/340642?lang=en&region=CZ

[114] CHEMSPIDER. *Triacetin* [online]. 2014 [cit. 2014-05-23]. Dostupné z: http://www.chemspider.com/Chemical-Structure.13835706.html

[115] Everlight chemicals. *Everlight chemicals* [online]. 2013, [cit. 2014-05-30]. Dostupné z: http://everlight-uva.com/

[116] Eversorb AQ1. In: *Eversorb AQ1* [online]. 2008 [cit. 2013-11-12]. Dostupné z: http://www.braschemical.com.br/fotos/produtos/EVERSORB%20AQ1.pdf

[117] Czech republic. Safety sheet - EVERSORB AQ2. In: *356/2003 Sb.* 2007.

[118] BYK GARDNER GMBH. *Manual - Glossmeter mikro-TRI gloss* [online]. 2010 [cit. 2015-03-16]. Dostupné z: http://www.byk.com/fileadmin/byk/support/instruments/downloads/support-downloads/public/Manuals/Appearance/Gloss/micro-gloss/Full%20Version%20English%20German/260020398_E_1008.pdf

[119] Film Applicators. 2014. *BYK Gardner* [online]. [cit. 2015-05-11]. Dostupné z: https://www.byk.com/en/instruments/products/film-application/film-applicators.html

[120] VolGa microsite. *Brno University of Technology* [online]. 2011 [cit. 2014-06-17]. Dostupné z: http://www.fch.vutbr.cz/cs/laboratore/volga.html

[121] The Known Colors Palette Tool. *Code project* [online]. 2015 [cit. 2015-11-06]. Dostupné z: http://www.codeproject.com/Articles/243610/The-Known-Colors-Palette-Tool-Revised-Again

[122] PŘÍZEMNÍ OZON (O_3). 2014. *Český hydrometeorologický ústav* [online]. [cit. 2015-05-13]. Dostupné z: http://portal.chmi.cz/files/portal/docs/uoco/isko/grafroc/13groc/gr13cz

[123] Table of critical values for the F distribution (for use with ANOVA). *University of Sussex* [online]. 2005 [cit. 2015-11-05]. Dostupné z: http://users.sussex.ac.uk/~grahamh/RM1web/F-ratio%20table%202005.pdf

[124] STANČÍK, Jiří. *Degradace inkoustových výtisků*. Brno, 2010. Disertation thesis. Brno University of Technology. Vedoucí práce Doc. Ing. Michal Veselý, Ph.D.

7 ABBREVIATION AND SYMBOL LIST

2D	two-dimensional
3D	three-dimensional
A	test area of the specimen
ATR	attenuated total reflection
a^*, b^*	colour space 1979 CIE $L^*a^*b^*$ *x, z–axis* coordinates
ASTM	American Society for Testing and Materials
B	blue filter
C	cyan dye
CAP	cellulose acetate propionate
Cd	Cadmium
Ch.	chapter
CIE	Commision Internationale de l`Éclairage (International commission for illumination)
CIELAB	CIE L*a*b* colour space
CO_2	carbon dioxide
CS	continual stream print
ČSN	Czech technical standard
δ	molecular bending
DIN	Deutsches Institut für Normung; the German Institute for Standardization
DOD	drop on demand print
d_p	depth of beam penetration in ATR
dpi	dots per inch
E_{max}	relative intensity maximum
E_r	relative intensity spectrum
e.g.	exempli gratia; for example
ΔE^*_{ab}	change in colour
ΔE_e	electron state transition energy
ΔE_r	rotation state transition energy
ΔE_v	vibrational state transition energy
et. al.	et alii; and others
etc.	et caetera, and so forth
F	value of test criterion in ANOVA test
F_{crit}	critical value of test criterion in ANOVA test
Fig.	figure
FTIR	Fourier transform infrared spectroscopy
G	green filter
GU	gloss units
H_0	null hypothesis in ANOVA test
H_2	hydrogen
H_a	alternative hypothesis in ANOVA test
HALS	hindered amine light stabiliser
HP	Hewlett Packard
hr	hour
*I**	I star, parameter set up by Wilhelm Imaging group
i.e.	id est; that is
Inc.	incorporated
ICC	International Colour Consortium

ISG	Ilford GALERIE Smooth Gloss inkjet paper
ISO	International Organization for Standardization
ISP	Ilford GALERIE Smooth Pearl inkjet paper
IR	infrared
IR-A	radiation in infrared region in wavelengths 780-1400 nm
IR-B	radiation in infrared region in wavelengths 1400-3000 nm
IR-C	radiation in infrared region in wavelengths 3000 nm-1 mm
K	black ink
KCl	potassium chloride
KNO_3	potassium nitrate
λ	wavelength
L^*	colour space 1979 CIE $L^*a^*b^*$ y-axis coordinate; lightness
M	magenta dye
MIS	MIS Associates INC.
M_r	molar mass
ν	molecular stretching
n	refraction index
N_2	nitrogen
NaOH	sodium hydroxide
Ni	Nickel
$Na_2C_4H_4O_6{\cdot}2H_2O$	sodium tartrate di-hydrate
NaCl	sodium chloride
NO_x	nitrogen oxides
nr.	number
O_2	oxygen
$^3O_2$	ozone
OBA	optical brightening agents
OTR	oxygen transmission rate
PP	polypropylene
P_{amb}	the atmospheric pressure
Pd	Palladium
Pt	Platinum
prep	preparation
Ψ	ellipsometrical angle
R	reflectance
R	red filter
R	resistance of the resistor
ϱ_{O_2}	volume percentage of oxygen in the test gas
$R(\lambda)$	spectral reflectance
resp.	respectively
RC	resin coated-double side coated with polyethylene
RH	relative humidity
SD	standard deviation
SO_2	sulfur dioxide
θ	incident angle
T	transmittance
U_0	zero level voltage
U_E	steady state voltage
UV	ultraviolet
UVA	radiation in range 315-400 nm

X, Y, Z	tristimulus values
$\bar{x}, \bar{y}, \bar{z}$	colour matching functions
$\bar{x}_{10}, \bar{y}_{10}, \bar{z}_{10}$	colour matching functions for 10°observer
Y	yellow ink
VIS	visible
VOC	Volatile organic compounds
VolGa	Volume of Gamut; software
w%	weight percentage